RCA REVIEW

a technical journal

RADIO AND ELECTRONICS
RESEARCH · ENGINEERING

VOLUME X   JUNE 1949   NO. 2

RCA REVIEW

a technical journal

RADIO AND ELECTRONICS
RESEARCH · ENGINEERING

CONTENTS

RCA REVIEW

BOARD OF EDITORS

REPUBLICATION AND TRANSLATION

METHOD OF MULTIPLE OPERATION OF TRANSMITTER TUBES PARTICULARLY ADAPTED FOR TELEVISION TRANSMISSION IN THE ULTRA-HIGH-FREQUENCY BAND*

By

GEORGE H. BROWN, WENDELL C. MORRISON, W. L. BEHREND AND J. G. REDDECK

Research Department, RCA Laboratories Division, Princeton, N. J.

Summary—A combining network has been developed which allows two transmitting tubes to be operated simultaneously into a common load without interaction between tubes and without reduction in band width. A number of variations of the combining network are discussed and a theoretical analysis is presented which shows that the necessary balancing adjustments are not critical.

A pair of tubes and a combining network may then be considered as a unit, with this unit combined with several other identical units to provide a transmitter with a large number of tubes in multiple operation. In this arrangement, each tube is free from interaction with other tubes.

Rather simple circuits which apply the principles set forth are described for operation at low radio frequencies. A complete television transmitter with a carrier frequency of 850 megacycles has been developed, using four tubes in multiple to demonstrate the principle of operation.

INTRODUCTION

THE ability to generate radio-frequency power has generally kept abreast of the demand for increases in power, particularly in the broadcast band of frequencies and in the medium-high frequencies. With large power tubes available and the techniques of multiple use of tubes in push-pull or parallel operation quite commonplace, transmitter design resolves itself into a problem of economics and good engineering practice. Estimates of power requirements for ultra-high-frequency television broadcasting, however, are far in excess of the power capabilities of any commercially available single tube or of any simple push-pull combination of these tubes.[1,2]

---

* Decimal Classification: R355.16 × 583.4.
[1] George H. Brown, J. Epstein, and D. W. Peterson, "Comparative Propagation Measurements; Television Transmitters at 67.25, 288, 510, and 910 Megacycles," *RCA Review*, Vol. IX, No. 2, pp. 177-201, June, 1948.
[2] George H. Brown, "Field Test of Ultra-High-Frequency Television in the Washington Area," *RCA Review*, Vol. IX, No. 4, pp. 565-584, December, 1948.

Several tubes may be used in essentially parallel operation by arranging the tubes in a circle on a common cavity.[3] In this method, the number of tubes is limited by practical considerations of high circulating currents in the tank circuit and criticalness of tuning, both effects due to the paralleling of the tube capacities. The authors have undertaken a study of circuit arrangements which alleviate these difficulties and have developed a simple bridge circuit which permits the multiple operation of transmitter tubes into a common load without interaction between tubes and with no limitation on band width other than that imposed by a single tube and tank circuit. In this method of operation, each final amplifier tube has its own associated tank circuit, feeds into a pure resistance load, and is entirely oblivious to the existence of the other amplifier tubes.

The Philosophy of the Use of a Bridge Circuit to Accomplish Multiple Operation of Amplifier Stages

The bridge circuit which forms the heart of this multiple operation method may be depicted for illustrative purposes by Figure 1. However, the reader should remember that this circuit *per se* is not readily applicable to the problem at hand. Circuits appropriate to particular frequency ranges will be described later in the paper.
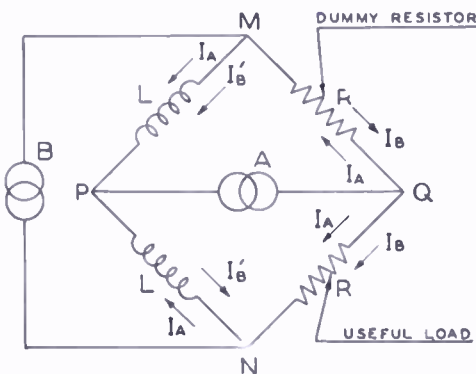
Fig. 1—A bridge circuit used to illustrate the principle of multiple operation.

The bridge of Figure 1 consists of two equal inductances and two equal resistances. This bridge is balanced, that is, the generator A produces no voltage across the terminals M-N and the generator B produces no voltage across the terminals P-Q. Thus, the two generators may operate simultaneously without interaction and the currents in the network produced by generator B simply superimpose upon the currents produced by generator A. The voltages generated by A and B are assumed to be sine waves of identical frequency.

Suppose for the moment that generator B is inoperative. Then generator A produces the two currents denoted as I_A in each of the resistors. One resistor in Figure 1 is called the useful load while the

[3] Donald H. Preist, "Annular Circuits for High-Power Multiple-Tube Generators at VHF and UHF," presented at the 1949 I.R.E. National Convention, New York City, March 9, 1949.

other is designated as a dummy resistor, for reasons which will soon become apparent. The power dissipated in the dummy resistor is $I_A^2 R$ and the power in the useful load is of exactly the same value. Hence the power delivered by generator A is

$$P_A = 2 I_A^2 R. \tag{1}$$

If generator A now becomes inoperative and generator B delivers power to the bridge, the currents in the two resistors will be I_B and the total power delivered by generator B is

$$P_B = 2 I_B^2 R \tag{2}$$

with this power divided equally between the two resistors.

Now let both generators become operative and assume that the voltage produced by generator B can be completely controlled with respect to both amplitude and phase. Control is exercised until the current I_B in the useful load is exactly equal to I_A in both amplitude and phase. Under this condition, the net current in the dummy resistor is zero and no power is dissipated in this dummy resistor. The power in the useful load is

$$P_U = (I_A + I_B)^2 R = (2 I_A)^2 R = 4 I_A^2 R \tag{3}$$

and the total power of the two generators is delivered to the useful load. The two generators remain uncoupled one from the other, with the total power concentrated in the single useful load. It is interesting to note that when one generator ceases to operate, the current in the useful load is halved and the power in this load goes to one quarter of the full load power.

When the bridge circuit was first considered, the ability to maintain sufficiently accurate balance of amplitude and phase was immediately questioned. A subsequent analysis, given below, soon showed the rather remarkable insensitiveness and practicality of the circuit arrangement. To illustrate this point, assume that the currents I_A and I_B are no longer equal and in phase but are related as follows:

$$I_A = K I_B \angle \beta \tag{4}$$

where K is a simple numerical coefficient. For this condition

$$P_B = 2 I_B^2 R \quad (5) \qquad \text{and} \qquad P_A = 2 I_A^2 R = 2 K^2 I_B^2 R \quad (6)$$

with the total power given by $P_A + P_B = 2(1 + K^2) I_B^2 R.$ (7)

Then the total current in the useful load is

$$\bar{I}_U = \bar{I}_B(1 + K \cos \beta + jK \sin \beta) \qquad (8)$$

and the power in the useful load is

$$P_U = (1 + K^2 + 2K \cos \beta) I_B^2 R. \qquad (9)$$

Likewise, the current in the dummy load is

$$\bar{I}_D = \bar{I}_B(1 - K \cos \beta - jK \sin \beta) \qquad (10)$$

and the power lost in the dummy resistor is

$$P_D = (1 + K^2 - 2K \cos \beta) I_B^2 R. \qquad (11)$$

One may easily note that the sum of the Equations (9) and (11) is identical with Equation (7).
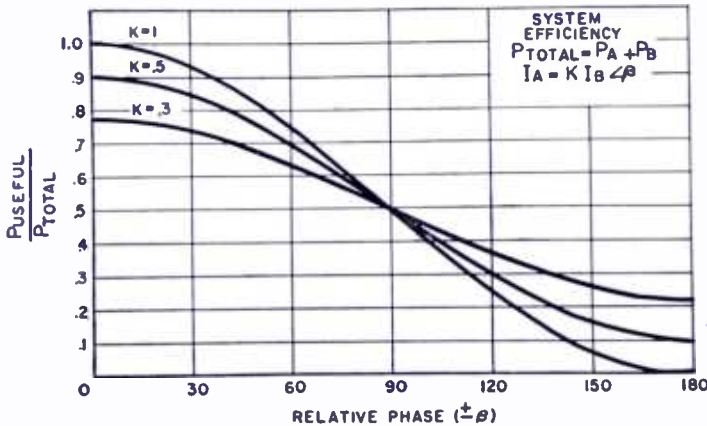
Fig. 2—Power in the useful load in terms of the total power as a function of the phase relationship between the currents produced by the two generators.

Dividing Equation (9) by Equation (7) gives

$$\frac{P_U}{P_A + P_B} = \frac{1 + K^2 + 2K \cos \beta}{2(1 + K^2)}. \qquad (12)$$

Equation (12) is plotted in Figure 2 as a function of the phase angle, β, with the numerical value of K as a parameter on each curve. This diagram reveals the inherent insensitiveness of the circuit to correct phase adjustment. To be specific, suppose that generators A and B are each delivering 500 watts to the circuit. Then with truly
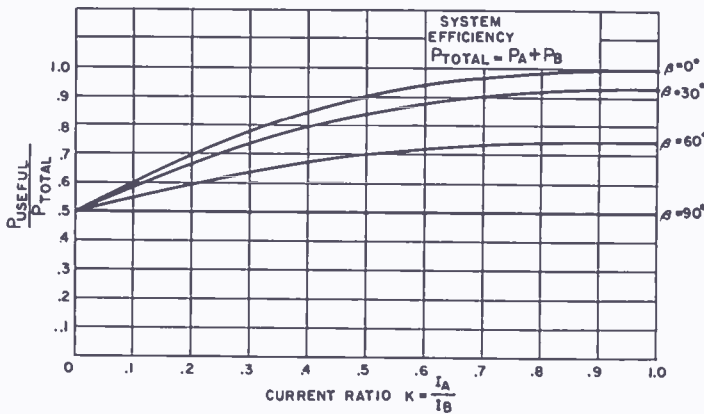
Fig. 3—Power in the useful load in terms of the total power as a function of the ratio of the currents produced by the two generators.

zero phase the power into the useful load will be 1000 watts. Reference to Figure 2 shows that with β equal to 30 degrees, the power into the useful load will be 933 watts. If the useful load is an antenna, the field strength will drop less than four per cent with this degree of phase misadjustment.

The calculations of Figure 2 have been replotted in Figure 3 to better illustrate the relative "flatness" of circuit conditions with variation in the parameter K.

So far in the analysis, it has been assumed that the two generators produced sine waves of identical frequency. It is reasonably apparent that if the signals are of complex wave form, but identical, cancellation in the dummy resistor will still be secured and the additive condition in the useful load realized. If the two generators represent modulated power amplifiers, the necessary conditions of operation are that the carriers are substantially in phase in the useful load and that the modulation of the two output stages is identical and simultaneous.

A pair of output tubes and a combining network may now be considered as a unit, with this unit combined with several other identical units to provide a transmitter with a large number of tubes in multiple operation. In this arrangement each tube is free from interaction with other tubes. Figure 4 illustrates the manner in which eight tubes are combined with seven bridges, or diplexers. It is now apparent that if n tubes are combined, the number n must be 2 raised to an integral power, that is, n must be 2, 4, 8, 16, and so on.
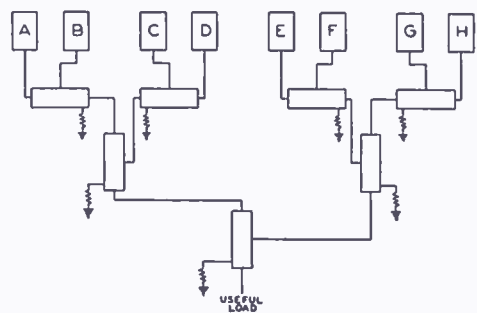
Fig. 4 — A combination of eight tubes and seven diplexers to accomplish simultaneous operation into a common load without interaction between tubes.

Also, the number of bridges required is $n-1$.

Since the currents in the outputs of the bridges are additive, it is a simple matter to estimate the overall efficiency and other operating conditions of interest without tracing through the rather involved bridge network. To accomplish this estimate, the following nomenclature has been set up:

P = power output of each output stage.

n = total number of stages.

nP = total power in useful load when all n stages are turned on.

mP = total power available when m stages are turned on.

I_n = current in useful load with n stages turned on.

I_m = current in useful load when m stages are turned on.

$I_m = (m/n) \; I_n$.

P_m = power in useful load when m stages are turned on.

$P_m = I_m^2 R = (m/n)^2 (I_n^2 R) = (m/n)^2 \cdot (nP)$.

Ratio of power into useful load with m stages turned on to total power available from n stages $= P_m/(nP) = (m/n)^2$.

Circuit efficiency when m tubes are on $= (P_m/mP) \cdot 100 = m/n \cdot 100$.

Table 1—Conditions of Operation in Seven Combining Networks and Eight Output Stages

m (Number of stages operative)	$\dfrac{mP}{nP} = \dfrac{I_m}{I_n}$	$P_m/(nP)$
8	1.0	1.0
7	0.875	0.766
6	0.75	0.562
5	0.625	0.391
4	0.5	0.25
3	0.375	0.141
2	0.25	0.063
1	0.125	0.016
0	0	0

As an example, suppose that each of eight tubes is capable of delivering 100 watts. Then a total of 800 watts is available for the useful load. With any three of the tubes turned on, the power delivered to the networks is 300 watts. The current in the useful load is m/n or $3/8$ of the current found there when eight tubes are on. The power into the useful load, P_m, is 112.5 watts, and the combining circuit efficiency is 37.5 per cent.

Table I illustrates still further the conditions of operation for n tubes, with n equal to eight.

<div align="center">

PRACTICAL BRIDGE CIRCUITS FOR LOW-FREQUENCY AND
HIGH-FREQUENCY OPERATION

</div>

A simple method of applying the bridge circuit principles at low frequencies, of the order of a few megacycles or less, is illustrated in Figure 5. It is apparent that this elementary application is a one-step bridge circuit which does not lend itself to the repetitive use outlined
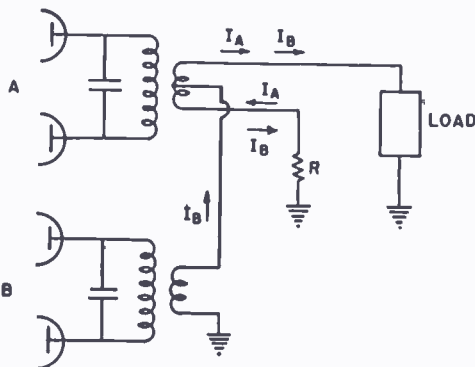
Fig. 5—A means of combining four tubes at a low frequency.
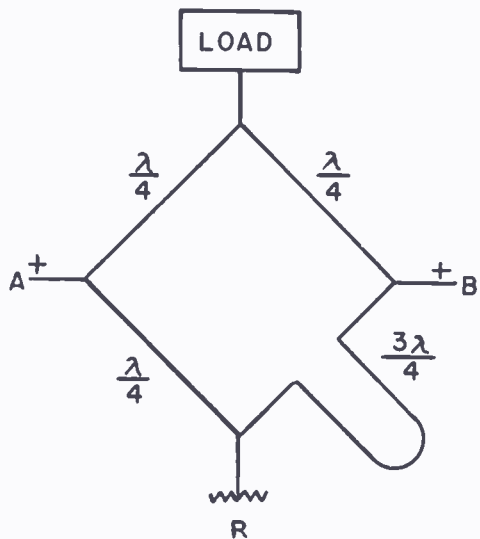
Fig. 6—A bridge arrangement constructed of lengths of transmission line.

above. A circuit much better suited to cascading at low frequencies may be best developed by referring to Figure 6. In this particular diagram, the arms of the bridge are coaxial transmission lines. Three of the arms are each one-quarter wave length at midband, while the fourth arm is three-quarters of one wave length. For the sake of simplicity, only the inner conductors are shown in Figure 6. Perfection of uncoupling between points A and B depends upon the exactness of these line lengths and the device is strictly limited to a narrow band of frequencies. When the useful load and the dummy resistor have a resistance of R ohms, and the characteristic impedance

of the transmission line arms is chosen as $\sqrt{2} \cdot R$, the resistance look-
ing in at points A or B will be R ohms at midband. While the above
choice of characteristic impedance plays no part in the balancing
action at midband, affecting only the input impedance, this same choice
does help in broadbanding the circuit.

The circuit of Figure 6 may now be used as a guide in forming a
lumped-circuit network for use at low frequencies. This has been
done in Figure 7. Each one-quarter-wave line has been replaced by a
Pi network consisting of two capacitors and one inductance coil. The
inductance and capacitance values have been so chosen that X_L equals
X_C at midband. The fourth arm is formed from two inductances and
one capacitance to be the equivalent of the three-quarter wave long
branch. When $X_L = X_C = MR$, the input impedance at A and B is
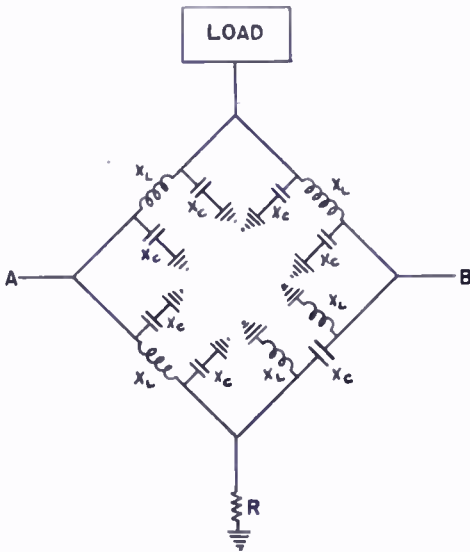
Fig. 7 — A bridge circuit con-
structed of lumped elements, to be
the equivalent of Figure 6.
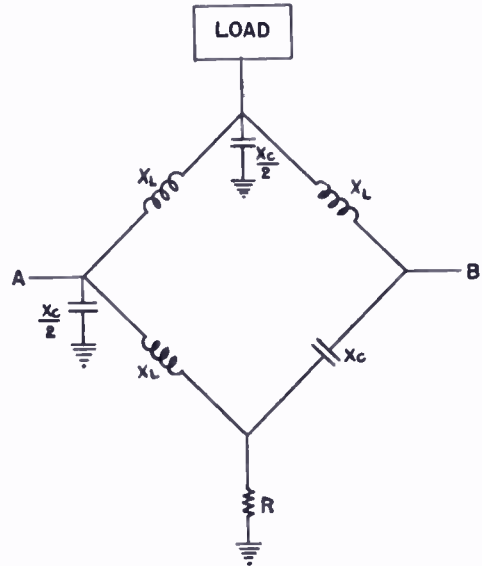
Fig. 8—A simplified circuit, equiva-
lent to Figure 7.

$M^2R/2$ ohms. Again a choice of M equal to $\sqrt{2}$ gives maximum broad-
banding for the input impedance. Figure 7 may be considerably simpli-
fied as shown in Figure 8 when it is noted that an inductive reactance
in parallel with an equal capacitive reactance forms a parallel resonant
circuit and both elements may then be omitted from the system.

The narrow-band limitations of Figure 6 may be avoided by the use
of the circuit shown in Figure 9. Here the balance between feed points
is independent of frequency and the variation of impedance at the
feed points establish the limits on the frequency band.

If a circuit balanced to ground is desired, the circuit shown in
Figure 10 is useful. Here the arms of the bridge may be either parallel
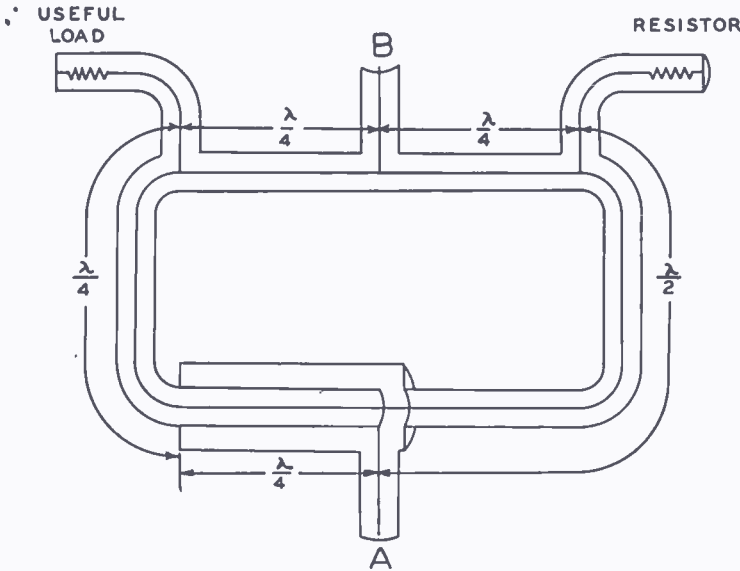
Fig. 9—A high-frequency bridge which is not sensitive to frequency change.

wire lines or two coaxial cables. This circuit does not depend on the line lengths being one-quarter wave for balance. The line lengths shown do establish the midband frequency as far as the input impedance is concerned. Here again a choice of characteristic impedance equal to MR ohms yields an input impedance of $M^2R/2$ ohms and a value of M equal to $\sqrt{2}$ gives the broadest input impedance characteristic. The circuit of Figure 10 with M equal to unity is described by Westcott.[4] The authors have found that a choice of M equal to $\sqrt{2}$ yields a much more desirable input impedance versus frequency characteristic.

For higher frequencies, particularly the ultra-high frequencies, the authors have found the bridge or diplexer of the slotted type shown in Figure 11 to be the simplest and most easily balanced. This is the same diplexer which has been used so very successfully to diplex a Turnstile antenna, a method of operation which permits both picture and sound transmitters to be fed to a single Turnstile.
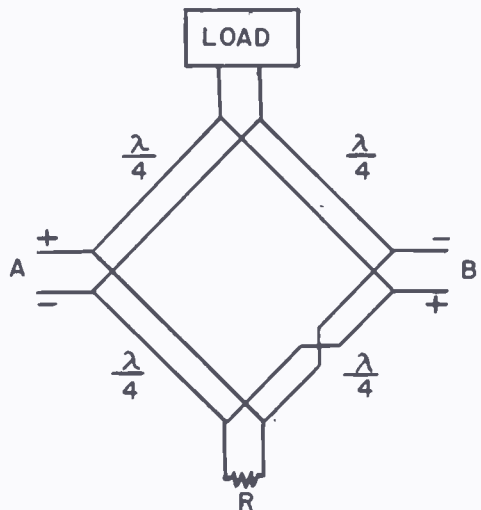
Fig. 10 — A bridge arrangement which is balanced to ground.

[4] C. H. Westcott, "Transmission-Line Bridge," *Wireless Engineer*, Vol. XXV, No. 298, p. 215, July, 1948.
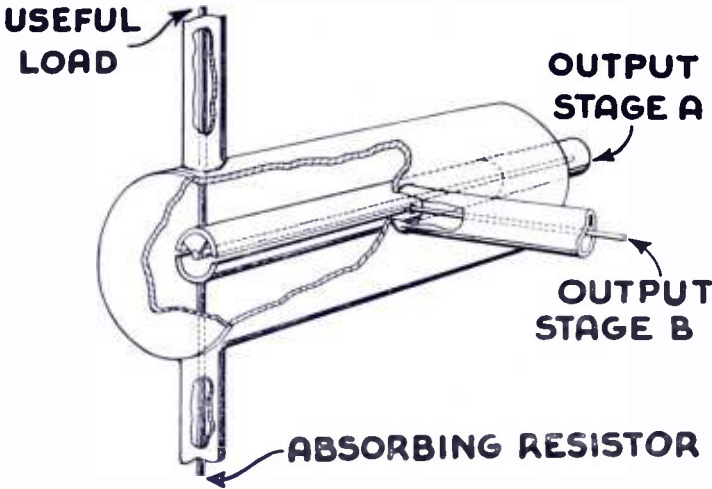
Fig. 11 — A slotted diplexer or bridge which is particularly useful at ultra-high frequencies.

AN ULTRA-HIGH-FREQUENCY TELEVISION TRANSMITTER APPLYING THE BRIDGE ARRANGEMENTS FOR MULTIPLE OPERATION OF OUTPUT STAGES

To demonstrate the principle of multiple operation, the authors developed a television transmitter using four RCA-5588 tubes in the output stages, to produce a total power of 400 watts. The circuit arrangement is shown in Figure 12. A crystal oscillator operated at a frequency of 7870.4 kilocycles. When the output of this oscillator was passed through suitable frequency multiplying stages, the exciter developed a signal with a frequency of 212.5 megacycles. At this point, the chain was broken into four parallel paths. Each path then led through two doubler stages to furnish driving voltage to a final amplifier stage at 850 megacycles. Three diplexers and three absorbing resistors were used as shown to combine the four output stages into a
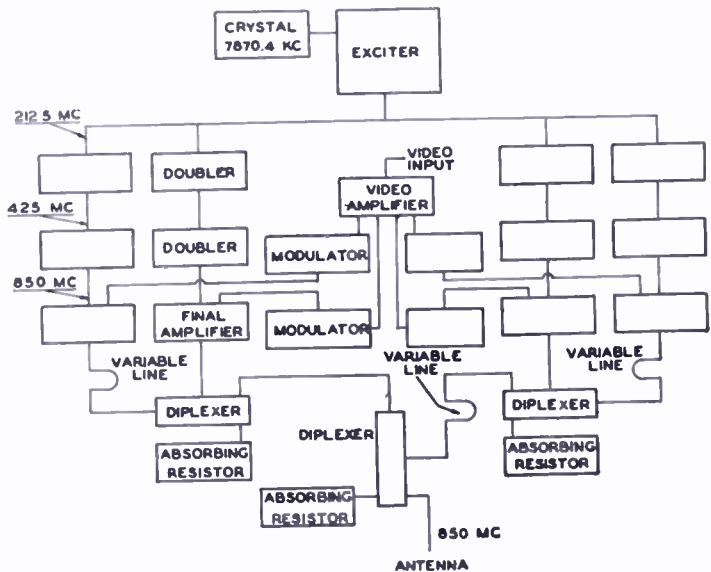
Fig. 12—A block diagram of an 850-megacycle television transmitter using the principle of multiple operation.

single antenna. Each final amplifier was cathode modulated from a single picture source to accomplish simultaneous modulation of each final amplifier. The diplexers were of the type shown in Figure 11.

Three variable length lines, shown in Figure 12, were used to provide phase adjustment of the radio-frequency carriers. These variable length lines were constructed of overlapping tubes, adjusted by a rack and pinion. Experience has indicated that these lines may be omitted and small phase adjustments accomplished by slight tuning of amplifier tank circuits in the doubler stages.
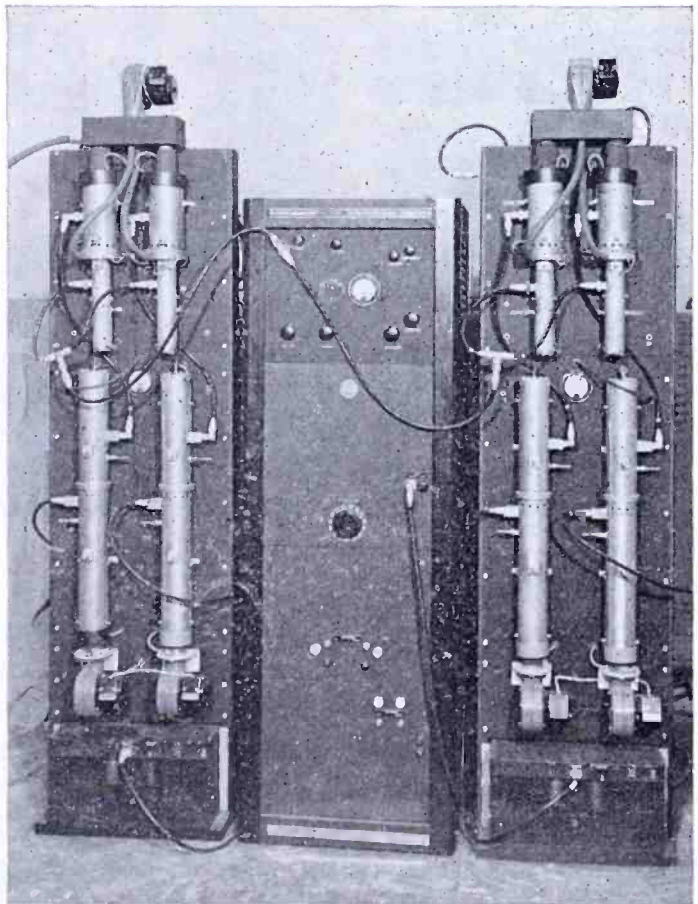
Fig. 13—The experimental 850-megacycle television transmitter.

One or more of the final amplifier stages could be turned on or off without reaction on the remaining stages. Signal strength in the antenna circuit changed according to theoretical predictions.

The transmitter is shown in Figures 13 and 14, with the diplexers visible in Figure 14. This transmitter was operated under an experimental license as Station W3XCY in Washington, D. C. in the fall of 1948 and has since been in operation in Princeton, N. J., as Station KE2XAY for the purpose of providing further test data in connection with the principle of multiple operation.
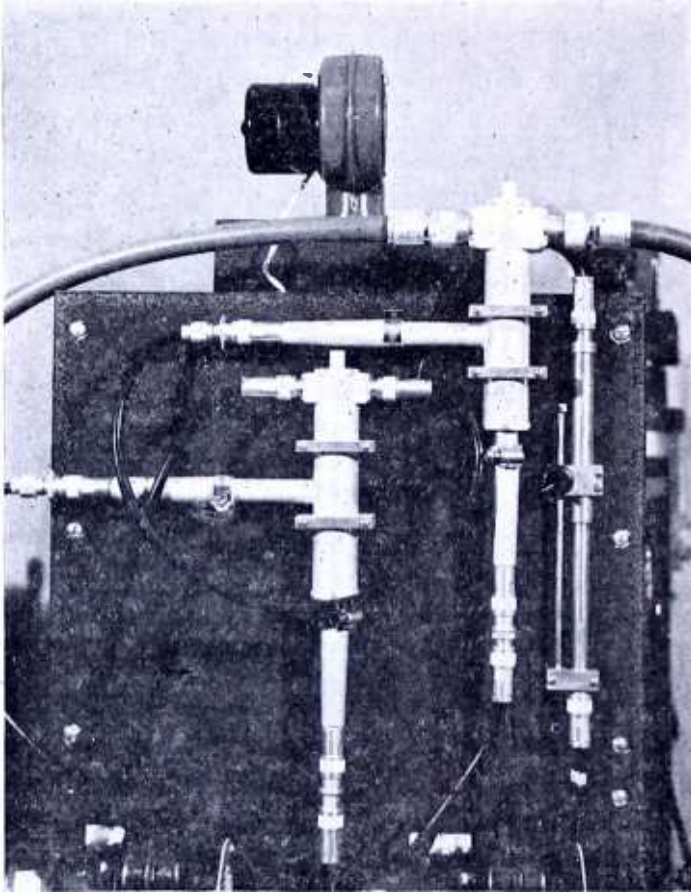
Fig. 14—Another view of the 850-megacycle television transmitter, showing the diplexers used in securing multiple operation.

CONCLUSION

A combining network has been developed which allows transmitting tubes to be operated simultaneously into a common load without inter-action between tubes and without reduction in band width. A transmitter has been constructed which shows the method to be applicable to the design of ultra-high-frequency transmitters for television use. While relatively low power tubes were used in this demonstration transmitter, it was done for purposes of expediency and to demonstrate the principle of operation. The authors do not mean to imply that several small tubes are to be preferred to one large one. However, when the largest tube available does not approach the power desired for the particular service under consideration, multiple operation with diplexing circuits seems to be indicated as a practical solution.

A RECORD CHANGER AND RECORD OF COMPLEMENTARY DESIGN*

By

B. R. Carson†, A. D. Burt† and H. I. Reiskind‡

Summary—This paper describes a record changer and a record designed to accomplish fundamental improvements in the phonograph. The practical and theoretical limitations of other systems have led to the establishment of design and performance objectives for a new system. The accomplishment of these objectives as they apply to the 45-rpm record changer and record is discussed.

Introduction

WHEN the phonograph and record industries had their commercial beginnings almost a half century ago in the Camden machine shop of Eldridge Johnson, the size of the records and the rotational speed of the turntable were established on a basis which was largely a matter of experimental compromise based on the state of the art at that time. The standards which finally evolved (10 and 12 inches for diameter, and 78.26 revolutions per minute for speed) have remained unaltered for many years. While there have been some noteworthy refinements of record making and playing techniques, these were accomplished within the pre-established limitations of record size, groove dimensions, and turntable speed. Record changing mechanisms, in particular, have been handicapped by the requirement that they accommodate both 10-inch and 12-inch records. Further, records have been costly, fragile, subject to wear, of limited quality, and inconvenient to handle and to store. The result of this situation has been that a truly satisfactory performance seemed to be unattainable within the limitations of the system as established. It, therefore, became evident that an entirely new approach was indicated, namely, one specifically designed to eliminate these problems and limitations.

Experience has shown that any major change in an existing, long-established system must do more than solve problems related to the accomplishment of just satisfactory performance. It might be stated that such a change can only be justified if its accomplishments reason-

ably approach the requirements of an ideal system. About seventeen years ago there began a program aimed at a fundamental improvement in the reproduction of recorded music. Unhampered by any previous restrictions, attempt was made to develop an ideal method of bringing recorded music into the home. Factors of cost and convenience to the customer, playing time, record life, freedom from distortion and numerous technical considerations were established with the "ideal" being the objective. Some nine years of research and experimentation culminated in a new record playing means which, after eight more years of testing and refinement, finally emerged in a record changer and record to be discussed in this paper.

Factors Influencing Record Changer Design

As long as records were played manually, the two diameters (10-inch and 12-inch), the variations in the dimensions of the starting, lead-in, lead-out, and tripping grooves, and the variations in record thickness were comparatively unimportant. However, with the advent of automatic record playing devices, these dimensional variations became important since they seriously complicated the mechanical design of record changers. Over a period of years the record industry standardized the physical dimensions of the 10-inch and 12-inch records. Unfortunately, standardization did not solve the fundamental problems which confronted the record changer designer, since they are associated with the basic design of the record. Considered solely from the standpoint of record changer design, these problems are due to the fact that the record changer is required to operate with records:—

1. Of constant thickness over their entire area,
2. Having a small center hole,
3. Of two different diameters.

All record changers require a selecting mechanism of some sort to separate individual records from the stack. With records of constant thickness, all practical designs of selecting means cause some damage to the edge, body, or center hole area since the records have to be forced apart or slid one against the other to effect selection. With a small center hole and the heavy records commonly used, high stresses occur around the center hole and record damage results. A small center hole does not permit record stability on the spindle without edge support or complex spindle mechanism. Further, the small hole makes loading difficult.

The necessity of accommodating records of two diameters brings

about record changer complexity and customer inconvenience. The very magnitude of the diameters makes the record changing mechanism big. Cabinets to accommodate such record changers and also provide record storage become large and therefore expensive. The relatively high rotational speed of the turntable necessitates the use of speed reducing mechanism to give the record changer time to perform its several functions reliably.

DETERMINATION OF THE RECORD CHANGER DESIGN

The solution to these problems, when considered against the ideal of minimum space requirements, minimum cost, maximum performance, and maximum convenience of customer operation, dictated a major change from existing practice. After study of the problem, it was concluded that a simple record changer design could be accomplished if the following conditions were satisfied:—

1. A large center spindle housing the separating means. It was found that a 1½-inch diameter spindle would house an economical selecting mechanism, provide adequate record stability on the spindle without external support, and make for easy loading of records on the spindle.

2. Provision of a depressed area around the center hole of the record so that the selector blades would not touch the records during the separating operation.

3. A single diameter record having fixed dimensions for starting and tripping grooves so as to reduce record changer complexity.

4. A small diameter record, rotating at a low speed. The small diameter results in a reduction in size of the record changer. It also permits a decrease in length of the tone arm and thus decreases its inertia. This decreased inertia of the tone arm permits a reduction in cycle time since the low-inertia tone arm may be moved more rapidly during the change cycle. Then by choice of a low rotational speed, it is possible to accomplish the complete change cycle in one revolution of the turntable. The cycling cam may thus be made integral with the turntable, eliminating the speed reducing means. With such a design it was found by experiment that the cycle time could be reduced to 1.2 seconds as a minimum, but that some additional time was desirable to provide reliable operation. It was therefore concluded that satisfactory operation could be expected at any turntable speed below 50 revolutions per minute.

DESCRIPTION OF RECORD CHANGER

Figures 1, 2, 3 and 4 show the principle of operation of the record selector mechanism. Two oppositely positioned and inwardly retractable shelves (*a* in the four figures) are located in the spindle. In direct association are two outwardly rotatable blades (*b* in the four figures) spaced at a definite distance above the shelves. The design is such that in the playing position (Figures 1 and 2) the shelves extend beyond the periphery of the spindle supporting the record stack and the blades are housed within the spindle. The cycling operation causes the blades to rotate out beyond the outside diameter of the spindle just before the shelves are retracted. Figures 3 and 4 show the positions of the blades and shelves just after the record has been selected. To
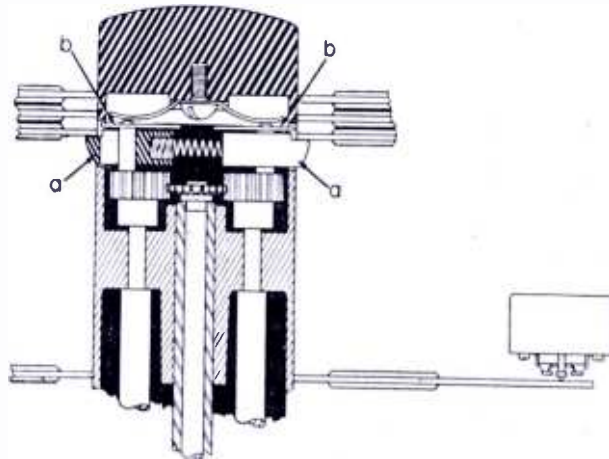
PLAYING POSITION
[OUT OF CYCLE]
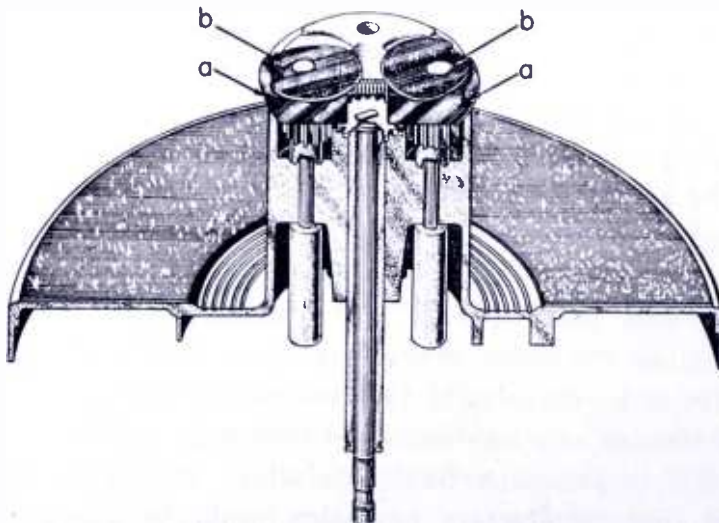
Figs. 1 (above) and 2 (below)—Principle of operation of large spindle record changer using depressed center area records — changer in playing position.

complete the cycle, the shelves move back to their normal extended position just before the blades are rotated back to their normal retracted position.

As may be seen from Figures 1 and 3, the center area of the record about the center hole is depressed on either side of the record, so that, when two records are stacked together, an air space is provided between them. The dimensions of the depressed area and the spacing between the record changer shelf and blade are such as to bring the center of the blade in line with the center of the air space provided between the records. This design offers a distinct advantage in that the records are not knived or otherwise separated, or even touched by the blade during the selecting operation. The aforementioned shelves
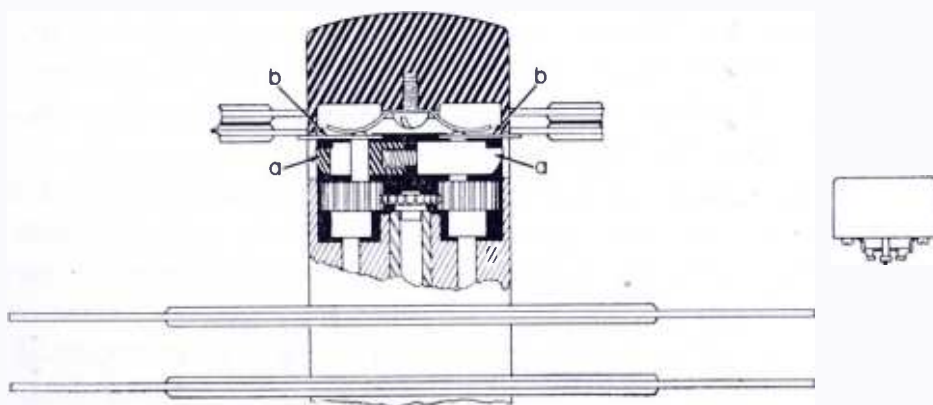
SEPARATING POSITION
[ONE HALF THROUGH CYCLE]
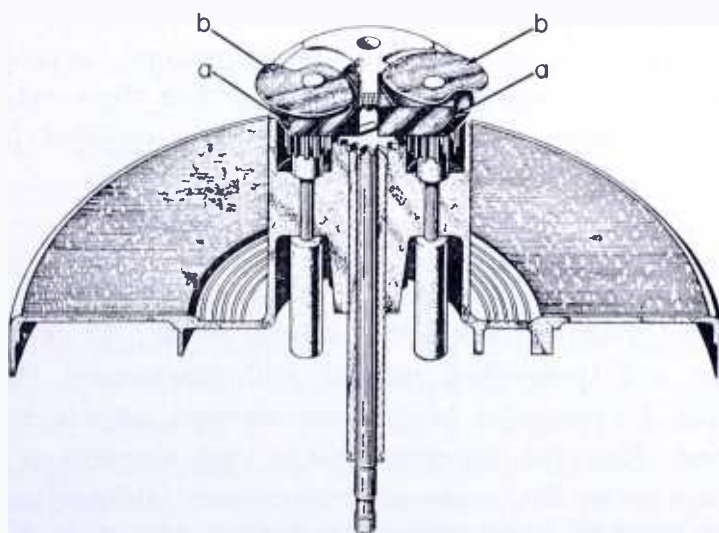
Figs. 3 (above) and 4 (below)—Principle of operation of large spindle record changer using depressed center area records — changer half way through change cycle.

are held outward by a spring and their lower portion is shaped so as to be contained within the body of the spindle. This design causes the shelves to be cammed inwardly when records are removed from the turntable. The large diameter spindle and record center hole result in easy loading of the record changer, and the retractable shelves result in easy unloading.

The pickup unit, tone arm and tripping mechanism are designed to be consistent with the requirements of the record. (See SELECTION OF DESIGN PARAMETERS below.) The tripping mechanism is of particular interest. It is designed so that the work to trip the mechanism into cycle does not require any appreciable force between the reproducing stylus and the record groove. A small lever having very low friction is moved, by the inward motion of the tone arm, to a specific position where a lug on the turntable picks up the lever and causes it to cam the mechanism into cycle. The work of putting the mechanism into cycle is thus supplied by the moving turntable rather than by the pickup stylus and record groove.

Record changer tripping mechanisms of the common diameter type are well known for their reliability of operation and simplicity of design. With this type of trip the record can end in a concentric finishing groove rather than the $\frac{1}{8}''$ eccentric finishing groove commonly employed. This is of a very definite advantage as the finishing grooves can be cut with same cutting stylus as used for recording and without removing the wax or lacquer from the recorder. Furthermore, the complexity of cutting the eccentric finishing groove on the recorder has resulted in the practice of transferring the wax or lacquer to a special machine designed for that purpose. This practice requires extreme care to prevent damage to the recording and to produce a quiet groove as another cutting stylus is used. For these reasons a common diameter type of tripping mechanism was selected for the record changer.

FACTORS INFLUENCING RECORD DESIGN

With the requirements established for an improved record changer, consideration was given to the existing record design. 78 revolution-per-minute ten- and twelve-inch records still represented the best available medium for recorded home entertainment considering convenience and cost. However, improvements in such elements as record breakage, surface noise, life, consumer convenience (storage and handling), and reproduction quality were highly desirable. Record breakage has been a problem to manufacturer, dealer and consumer ever since the present design of 78 revolution-per-minute records was adopted.

The advent of synthetic thermoplastic resins made it possible to produce unbreakable records.[1] However because of high raw material costs, such resins were not economically practical to use for commercial records.

Record surface noise has also come in for its share of criticism and has a long history. In the past, many factors have contributed to its production; recording materials, cutting styli, metallizing and plating processes, and record compositions. Over the years, improvements in all these elements have been made until, in recent years, the particle size of the mineral fillers used in commercial record compositions has largely determined surface noise. The introduction of the lightweight jewel-point pickup and the frequency balance developed for home instruments just before the war, further reduced the apparent loudness of record surface noise and resulted in quite acceptable performance on home instruments. However, for reproduction with increased frequency ranges, the surface noise of the average commercial record composition is higher than desirable. The elimination of mineral fillers from shellac type compositions is impractical since it results in an extremely brittle, poor-wearing composition; even a reduction in filler particle size seriously increases brittleness. Further, the noise reduction that can be obtained by using the finest available fillers does not approach that obtained with unfilled resins. The solution to this problem is the same as breakage; the use of unfilled synthetic thermoplastics and again economics enters. Toughness, which results in greatly increased record life, is another characteristic of many of the synthetic thermoplastic resins that makes their use desirable in phonograph records.

It is obvious that for an economic solution of these problems, the amount of material in the record should be reduced and that this is compatible with the requirements of improved record changer design and reduced storage space. A drastic reduction in record size was therefore indicated as a major design requirement.

High fidelity reproduction of recorded sound has been an engineering objective for some time. It has been shown[2] that with a purely acoustical system (where noise and distortion are absent) a definite preference is shown for an unrestricted frequency range. It appeared desirable, therefore, in designing a completely new record, that the parameters be chosen so as to reduce inherent distortion to a minimum.

---

[1] F. C. Barton, "Vitrolac Records," *Jour. Soc. Mot. Pic. Eng.*, Vol. 18, pp. 452-460, April, 1932.

[2] H. F. Olson, "Frequency Range Preference for Speech and Music," *Jour. Acous. Soc. Amer.*, Vol. 19, No. 4, pp. 549-555, July, 1947.

The major causes of distortion in disc records have been: first—polishing the metal parts in the plating operations, and second—the inability of the stylus to trace the recorded groove. The effect of the first has been recognized for some time[3] and, through the development of improved plating methods, completely eliminated in good manufacturing plants. The second, tracing distortion, has also been known for many years[4,5] but comparatively little work has been done to evaluate it subjectively. Rather than attempt to determine a "tolerable" value, it was considered advisable to limit distortion to less than "perceptible" and a specification was therefore set up that:

> "The maximum tracing distortion in any portion of the record shall not be more than is barely perceptible to trained observers when the record is reproduced through a wide-range audio system having overall response extending to 15 kilocycles."

The two-frequency method of distortion testing has proven to be a powerful tool[6,7]. Investigations carried on during the past several years have shown that this method gives excellent correlation between measurements, theory and listening tests[3]. It was therefore decided to use it in this work. In cooperation with engineers of the National Broadcasting Company, voice and music recordings were made and processed under a variety of conditions. Intermodulation frequency bands (400-4000 cycles) were recorded at the beginning and end of each record at a velocity equal to the peak velocity of the speech or music. It was observed that in all cases where the intermodulation distortion measured less than 10 per cent, no aural distortion was perceptible when the records were reproduced on wide-range equipment, while conditions which produced measured values above 10 per cent also produced aural distortion. It was also observed that distortion was audible in the last third of well-processed high-quality 12-inch commercial records when similarly reproduced, and that a comparable condition obtained with transcription records.

[3] H. E. Roys, "Intermodulation Distortion Analysis as Applied to Disc Recording and Reproduction Equipment," *Proc. I.R.E.*, Vol. 35, No. 10, pp. 1149-1152, October, 1947.

[4] J. A. Pierce and F. V. Hunt, "Distortion in Sound Reproduction from Phonograph Records," *Jour. Acous. Soc. Amer.*, Vol. 10, pp. 14-28, July, 1938.

[5] W. D. Lewis and F. V. Hunt, "A Theory of Tracing Distortion from Phonograph Records," *Jour. Acous. Soc. Amer.*, Vol. 12, pp. 348-365, January, 1941.

[6] J. G. Frayne and R. R. Scoville, "Analysis and Measurements of Distortion in Variable-Density Recording," *Jour. Soc. Mot. Pict. Eng.*, Vol. 32, p. 648, June, 1939.

[7] J. K. Hilliard, "Distortion Tests by the Intermodulation Method," *Proc. I.R.E.*, Vol. 29, pp. 614-620, December, 1941.

In their paper on tracing distortion, Lewis and Hunt[5] give an equation (Equation (30), page 356) for the distortion resulting when two frequencies are combined. It has been shown[8] that

Per Cent Intermodulation =

$$\frac{\dfrac{\pi^2}{4} \dfrac{r^2 u_1^2 u_2}{S^4} \left[(2f_1 + f_2)^2 + (2f_1 - f_2)^2 \right]}{u_2 - \dfrac{\pi^2}{2} \dfrac{r^2 f_2^2}{S^4} \left(\dfrac{u_2^3}{2} + u_1^2 u_2 \right)} \times 100$$

$u_1 =$ lower frequency lateral velocity (peak)

$u_2 =$ upper frequency lateral velocity (peak)

$r =$ reproducing stylus radius

$f_1 =$ lower frequency

$f_2 =$ upper frequency

$S =$ groove velocity

Figure 5 shows the calculated intermodulation distortion for 12-inch commercial and 16-inch transcription records using the following conditions:

	12-inch Commercial Records	Transcription Records
Revolutions per minute	78.26	33⅓
Diameter of music start (inches)	11½	15½
Diameter of music end (inches)	3¾	7½
Reproducing stylus radius (mils)	3.0	2.3
Peak recording level (centimeters per second)	22.	14.

It will be noted that in both cases the intermodulation distortion exceeds 10 per cent part way through the record and confirms the listening tests. The cumulative evidence of these tests resulted in the decision to select design parameters for the new record such that the intermodulation distortion at the innermost groove would not exceed 10 per cent.

---

[8] H. E. Roys, "Analysis by the Two-Frequency Intermodulation Method of Tracing Distortion Encountered in Phonograph Reproduction," Equation (7), p. 268 of this issue.

Selection of Design Parameters

From the equation shown earlier, it may be seen that for a given distortion a reduction of reproducer stylus radius allows a reduction in linear speed of the record and therefore a smaller record. (This is obvious since keeping the ratio of r^2 to S^4 constant requires that $S \propto \sqrt{r}$.) Experience dictated the choice of a 1-mil radius as the minimum for the reproducer stylus and a 90-degree, 0.25-mil bottom radius groove. Since stylus and record wear are dependent on pressure, it was considered desirable to reduce the vertical stylus force. A sapphire was chosen for the stylus in order to achieve long life.

Tests have proven that with a vertical force of five grams, stylus life is equal to or better than that obtained in the present day home phonograph. Unfilled vinyl records reproduced under these conditions show life far in excess of commercial filled compositions played on present day phonographs.
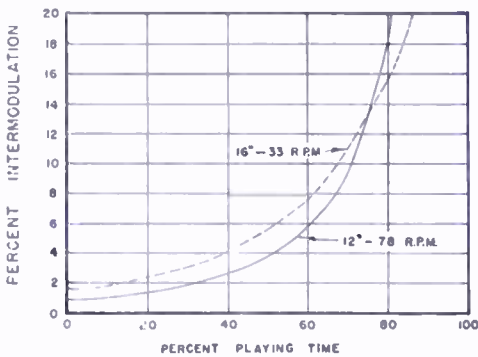
Fig. 5—Calculated intermodulation distortion of commercial and transcription records.

The remaining parameters to be determined in order to design the record are peak recording level, maximum permissible grooves per inch and playing time.

The selection of the first two must be largely a compromise of several factors. Increasing recording level increases signal-to-noise ratio. However, it also increases record size for a given playing time, both because a higher terminal linear speed is required for a given quality level, and because the maximum permissible number of grooves per inch must be decreased. Experience indicated that with the improved processing methods available and the use of unfilled vinyl compositions, highly satisfactory signal-to-noise ratios could be obtained with a peak recording level of 14 centimeters per second (about 4 decibels below standard 78 revolution-per-minute records). Any further reduction in recording level (and therefore signal-to-noise ratio) was considered inconsistent with the objectives of high quality reproduction. This recording level permitted the selection of 275 grooves per inch as a maximum. These selections of recording level and reproducing stylus size resulted in the requirement that the minimum terminal linear speed be 11.5 inches per second for 10 per cent intermodulation distortion in the innermost groove.

While playing time is primarily determined by artistic and commercial considerations rather than technical, it must be discussed here since, in the final analysis, it determines record size. It was pointed out earlier that the use of one size of record, rather than the two now common, would make possible a material improvement in the cost and reliability of the record changer. Unfortunately for the design engineer composers have found it necessary to write selections as short as 1½ minutes and longer than two hours. To determine if any common denominator existed that would minimize musical breaks without being too wasteful for short selections, an analysis was made of the music in the Victor Catalog. Because of its great size, only that portion of the catalog known as "The Music America Loves Best" was chosen.
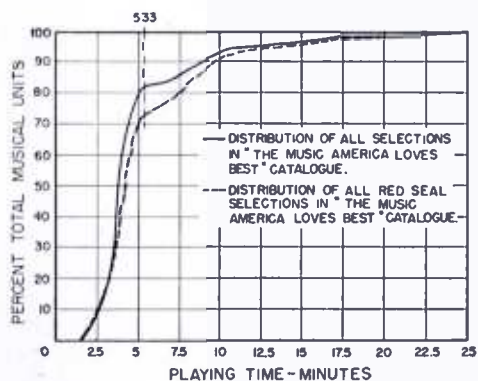
Fig. 6—Playing time distribution of "The Music America Loves Best" catalog, showing the percentage of music units shorter than any specific time.
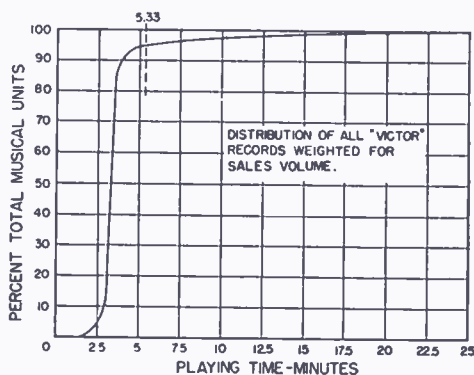
Fig. 7—Playing time distribution of all Victor records showing the percentage of musical units sold which are shorter than any specific time.

This consists of those selections, other than current popular tunes, that show continued popularity. The playing time of each musical unit was determined and cumulative distribution curves prepared. By "music unit" is meant a selection or a part of a work, such as a movement of a symphony, that was written to be played without a break. The "Red Seal" or "classical" portion of this catalog was analyzed separately, since it is in this type of music that long units are most frequently encountered. Distribution curves of both the "classical" portion and the entire "Music America Loves Best" catalog are shown in Figure 6. It is rather surprising to note that 70 per cent of the musical units in the "classical" portion of this catalog are less than five minutes long. It would appear from this that undue weight may, at times, have been given to the importance of long playing time.

Current popular tunes which make up the bulk of record sales must be considered in any determination of record playing time requirements. Figure 7 shows the playing time distribution of all Victor

records weighed for sales volume. In this case it will be noted that 96 per cent of all Victor musical units sold have a playing time of less than five minutes. It is felt that, had industry figures been available, an even higher percentage would have been obtained. It was decided, as a result of this analysis, that a playing time of a little more than five minutes, or the same as the 12-inch 78-revolution-per-minute record, would represent the best compromise.

The parameters necessary to design the record have therefore been chosen as follows:

    1. Playing time—5⅓ minutes
    2. Terminal linear velocity—11½ inches per second.
    3. Maximum grooves per inch—275.

SELECTION OF ROTATIONAL SPEED AND RECORD DIAMETER

The record diameter to satisfy the above parameters may be determined for any rotational speed from the relations

$$P = \frac{D_0 - D_i}{2R} N \quad \text{and} \quad S_i = \frac{\pi D_i R}{60},$$

where P = playing time in minutes

        D_0 = start of recording, inches diameter

        D_i = end of recording, inches diameter

        R = rotational speed, in revolutions per minute

        N = grooves per inch

        S_i = terminal linear velocity, inches/second.

A study of the characteristics of the record changer indicated that it would be desirable to provide a landing area of ⅛-inch radial length outside the music grooves. By combining the above equations, substituting the desired parameters and adding the landing area, the relation between rotational speed and diameter may be expressed as

$$D \text{ (record diameter in inches)} = 0.0388\, R + \frac{219.6}{R} + 0.250 \ .$$

While it has been shown[9] that the minimum diameter record is obtained when $D_0 = 2D_i$ or $R = \sqrt{\dfrac{60\, S_i N}{2\pi P}}$

[9] J. P. Maxfield, U. S. Patent #1,637,082, filed January 17, 1925.

other factors must also be considered in selecting the rotational speed. The criteria involved are:

1. The record should contain a minimum volume of material (this, as will be shown later, is not necessarily consistent with the minimum diameter constant thickness record).
2. The rotational speed should be selected considering optimum mechanical performance of the record changer.
3. An adequate label area (to provide identification of the music) should be included.

Another factor evolved from the fact that the records are separated from the center and that record changer operation therefore is not affected by the thickness of the outside edge of the record. It is then possible to reduce the thickness of the record in the music area and consideration was given to the design shown in Figure 8(b). This design has two major advantages; first, the volume of material re-

quired for a given diameter of record is appreciably reduced; and second, the music areas of adjacent records do not touch in normal handling or playing. This reduces the probability of scuffing the music grooves. It is, however, necessary that the radial length of the label area (A_R, Figure 8(b)) be large enough to provide adequate driving force and preclude the possibility of slippage.
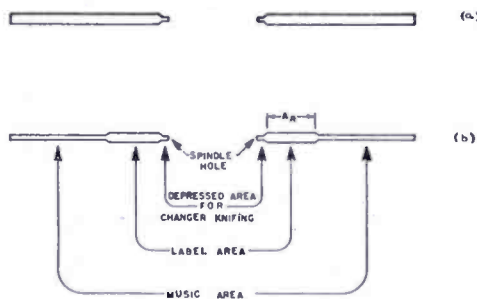
Fig. 8—Cross section of 45 revolution-per-minute records. (a) Constant thickness, (b) Depressed music area.

Earlier in this paper it was pointed out that the maximum permissible rotational speed of the record changer was 50 revolutions per minute, and that to secure reliability of operation, a somewhat lower speed would be desirable. A speed of 45 revolutions per minute was tentatively adopted as a practical maximum. The desirability of making use of one of the two existing standard speeds (33⅓ and 78.26 revolutions per minute) was recognized, and consideration was therefor given to these three speeds (33⅓, 45 and 78.26 revolutions per minute).

Considering the record changer only, no serious disadvantages occur from operation at 33⅓ revolutions per minute. However, as will be shown later, major disadvantages are encountered from the standpoint of the record.

Again considering the record changer alone, operation at 78 revolu-

tions per minute would require the addition of a speed reducing mechanism to enable it to function reliably. This would complicate and add cost to the design and was therefore considered undesirable unless very large advantages would accrue from the standpoint of the record.

A study was then made of the volume of material in the record and the radial length of the label area for different rotational speeds. Considerable study of the changer and of record manufacturing operations resulted in the following decisions:

1. A radial distance of 3/16-inch is desirable between the last music groove and the concentric finishing groove to provide reasonable tolerance for the trip mechanism and allow a very slight interval between the last note and actual tripping.

2. A radial length of 3/16-inch is desirable between the concentric groove and the outside diameter of the thicker center section. This is necessary partly to provide for normal variations in label diameter and label centering but also to allow the metal stampers to be formed to the reverse of the record contour after electro-forming. This radial length is sufficient to prevent distortion of the concentric groove by the forming operation and to allow for a taper between the thin and thick sections.

3. The depressed center area of the records which forms the air space in which the selector blades operate should have a radial length of approximately ⅛ inch.

The radial length of the label results from the equation

$$A_R = \frac{1}{2}\left(\frac{60 \, S_t}{\pi R} - 2.531 \right)$$

or using the previously chosen parameters

$$A_R = \frac{109.9}{R} - 1.265.$$

The radial length of the label and the volume of material in the record for the depressed music area design (Figure 8(b)) are shown in Figure 9. It will be noted that at 78 revolutions per minute the radial length of the label is approximately 1/10 inch and it is therefore obvious that even though the record volume approaches a minimum at this speed, such a record design is impractical since the label area is much too small either to provide adequate traction or to allow space

for printing. It will also be noted that as the speed is reduced the volume of material required increases rapidly and that therefore 33⅓ is a much less efficient speed than 45 revolutions per minute.

Careful testing of large numbers of records played with a pickup of 5 grams stylus force under different conditions of stylus and record wear, developed the fact that the minimum label diameter to provide adequate traction was 3½ inches. This required that the minimum diameters of the concentric finishing groove and the last music groove be 3⅞ inches and 4¼ inches respectively. This diameter provides a radial length of about ⅞ inch, which is sufficient for printing requirements.

Figure 10, curve b, shows the relation between record volume and rotational speed of the depressed music area record with a label diameter of 3½ inches. Minimum volume for this design is obtained
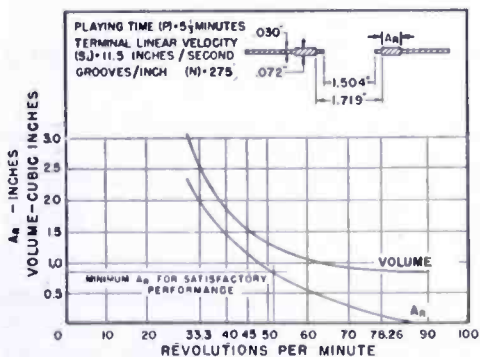
Fig. 9—Relation of record volume and radial length of label to rotational speed—depressed music area design.
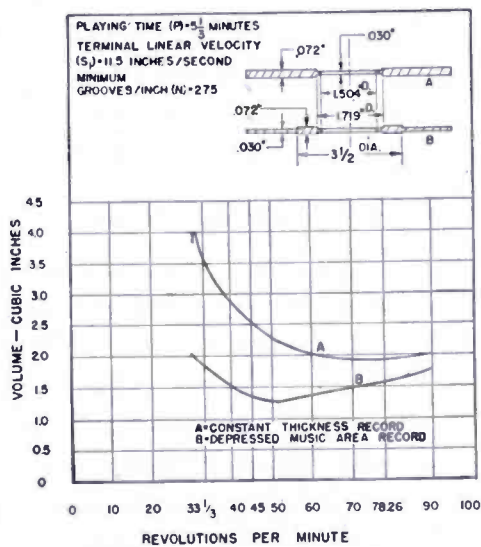
Fig. 10—Relation of record volume to rotational speed for (A) Constant thickness record, (B) depressed music area record with constant diameter label.

at 51½ revolutions per minute. Since the diameter of the last music groove cannot be decreased below 4¼ inches, operation at higher speeds requires an increase in the outer diameter of the record and results in the essentially straight portion of the curve. While it is true that increased terminal velocity is obtained and results in a theoretical reduction in distortion, it is considered that this is an academic point since no subjective improvement would be noticed.

It was pointed out earlier that 45 revolutions per minute had been tentatively selected as the maximum practical rotational speed for the record changer. At this speed, the minimum music diameter is 4.9 inches. By utilizing the remaining music area of the record (to the

limiting diameter of $4\frac{1}{4}$ inches), a playing time of $7\frac{1}{4}$ minutes is possible with a terminal groove velocity of 10 inches per second. While the reproduced quality at the inside of such a record will be inferior to the criterion of 10 per cent intermodulation distortion, it is, however, superior to that obtained from 78.26 revolution-per-minute records. Such a design might be of interest for use with "popular type" or "children's" records, since it provides quality adequate for this type of program material.

Figure 10 also shows the volume of the constant thickness record as a function of revolutions per minute. It is interesting to note that the depressed music area record has a smaller volume for any speed above 31 revolutions per minute than the constant thickness record at its theoretical optimum speed.

The advantages and disadvantages of the three speeds in record designs that satisfy the previously established parameters ($5\frac{1}{3}$ minutes playing time, 275 grooves per inch, $11\frac{1}{2}$ inches per second terminal velocity) may be listed as follows:

78.26 revolutions per minute

1. A speed reducing mechanism must be incorporated in the record changer increasing its complexity and cost.
2. The minimum volume depressed music area design is impractical. If the constant thickness design is used, more material is required than is used by the depressed music area design at the other speeds under consideration.
3. The label area in the constant thickness minimum volume design is entirely inadequate.
4. The diameter of a $3\frac{1}{2}$-inch label depressed music area record would be $\frac{5}{8}$ inch greater than at 45 revolutions per minute and require 17 per cent more material.

$33\frac{1}{3}$ revolutions per minute

1. The record diameter must be increased by $1\frac{1}{4}$ inches and the volume of material by 33 per cent over that required at 45 revolutions per minute. The limiting groove velocity of 11.5 inches per second is reached at a diameter of 6.6 inches. This diameter is greater than the diameter of the first music groove of the 45 revolution-per-minute record.

45 revolutions per minute

1. The volume of material in the record is less than that required at either $33\frac{1}{3}$ or 78.26 revolutions per minute.

2. With the depressed music area design, which reduces record scuffing, the diameter is 6⅞ inches compared to 8⅛ inches at 33⅓ or 7½ inches at 78.26 revolutions per minute.

3. The record changer design provides reliable performance.

4. A playing time of 7¼ minutes may be obtained at a reduced terminal quality (though superior to 78 revolution-per-minute records).

Based on the above considerations, the speed of 45 is obviously superior to either 78.26 or 33⅓ revolutions per minute, and was therefore chosen for this system.

RECORDING AND REPRODUCING CHARACTERISTICS

The recording characteristic used for these records is shown in Figure 11. For use in calibrating reproducing systems, a frequency
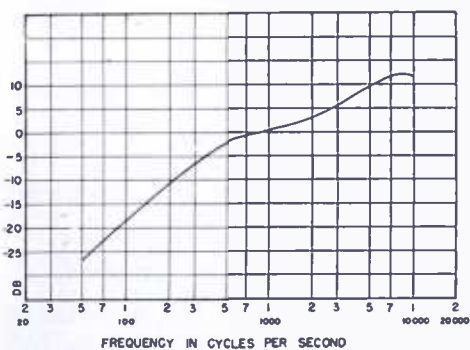
Fig. 11—Overall frequency characteristic (microphone pre-amplifier to cutting stylus) used in recording 45 revolution-per-minute records.
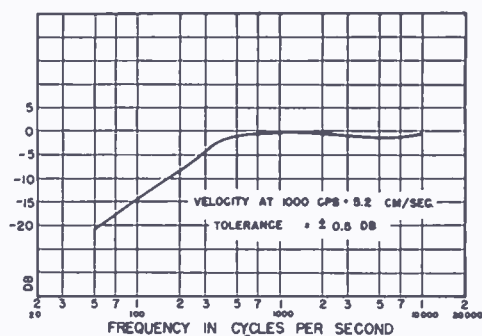
Fig. 12—Average calibration of 45 revolution-per-minute test record 12-5-31.

record has been prepared. Calibrations by both the variable speed turntable and the light pattern methods were found to be in good agreement. The calibration of the record is shown in Figure 12.

CONCLUSIONS

In Figure 13, the finished record changer and records are pictured. It is believed that the system described here represents a basic advance in disc record reproduction. The desired improvements in quality, both noise and distortion, size reduction, long life, simplified and rapid record changer operation and elimination of record breakage have been achieved. This record meets the requirements for high fidelity reproduction.
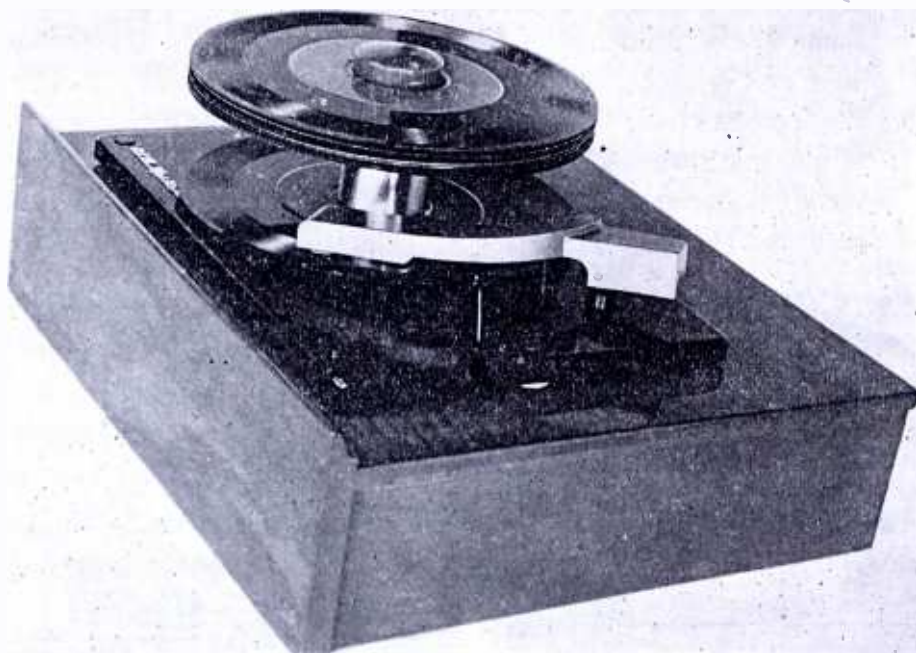
Fig. 13—Record changer and mounting with records in operating position.

ACKNOWLEDGMENT

DEVELOPMENT AND PERFORMANCE OF TELEVISION CAMERA TUBES*

By

R. B. JANES, R. E. JOHNSON AND R. S. MOORE

Summary—Three new television camera tubes have resulted from an intensive development program extending over several years. These are (1) the well-known 2P23 image orthicon which is especially suited for remote pickups where a wide range of illumination is encountered and versatility is of the greatest importance; (2) the 5655 image orthicon which is capable of producing pictures of studio quality when the illumination can be controlled; (3) the 5769 image orthicon which may be used for either remote or studio pickups. The construction and operation of these tubes are described in detail. The development of image orthicons is traced by an examination of their limitations and the improvements which have resulted from changes in their construction.

INTRODUCTION

DURING the past fifteen years a number of television camera tubes have been developed. The first to be considered here is the iconoscope[1]. This tube is still used for the transmission of motion picture films and has been extensively used in studio work. When carefully used with the needed complicated correcting circuits, bias and frame lighting, it is capable of producing a high-quality picture. Its resolution is satisfactory and its half-tone response is good. It is also completely stable at all light levels. However, in order to obtain satisfactory pictures, incident light levels of 800 to 1,200 foot-candles are needed on the subject. Even under these conditions "dark spot" and "flare" can be troublesome, particularly for rapid changes of illumination and for scenes that contain dark areas near the bottom of the picture. Although the signal-to-noise ratio may be satisfactory at lower light levels, shading becomes nearly impossible to correct unless the scene is evenly lighted. Lowering the beam current to decrease dark spot is of little help because the signal output drops nearly as rapidly as the dark·spot and the tube becomes unusable because of low signal-to-noise ratio.

The type of iconoscope presently available is the 1850-A, which has a diameter of 6¾ inches and a mosaic area of 17 square inches.

---

[1] V. K. Zworykin and G. A. Morton, TELEVISION, John Wiley and Sons, Inc., New York, N. Y., 1940.

The signal output in microamperes for a typical tube is shown in Figure 1 plotted against illumination on the mosaic in foot-candles for two values of beam current. These two values of 0.15 and 0.2 micro-ampere are, in general, the values used in operation. As the operating personnel become more conscious of dark spot and flare, they tend to use the lower value of beam current. However, some may prefer the greater signal and signal-to-noise ratio obtained from the higher value. With a beam current of 0.2 microampere and a mosaic illumination of 6 foot-candles, a signal-to-noise ratio (assuming 3×10^{-3} micro-amperes of amplifier noise) of 60 can be obtained. Because this is

"peaked-channel noise", i.e., noise of high frequency which conse-quently appears to the eye as fine grain, it is not objectionable; it is equivalent to a flat-channel noise ratio[2] of 180 to 1. The use of "high peaking" to improve resolution may reduce this ratio to about 100 to 1. It should be noted that these signal-to-noise ratios are expressed as the ratio of highlight signal to root-mean-square noise.

Fig. 1 — Typical signal output characteristics for iconoscopes type 1850-A and type 1848.

Another type of iconoscope which has been manufactured is the 1848. It has a 4½ inch diameter and a mosaic area of a little over 6 square inches. The signal output in microamperes is shown in Figure 1 plotted against illumination on the mosaic in foot-candles for 0.15 and 0.2 microampere beam current. At 6 foot-candles and with the same amplifier noise as for the 1850-A, the value of signal to peaked-channel noise is about 30 to 1. To many users this perform-ance has not been acceptable when compared with that of the 1850-A. The 1848, however, has certain advantages over the 1850-A. When the amount of mosaic illumination is the same, the depth of focus of the 1848 is better because only about ⅓ as much total light is needed to obtain the same mosaic illumination. Not only is the shading of the 1848 usually somewhat easier to handle, but its smaller size makes the final equipment less bulky. Because of its size the 1848 has been used to a certain extent in portable outdoor equipment but here its low sensitivity has not made it popular. In motion picture applications where design factors of size and depth of focus are not important, the

---

[2] For a comparison of peaked- and flat-channel noise, see O. H. Shade, "Electro-Optical Characteristics of Television Systems", Part I, *RCA Review*, Vol. IX, No. 1, pp. 32-34, March, 1948.

1850-A, because of its greater signal-to-noise ratio, appears to be the logical choice. For studio work, the choice between the 1848 and 1850-A is more difficult.

There have been many proposals for increasing the sensitivity of iconoscopes to make them more useful for studio and perhaps outdoor pickup. One involves the use of an image stage of multiplication.[3] This proposal permits the use of a continuous photocathode instead of a photosensitive mosaic with a possible increase in photosensitivity of 2 or 3. However, in order to keep the tube to a practical size, the photocathode area has to be small, usually about three square inches in size. This size requires the use of a small diameter lens. Although the depth of focus improves, there is little, if any, reduction in the light level needed, because the signal from a pickup tube depends on the total amount of light striking the photosensitive surface rather than upon the illumination per unit area. There is, however, a gain of four or five because of the secondary-emission gain at the mosaic or target. Focusing the electron image from the photocathode to the mosaic is tricky even with magnetic focusing with the result that a loss of resolution and distortion of the picture is likely. Also, care must be taken to prevent interaction between the image-focusing coil and the beam-deflecting coil. Because the gain in sensitivity of such a tube is small unless very high photosensitivities can be obtained, it has not been considered as desirable as the tubes described later in this article.

Another possibility for increasing sensitivity of the iconoscope is the use of signal multiplication. This method involves collecting the secondary emission from the iconoscope mosaic and putting it through a multiplier. This procedure is very difficult with the iconoscope because the large area from which electrons must be collected adds spurious signals. Furthermore, neither image multiplication nor signal multiplication offers any hope of eliminating an inherent fault of the iconoscope—the dark spot.

The next pickup tube to be developed was of the orthicon type[4], the now obsolete 1840. In design and operation this tube was a tremendous departure from iconoscope tradition. Instead of the use of a high-velocity electrostatically focused beam to discharge the mosaic, a low-velocity beam focused by a long magnetic field was used. The vertical deflection is magnetic but in order to avoid the need for high

---

[3] H. A. Iams, G. A. Morton, and V. K. Zworykin, "The Image Iconoscope", *Proc. I.R.E.*, Vol. 27, No. 9, pp. 541-547, September, 1939.

[4] A. Rose and H. A. Iams, "The Orthicon", *RCA Review*, Vol. 4, No. 2, pp. 189-199, October, 1939.

power the horizontal deflection is electrostatic. Because the beam strikes the mosaic at a velocity of only one or two volts in the lighted areas and not at all in the dark areas, there is no secondary-electron redistribution and, consequently, no dark spot. Also, the sensitivity of the tube is greater because of more efficient collection of the photoelectrons emitted during storage. A curve of signal output is given in Figure 2. As the curve shows, the signal-to-noise ratio is the same at 1 to 2 foot-candles on the mosaic as at 6 for the iconoscope. In addition, even lower light levels can be used because of the absence of dark spot. Part of this sensitivity is usually used to provide greater depth of focus because of the smaller mosaic size (4 square inches). The tube was very useful in picking up scenes where the incident illumination was only 100 to 200 foot-candles.

Fig. 2—Typical signal output characteristics for orthicon type 1840.

Although the 1840 has two advantages over the iconoscope: freedom from dark spot and greater sensitivity, it has many disadvantages. The iconoscope is stable at all light levels, but the orthicon will tend to charge up in areas of bright illumination because the mosaic potential is not limited to small values. The "sharpness" of the picture in still scenes approaches that transmitted by the iconoscope, but in moving scenes the tube loses resolution much more readily because, in part, of its much longer storage period. Scenes reproduced by the orthicon, moreover, show a smaller range of intermediate grays than the same scenes reproduced by the iconoscope. The lack of any detail in the low lights is particularly noticeable and is the result of the linear signal output characteristic of the orthicon as compared to the non-linear output characteristic of the iconoscope which saturates at high light levels.

In order for the orthicon to handle the very large signals from local highlights, the grays are pushed down into the noise. It is nearly impossible to transmit any information in dark areas of the picture when other parts are bright. This limitation is a severe disadvantage at baseball or football games when shadows begin to fall across the field. Although the orthicon is useful because it can transmit scenes which the iconoscope cannot, its versatility is severely limited.

Further development work has been done to overcome some of

these limitations. Best results were obtained from a tube of the orthicon type which uses all-magnetic scanning and a 5-stage signal multiplier. With all-magnetic scanning any difficulty with "sharpness" of the picture on stationary scenes disappeared, although on moving scenes the same loss of resolution was still apparent. The tube had greater sensitivity than the 1840 because of the use of the signal multiplier, but such factors as instability and the inability to transmit the darker areas in scenes were not improved. The greatest advantage of the tube is that its resolving power for still scenes exceeds that of any other tube. The signal-to-noise ratio was also adequate for light levels of 100 foot-candles but not all of the most severe limitations of orthicons were overcome in this developmental tube.

GENERAL DESCRIPTION OF THE IMAGE ORTHICON

The most important development in camera tubes for the past several years has been the now-well-known image orthicon. This tube,
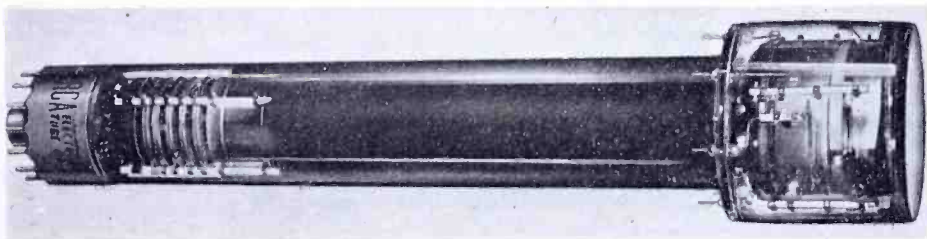
Fig. 3—Typical image orthicon.

on which fundamental work was done by Rose, Law, and Weimer[5], appears to offer the most promise, both for outdoor and studio pickup. The development has led to three commercial types, the 2P23 for poorly lighted, remote pickups, the 5655 for studio work, and the 5769 for general use.

The image orthicon, pictured in Figure 3, combines the features of several of its predecessors. It includes in one envelope an image section, a target or mosaic assembly, low-velocity scanning of the orthicon type, and a 5-stage signal multiplier. Before its performance is described, a brief summary of its construction and operation will be given.

The tube itself consists of a three-inch-diameter image section and a two-inch-diameter scanning and multiplier section. The over-all length is 15½ inches. This size has proven to be a good compromise between camera performance and portability. Although a smaller size

---

[5] A. Rose, P. K. Weimer and H. B. Law, "The Image Orthicon — A Sensitive Television Pickup Tube", *Proc. I.R.E.*, Vol. 34, No. 7, pp. 424-432, July, 1946.

would make a lighter-weight camera possible, the loss in performance would be objectionable. For convenience, the image orthicon may be described in three parts — one covering the image section, one the scanning section, and one the multiplier section. Figure 4 is a schematic drawing of the tube.

The image section contains a semi-transparent photocathode on the inside of the face plate, a grid (grid No. 6) to provide an electrostatic accelerating field, and a target which consists of a thin glass disc with a fine mesh screen very closely spaced to it on the photocathode side. Focusing is accomplished by means of a magnetic field produced by an external coil, and by varying the photocathode voltage. Light from a scene being televised is picked up by an optical lens system and focused on the photocathode which emits electrons from each illuminated area in proportion to the intensity of the light striking the area. The
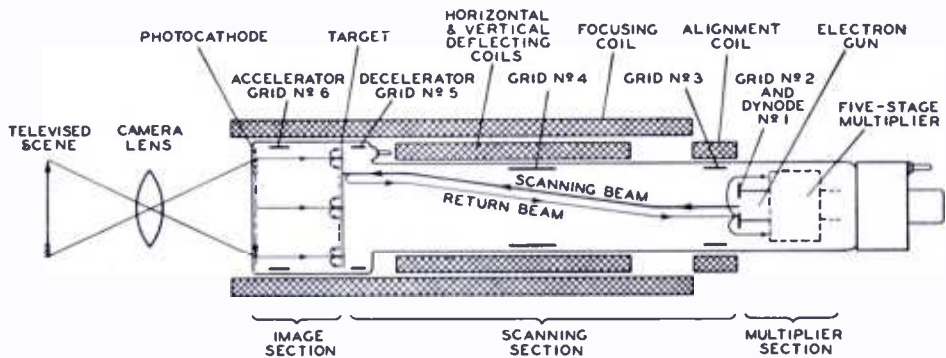
Fig. 4—Schematic arrangement of image orthicon.

streams of electrons are focused on the target by the magnetic and electrostatic fields.

On striking the target, the photoelectrons cause secondary electrons to be emitted from the glass. The secondaries thus emitted are collected by the adjacent mesh screen which is held at a definite potential of 1.5 to 2.5 volts above that of the scanned side of the glass target. The potential of the glass disc, therefore, is limited for all values of light and stable operation is achieved. Emission of the secondary electrons leaves on the photocathode side of the glass a pattern of positive charges which corresponds with the pattern of light from the scene being televised. Because the target is a very thin sheet of partially conducting glass, the charge image is also seen on the scanned side of the target by the scanning beam.

The electrons are emitted from the gun through a small defining aperture and are focused into a fine beam by means of the magnetic field of an external focusing coil and the electrostatic field of grid No. 4. Magnetic deflection is used to scan the target. Grid No. 5 serves to

adjust the shape of the decelerating field between grid No. 4 and the target in order to obtain uniform landing of the scanning beam over the entire target area. The electrons stop their forward motion at the surface of the glass and are turned back, except when they approach the positively charged portions of the pattern and are deposited on the glass. This deposition leaves the glass with a negative charge on the scanned side and a positive charge on the photocathode side. These charges will neutralize each other by conductivity through the glass in less than the time of one frame.

The electrons turned back at the target form the return beam which has been amplitude modulated by absorption of electrons at the target in accordance with the charge pattern. The returning modulated beam strikes the first dynode which as a result, emits secondary electrons. These secondaries in turn are drawn down through a series of multipliers of high secondary emission which increase the signal a 1000 fold. The increased signal is finally collected at the anode of the multiplier and fed to a pre-amplifier through a resistance of the order of 10,000 to 30,000 ohms.

As this brief summary shows, the image orthicon has all the advantages of the orthicon together with the added advantages of greater sensitivity due to the image section, and of greater stability due to the mesh screen near the target. Its sensitivity is about 100 times greater than that of the iconoscope and it is stable over a light range of several hundred to one. These features make it very versatile and especially useful for outdoor scenes. Without any change in adjustment, the tube can handle a high light scene and then be used for a scene in deep shadow. It is also far superior to the orthicon in reproducing scenes containing both high lights and shadows.

This gain in sensitivity, particularly for the earlier image orthicons, was achieved only with a loss of signal-to-noise ratio and useful resolution. Also, the half-tone response differs from that of the orthicon. Why the tube possesses these properties can probably be best explained by a detailed examination of its construction and a description of how each section of the tube contributes to these properties. Image orthicons now available include the 2P23, 5655 and 5769. Because the 2P23 is the oldest and most widely used, it will be described first.

CONSTRUCTION AND OPERATION OF THE 2P23

Photocathode

The photocathode of the 2P23 consists of a semi-transparent layer of the cesium-silver-oxide type. As in the 1840 orthicon, the layer must

be semi-transparent because the light strikes it from one side and photoelectrons are emitted from the other. However, the 2P23 has the advantage over the 1840 in that this layer can be continuous. Higher sensitivities are possible with such a layer, the sensitivity to incandescent light being of the order of 10 to 20 microamperes per lumen compared to about 3 for the 1840. (This figure for the 1840 includes the loss in the semi-transparent signal plate needed in that tube.) It has proven difficult, however, to obtain a reproducible color response from tube to tube in the 2P23. Figure 5 shows the spectral response characteristics for typical low and high sensitivity tubes. Individual tubes may have spectral response characteristics anywhere between these two extremes. The high infrared sensitivity of some 2P23 tubes leads to very good sensitivity when low-temperature incandescent lighting is used but also leads to peculiar renditions of certain colors or objects. In outdoor use, for example, green grass appears to be white or very light gray. A fairly good color response with a two-fold or more loss of sensitivity can be obtained by the use of fluorescent lighting or by proper filters with incandescent light. Care must also be taken in the processing of the tube to keep the conductivity of the photosurface fairly high. Otherwise, for high light scenes, the picture will be distorted geometrically because of the voltage drop in the photosurface.

Fig. 5—Approximate spectral sensitivity characteristics of image orthicon type 2P23.

The size of the target limits the size of the picture on the photocathode to a rectangle with a diagonal of about 1.6 inches. This size is much smaller than that of any of the other pickup tubes so far discussed and means that available short-focal-length lenses having a rather small diameter may be used. Part of the increased photosensitivity, therefore, will have to be used to obtain greater depth of focus. Because of the high sensitivity of the tube the exchange of depth of focus for sensitivity is not a disadvantage. On the other hand, the use of small lenses makes it much easier to use a revolving turret containing three or four lenses of different focal length. The use of such a turret has become universal in the latest camera design.

Focusing of electron image

The use of a magnetic field to focus the emitted photoelectrons onto the target gives uniform resolution with little distortion. In general, this resolution is much higher than that of other sections of the tube. When a magnetic field of about 75 gauss and a photocathode voltage of about —400 volts are used, the electrons will make one "loop" in going from the photocathode to the target. Only a small improvement in resolution is possible at higher fields and voltages, but a serious deterioration of the resolution and signal occurs with a photocathode voltage below —200 volts. The voltage on grid No. 6, a cylindrical-type grid nearest to the photocathode, is adjusted to minimize picture distortion (in particular, the so-called "S" distortion) and to improve corner resolution. Best results are obtained when the voltage of this grid is about 80 per cent of the photocathode voltage. A lower grid No. 6 voltage produces "S" distortion in one direction and a higher voltage, "S" distortion in the opposite direction. With the focusing coil usually used with the 2P23 there is a small reduction in the image size at the target. Because the image section is near the end of the focus coil where the magnetic field is flaring, the image size at the target has a diagonal of about 1.4 inches for a 1.6 inch diagonal on the photocathode.

Image section crosstalk

Although the image section is not a serious limit to the resolution of the 2P23 directly, the resolution in this section can be seriously impaired by leakage of the strong magnetic deflection fields from the scanning yoke into the image section. The leakage fields cause a vibration of the image electrons from the photocathode around their normal path during the 1/30-second storage time on the target and, as a result, blur the charge image. Because the storage time decreases with increased illumination, this "crosstalk" effect on resolution is more serious at low light levels on the photocathode. Since the tube is generally used so that the high lights are just out of the storage range, "crosstalk" control is a serious problem. Although the effect may be reduced within limits by going to high magnetic fields and photocathode voltages, more than 75 gauss is not practical in portable equipment because of the added scanning power needed. Other approaches to the problem offer better practical solutions.

Magnetic shielding to reduce crosstalk

A number of methods will reduce "crosstalk" difficulty, all of which, in one way or another, involve the shielding of the image section from

the stray magnetic fields of the deflecting coils. One method which has worked out quite well is to wrap the outside of the external focusing coil with some magnetic shielding material such as silicon steel or Mu metal. In order to avoid high absorption of scanning power, the shielding material should be thin strips and wound in several layers separated by insulating material. For the same reason, the strips making up each layer should not be too wide. The use of such a winding tends to pull the stray flux lines away from the photocathode into the shielding material. Resolution gains of as much as 200 lines have been achieved by this method.

Loss of resolution due to initial velocities of emission

There is another cause that can impair the resolution in the image section: the initial emission velocity of the photoelectrons from the photocathode. This problem has been analyzed in a paper by H. B. DeVore[6]. The loss of resolution is most noticeable when blue light is used to illuminate the scene being televised and the photocathode of the camera tube has red and infrared response. Under such conditions the initial emission velocities of the photoelectrons are appreciable and can visibly limit the resolution. Because many 2P23's have high red and infrared response this limitation applies chiefly to this tube. The photocathodes used in the 5655 and the 5769 on the other hand, have little red and no infrared response, so the loss of resolution is not appreciable. In scenes where there is considerable "blue" light such as in skylight, the resolution of the 2P23 will be inferior.

Target mesh structures

When light causes photoelectrons to be emitted from the photo-cathode, the image section focuses these photoelectrons onto the target mesh assembly. This assembly is truly the heart of the tube and is the main reason for its amazing performance. This type of target differs from any which have been used before in commercial pickup tubes in that the signal is impressed on one side and taken off the other. Such a structure is called a two-sided target or mosaic.

There have been many attempts in the past to fabricate a successful two-sided target. The patent literature is evidence of many types, most of which have proven to be too difficult to manufacture. The use of two-sided mosaics was first attempted in connection with icono-scopes. An image section was also used and the mosaic or target consisted of an insulated (generally enameled) wire mesh in which

---

[6] Henry B. DeVore, "Limiting Resolution in an Image Orthicon Type Tube", *Proc. I.R.E.*, Vol. 36, No. 3, pp. 335-346, March, 1948.

the openings were closed with metal plugs. Such tubes actually operated, but the difficulty of making a target free of blemishes such as pinholes and surface irregularities proved almost insurmountable. If low-velocity scanning is used, such a target would also have too high a capacitance and lead to bad lag effects under low lighting conditions. The two-sided problem was solved through an entirely different approach*. This consisted of a very thin glass membrane of controlled resistance together with a fine mesh screen mounted close to it on the image or photocathode side. Such a glass membrane can readily be made free of pinholes and bad surface imperfections. Many problems, however, had to be solved in order to obtain a practical assembly that was free enough from other imperfections to be used in commercial television.

Target resistivity

The operation of the tube makes several demands on the glass target. The photoelectrons striking the image side of the glass through the mesh openings give rise to secondary electrons that are collected by the mesh. At low light levels the potential of the glass target does not ordinarily reach that of the mesh screen during the 1/30-second storage time. In order to obtain good resolution for such a storage time, the lateral leakage or leakage between elements is kept as low as possible, by the use of a high-resistance glass and by the use of a target as thin as possible. When the scanning beam approaches the scanned side of an element that has been charged, the beam "sees" the same potential as that of the charged side because of the thinness of the target. Electrons are deposited from the beam on the target until the potential returns to nearly the equilibrium potential under the beam when no light is present. After the beam leaves the element, the positive charge on the image side and the negative charge on the scanned side must combine in less than a frame time or 1/30th second. Otherwise, a "sticking picture" which will be of opposite polarity from the original picture will be seen if the picture is moved. If the picture is stationary the signal output from lighted areas will decrease. If the glass resistivity is very high the signal output for a stationary picture will, after a few scans, fall nearly to zero. If the resistivity is only slightly too high, the sticking picture will disappear as the tube warms up in the camera because the resistivity of glass falls about 2 or 3 to 1 for each 10-degree-centigrade rise in temperature. A satisfactory upper limit for the glass resistivity has been found to be about 9×10^{11} ohms per centimeter measured at 20 degrees

---

* See reference (5).

centigrade temperature. For the 2P23 a temperature of about 35 degrees centigrade at the target is needed to eliminate picture sticking entirely, when the glass has this value of resistivity.

The "sticking picture" puts a top limit to the resistivity of the glass. Mechanical handling puts a lower limit of about 0.0001 inch on the thinness of the target. A lower limit for the glass resistivity, necessary to keep lateral leakage low, is approximately 3×10^{11} ohms per centimeter measured at 20 degrees centigrade. With such a resistivity the tube can be operated at a temperature of about 65 degrees centigrade before serious loss of resolution sets in. At higher temperatures the resistivity will fall below 10^{10} ohms per centimeter, and a serious loss of resolution will occur particularly at low lights.

Target surface effects

Besides the mechanical difficulties of making a glass target of sufficient thinness and of the necessary strength, many other problems arise during the processing of the tube. In order to obtain sensitivity, the image side should have as high a ratio of secondary-electron emission as possible. Enough cesium reaches the image side of the target during processing of the photocathodes to give a ratio of 4 or 5 to 1. At times, however, too much cesium gets on the image side, the lateral leakage falls, and the target becomes "leaky", i.e., the resolution of the picture is poor. Such leakage, of course, shows up first at low light levels, where storage is complete over a frame time. During operation or shelf life, it sometimes happens that enough cesium will migrate to the target to cause "target leakage". This trouble can be minimized by operating the tube at the lowest possible temperature. (A minimum lower limit would, of course, be 35 degrees centigrade because of the target resistivity problem.)

Target contact-potential effects

There are other changes which occur in the glass that are largely the same in all tubes. During operation the scanned area on the beam side changes slowly in contact potential with respect to the unscanned area. With uniform light on the photocathode, overscanning will show the previously scanned area to be, in general, darker than its surroundings because the contact potential of the scanned area changes with respect to the thermionic cathode. When the tube is placed in operation the maximum area of the target which makes the picture magnification smallest should be used, because later it will be impossible to increase the area used because of the white edges that will show in the picture.

In addition to the "sticking picture" that can occur when the tube

· target is too cold, another type of sticking can develop. If the camera is stationary and the tube "looks at" a strongly lighted area for a period of time (5 minutes or more), a sticking picture of the same or most often of opposite polarity can develop. This trouble is more likely to occur when the tube is cold, but it will develop in all tubes if the picture is left stationary too long, regardless of temperature. Unlike resistivity sticking, the sticking or "burning-in" disappears slowly. This type of sticking can be avoided only by care in handling the camera. In order to remove a sticking picture once it has been developed, point the camera at a flat lighted scene and operate it for several hours.

Target secondary emission

One last point should be mentioned before leaving the rather complicated glass target. Whereas the image side should have high secondary emission to produce as much signal as possible, the scanned side should have low secondary emission. Although the scanning beam approaches the target at nearly zero velocity and is turned back in the dark areas, it strikes in the lighted areas with a velocity corresponding to one or two electron volts. Even at such potentials, some secondary emission will occur. Any such emission increases the number of electrons returning to the multiplier from the lighted areas and thus increases the noise, because more beam current is needed to discharge lighted areas. The secondary emission of the scanned side is reduced by evaporating on it a very light layer of some metal such as silver which has low secondary emission. The reduction in the amount of noise is readily noted after such an evaporation. During operation there is generally a slow increase in the secondary emission so that after several hundred hours of operation the picture becomes more noisy. A re-evaporation of silver at this time by the manufacturer will once more reduce the secondary emission.

Loss of scanning

It is important to note what damage can be done to the target by a stationary beam. With light on the photocathode and a sharply defined beam, a hole can actually be started in the target. If the beam is defocused the bombarded area may become either darker or lighter than the rest of the target. Removing the multiplier voltage will not, of course, be of any help because the beam still will strike the target. Removal of the photocathode voltage is only a partial solution because light can pass through the photocathode and strike the target, which being nearly always somewhat photosensitive, will charge up and allow the beam electrons to land. The only positive method of preventing

damage in case of scanning failure is to bias off the beam or target. This precaution should always be taken when the equipment is not being monitored.

Target-to-mesh spacing — close spacing

For proper functioning of the glass target, a fine mesh screen the potential of which can be varied is needed on the image side. This mesh serves a two-fold purpose—as an element to increase the capacitance of the target, and as a limiter to prevent the target from charging to high potentials such as occurs in the 1840 orthicon. The maximum amount of charge that can be deposited on an element of the target depends on the capacitance of the element and the potential of the mesh above the potential of the scanned side of the target. This
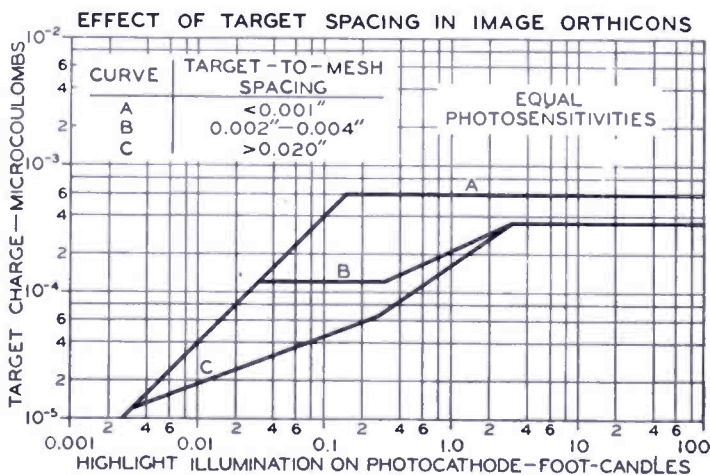
Fig. 6 — Effect of target-mesh spacing in image orthicons.

maximum charge also determines the maximum signal-to-noise ratio of the tube. At low light levels the target element never reaches mesh potential so that the charge rises linearly with light. In this region the tube has the same characteristic as a regular orthicon, namely, a loss of resolution for scenes in motion. For a spacing of the mesh to the target much less than the diameter of a picture element (for a 500-line picture this diameter is somewhat less than 0.002 inch), the charge rises linearly with light until it becomes limited by the capacitance and mesh voltage. When this limit is reached the charge caused by the high lights cannot increase, although that due to the low lights continues to rise. Curve A, Figure 6 shows an extremely simplified ourve of the charge developed on the target during the time for a complete picture frame plotted against the illumination on the photocathode for a target-to-mesh spacing of less than 0.001 inch. Ordinarily, it would be assumed that the picture contrast would decrease

rapidly after the high light signal becomes constant. Redistribution of secondary electrons from the bright areas onto the lowlight areas, however, tends to preserve the contrast even when the high lights are well above the knee. If an intense small area of light, such as a direct reflection of the sun from the windshield of a car, is present in the picture, this redistribution gives rise to a disturbing black border around the light area. The image orthicon cannot faithfully transmit such a scene. Also, in pictures with large black and white areas the contrast is preserved only at the area boundaries when the high lights are well above the knee. In such pictures the blacks appear gray although the resolution and "snap" may appear to improve because of the outlining of the edges.

The redistribution of secondary electrons makes a valuable contribution to the resolution of moving objects. As the picture moves, the border around the high lights discharges the high light signal at its former position in less than a frame time so that only the latest image is seen when the picture is scanned. To obtain the best picture contrast and the most natural-appearing picture (that is, with blacks "black" instead. of gray) the high lights should be run just at the knee of the curve. To take advantage of the better resolution in motion some loss of contrast is usually taken by operation somewhat above the knee.

Target-to-mesh spacing — wide spacing

If the spacing between the mesh and the target is much greater than the diameter of an element, the charge curve becomes more complicated. In the case of the close-spaced target, the capacitance of an element to the mesh greatly exceeds the "free space" capacitance of the element itself. For a wide-spaced target the "free space" capacitance is larger than its capacitance to the mesh. For low lights the charge will rise linearly with light until the point is reached where it is limited by the product of the capacitance of the element to the mesh and the mesh voltage. This point, as curve C of Figure 6 shows, is lower than the equivalent point for a close-space target because of the much smaller mesh-to-target capacitance of each element. However, as the light is increased above this point, the charge of the wide space target can increase because of the free-space capacitance of each element. This increase is at a slower rate because the discharge of the first part of each lighted section also partially discharges sections beyond it. Because the "free-space" capacitance is largely between neighboring elements, the edges of a lighted section both horizontally and vertically will produce a greater signal because of the partial dis-

charge of nearby elements. As the light is increased, these partially discharged elements are more and more recharged before the beam reaches them. Finally, a point is reached where the free-space capacitance of an element and its mesh voltage limits further increase. As curve C of Figure 6 shows, this point occurs at a light level a hundred times above that needed to reach the first knee of the curve. The effect in the transmitted picture of the free space or interelement capacitance is that the blacks are outlined with a white edge at the transition to white, occurring at the right end and the bottom of the blacks when the beam is scanning from black to white or gray.

Experience has shown that the proper target-to-mesh spacing depends on what the tube is expected to do. Very wide spacings, where the interelement capacitance is the only one that needs to be considered, has the advantage of taking the mesh completely out of focus. However, because the signal-to-noise ratio is too small to be useful except at very high light levels and because the resulting white edges are very annoying, the useful range is limited to intermediate and close spacings. The best spacing is determined by actual tests.

Tests of target-to-mesh spacing

Tubes with a wide variety of target-to-mesh spacings have been tested. For very wide spacings in the order of 0.020 inch to 0.080 inch the signal is far too low and the white edges are annoying. Spacings of the order of 0.004 inch to 0.008 inch produce useful tubes, but even in this range the signal-to-noise ratio is borderline and the white edges are still troublesome. A range of 0.002 inch to 0.004 inch was finally selected as the best for the 2P23 and the 5769. The white edges have largely disappeared and the signal-to-noise ratio is improved. Such tubes are of "intermediate" spacing, since the spacing is only slightly larger than an element diameter. Nearly all the properties are those of close-spaced targets as curve B, Figure 6 shows; only at high lights is there an increase in charge due to "wide-spaced" characteristics. In general applications this increase is not evident and can largely be overlooked. The properties of tubes with "close spacings" will be discussed in connection with the 5655.

Target potential

With regard to the mesh, two further points are important. As we have seen, one of the items limiting the target charge is the capacitance of an element, which is determined by the spacing of the target to the mesh. For the 2P23 and 5769 the spacing is in the range of 0.002 inch to 0.004 inch. The target charge is also determined by the ex-

ternally applied mesh potential. Experience has shown that the optimum potential depends to a great extent on the picture content. For scenes with flat, even lighting, especially when the scene illumination remains constant, the mesh potential can be set in the range of 2 to 2.5 volts above the point where the picture is cut off. (In actual experience, this cutoff point is at −1.0 to −2.0 volts with respect to the thermionic cathode.) Above 2.5 volts the picture will be stable but may have a peculiar "differentiated" appearance. When the potential difference between the target and the mesh is more than 2.5 or 3 volts, the beam will be bent by the more positive areas of the high lights and a premature discharge of these areas will occur. This action is known as beam bending and gives a picture reproduction inconsistent with the charge distribution on the target. When the tube has to pick up a scene with high lights and then one that is largely in the shadows, a mesh potential range of 1.5 to 2.0 volts is preferable. In general, the mesh potential should be kept as high as possible, without endangering picture fidelity in order to obtain the best signal-to-noise ratio.

Development of a suitable mesh

The problem of a satisfactory mesh has been the subject of a long development program. The first experimental image orthicon tubes were made with woven screens. Attempts to obtain woven screens that had uniformly spaced wires proved unsuccessful. In addition, the finest weave that could be obtained with a usable opening was only 325 to the inch which severely limited the resolution because the size of the picture on the target has a diagonal of only 1.4 inches. Various methods of electroplating mesh have been tried in the past, but, although they are capable of producing mesh of up to 400 lines per inch, the open area is small, generally not over 25 per cent for the finer meshes. A new method of producing an electroplated mesh, was originated at RCA Laboratories[7], and has been developed to a degree that meshes of 500 openings to the inch with 50 to 65 per cent open area can be produced. Special methods of mounting and tightening the mesh, which is only a few tenths of a mil thick, were worked out. Because the mesh is so close to the target, it is nearly at the point of focus of the image electrons. If a wide-band amplifier is used, this mesh can be seen by looking carefully at the kinescope picture. With the standard television bandwidth it is just noticeable. However, a problem of a "beat" pattern does arise. Because the picture height on

---

[7] H. B. Law, "A Technique for the Making and Mounting of Fine Mesh Screens", *Rev. Sci. Instr.*, Vol. 19, No. 12, December, 1948.

the target is approximately an inch, there will be about 500 wires of mesh to a picture height. These wires can beat with the 525-line scanning frequency to produce a low-frequency beat pattern. In the construction of the tube this possibility is reduced to a minimum by mounting the mesh at a 45-degree angle to the scanning beam. Even in this case some regions of the picture may show beat patterns, particularly in highly lighted areas. These patterns, also can be eliminated at a sacrifice in resolution, by slightly defocusing the beam. In operation the beat pattern can be minimized by scanning as large a part of the target as possible so as to keep the picture height at a maximum.

Electron gun

The gun which produces the beam consists of a thermionic cathode which is held at ground potential, a control grid (grid No. 1) and an accelerating grid (grid No. 2). Grid No. 2 contains a small aperture about 0.002 inch in diameter which serves to define the beam. After emerging from this aperture, the beam with a velocity corresponding to about 300 volts, passes through the grid No. 3 region which is also at 300 volts. It then emerges into the focusing section which consists of a uniform electric field of about 200 volts and a magnetic field in the direction of the beam of 75 gauss. Any component of the electron beam which has only forward velocity will go straight down the magnetic field. Other components which have radial velocities will form loops around the magnetic field and return to a disc of focus at the end of each loop. By means of the fields previously mentioned the beam is focused on the target at the end of the 5th loop. When the beam passes through the focusing section, it is also deflected in vertical and horizontal directions by means of magnetic fields at right angles to the focusing field.

Landing of beam at target[8]

As the beam approaches the target it is slowed down. If no light is on the target the electrons in the beam will continue to land until the target potential drops to a value determined by the initial velocities of the thermionic electrons and the contact-potential difference between the thermionic cathode and the target. When this potential is reached, all of the beam will be turned back unless the tube is illuminated. In the lighted areas all the electrons of an ideal beam would land on the

---

[8] P. K. Weimer and A. Rose, "The Motion of Electrons Subject to Forces Transverse to a Uniform Magnetic Field", *Proc. I.R.E.*, Vol. 35, No. 11, p. 1273, November, 1947.

target until the target is driven back to equilibrium potential. This ideal condition, however, is not reached for several reasons. After the beam emerges from the aperture, its direction, as a whole, may not be along the magnetic field. In this case the radial velocity of the beam may be so high that none of it can land at the target under normal conditions. Nothing will be visible in the kinescope picture except noise, unless the mesh voltage is raised to a very high value. This condition is corrected by the use of an alignment coil which produces a magnetic field at right angles to the beam direction near the aperture. This field can be rotated and varied in intensity until the direction of the beam is along the magnetic field. Even after best alignment, however, all of the electrons will not land because of variations in the initial emission velocities which range from 0 to about 0.5 volt. For low light levels only those electrons with the highest initial velocity will land and the percentage landing or the "beam modulation" will be poor. However, even for higher light levels only a portion of the available electrons will land because of the radial velocities introduced by the gun and because of the secondary emission which occurs at the target. Some preliminary data indicate that even for a target on which silver is evaporated the secondary-emission ratio may be as high as 0.5 in the high lights. All of these effects combine to lower the possible signal-to-noise ratio since a larger beam current is needed to discharge the target. The failure to land at low lights can give rise to another condition which is described by the term "picture lag". So few electrons land that a picture is not discharged by the beam in 1/30 second. If the picture is moved there will be a trail behind it of the same polarity. This condition is not serious in the 2P23 except at very low light levels because of the very small target capacitance. The condition is more serious, however, in the 5655.

Edge landing

Besides the lack of 100 per cent landing in the center of the target, a problem of poor landing at the edges arises because of the radial velocities introduced by the deflecting field. In a transmitted picture with poor edge landing the signal will be the highest in the center and drop off progressively towards the edges. The radial velocities introduced by the deflection are largely counterbalanced by the use of a decelerator grid (grid No. 5) which is in the form of a short cylinder. This grid, when operated at a positive voltage between that of the target and the focusing grid (grid No. 4) produces a radial electrostatic field which is zero at the center of the picture and increases

toward the edges. This field gives the electron beam a radial velocity opposite to that produced by the deflecting field.

Landing can also be influenced by many other factors. In the design of the tube it has been found necessary to control accurately the shape of the glass near the decelerating region. Otherwise, the deflected beam tends to strike the glass in this region and not reach the target. Also, the deflecting coil, image socket, and focusing coil must be carefully designed. Best results have been obtained with a deflecting coil 5 inches long. With a longer or shorter coil, the flare fields are different and cannot be counterbalanced as readily with a simple grid. For the same reason the three-inch image section of the tube should be as close to the end of the deflecting coil as possible. This space is limited to 0.5 inch by the length of the image leads and the socket thickness. Slightly better results can be obtained with a spacing of 0.3 inch. The effect on landing of any shielding windings on either the deflecting or focusing coil must also be considered. It is general practice to wrap the deflecting coil with a layer of iron wire, to help prevent leakage of the deflecting field into the target lead which generally returns over the deflecting coil from the image section to the rear of the focusing coil. However, this winding has a slight deteriorating effect on the landing because of its modications of the flare field. When image focus was studied, it was found necessary to reduce the "crosstalk" from the deflecting field into the image section. As mentioned previously, "crosstalk" can be reduced by the use of an external shield over the focusing coil. Such shields, because they modify the flaring of the deflecting field, can also affect the landing. The shields, therefore, should be designed with this item in mind. In fact, proper arrangement of shields will actually lead to better landing than can be obtained with no shields.

In general, the beam imposes no severe limitation on the center resolution of the 2P23 in its present state of development if a field of approximately 75 gauss and a focusing voltage of about 200 volts are used. However, the corner resolution is somewhat deteriorated when the center is in best focus. This deterioration occurs chiefly in the beam section rather than the image section. Some improvement can be obtained by proper adjustment of grid No. 5 provided the landing is not seriously affected. The resolution limits of the beam will be considered more thoroughly in the discussion of the 5655.

Return beam

The portion of the beam that does not land on lighted sections of the target returns and strikes the accelerating grid (grid No. 2) which

'also serves as the first dynode of the signal multiplier. The amount of deflection received in going to the target is not quite balanced by that received in returning so that the beam scans a small area of the first dynode. The size of this scan is roughly ¼ inch. This ¼-inch scan poses quite a serious problem in keeping the dynode free from spots because it is magnified by 25 or more in the kinescope picture. Fortunately, the dynode is not quite in focus for best focus at the target. In operation, however, it is usually necessary to defocus the picture slightly in order to minimize the spots, especially for dark scenes. These spots are nearly always white, indicating a lower secondary emission. In general, for dark scenes these spots are the most severe limitation on resolution, while for well-lighted scenes the target mesh is the limiting factor. Several methods have been tried for reducing the dynode spots including the use of highly polished surfaces and uniformly roughened ones for the dynode both being coated finally with an evaporated film of a metal with a high secondary emission. No completely successful solution, however, has as yet been found. In any event, the spot due to the aperture opening is always present.

Signal multiplier

The first orthicons and image orthicons were generally made with only one stage of signal multiplication. The signal in the form of secondary emission from this stage was collected by a nearby electrode. In general, the gain from this single stage was found to be insufficient. The purpose of signal multiplication by secondary emission is to obtain a nearly noiseless multiplication of the small signal which modulates the return beam to a level well above the noise of the first stage of the video amplifier so that amplifier noise is no longer a limitation. As mentioned previously, the maximum charge that a target element can have is limited by the product of its capacitance and the mesh voltage swing. For the 2P23 with a mesh voltage of 2 volts, the total charge for the whole target, if it is entirely highlighted, is about 1.6×10^{-10} coulombs. Because this capacitance is discharged in 1/30 second, the calculated signal current at the target is only about 5.0×10^{-9} amperes from the highlights. If the first video amplifier is connected directly to the target, a root-mean-square noise current of 3×10^{-9} amperes may be assumed. It can be seen that the highlight signal-to-noise ratio is less than 2 to 1 with the amplifier the limiting item. The gain of the multiplier should at least be such that the beam noise is the limiting item. This noise which is, of course, due to shot effect of the temperature-limited thermionic emission, is given by the expression $(2ei\Delta f)^{1/2}$. In this expression, e is the charge

of an electron (1.59×10^{-19} coulombs), i is the beam current in amperes, and $\triangle f$ is the frequency bandwidth of the picture in cycles per second. For a bandwidth of 4.25 megacycles and if it is assumed that all of the beam is useful in discharging the picture, the beam noise is 0.08×10^{-9} amperes. A gain of at least 40 is needed to bring this value up to the level of the amplifier noise. If the tube is to be used to pick up lower light scenes with no highlights so that the beam current can be reduced, a higher gain is useful. This condition is unusual in the field. Another reason for higher gains, however, is to reduce the number of electron tube amplifier stages required. For this purpose, a gain of several hundred is useful.

In order to obtain a gain of several hundred several multiplier stages are needed because the average gain per stage is usually only about 4. Many multiplier designs have been suggested and tried. Because the second stage must collect all of the electrons from an appreciable area of the first stage (because of the scanning of this stage), it has been found advisable to use a symmetrical multiplier. Such a multiplier can be a series of screens set one below the other around the gun and first dynode. The principal problem has been to get all the secondaries from the first stage over to the second stage. The best solution has proven to be the use of an extra cylindrical grid (grid No. 3) above the first dynode. The voltage of this grid is generally set at or slightly below the first-dynode potential. The beam, which emerges from the aperture in the first dynode with a 300-volt velocity, passes through an aperture in the top of grid No. 3 into the grid No. 4 section without being affected. However, the slow-velocity secondaries emitted by the return beam find themselves in a region of uniform potential except for the second dynode and will be attracted to it. This second dynode is parallel to the first but generally slightly below it. The magnetic field should also be weak near the first dynode to prevent the secondaries from spiraling about it and eventually returning to the first dynode. Any failure to collect all the secondaries at the second dynode will lead to a picture that is darker in one section than another. As in the iconoscope, this condition shows up most clearly when there is no signal due to light so it also is referred to as "shading". This shading signal differs from iconoscope shading in that it is smaller than the picture signal and can usually be cancelled by the insertion of a simple horizontal-sawtooth component in the amplifier. It does not vary greatly with illumination as does the iconoscope shading but depends almost entirely on the beam current. Consequently, the shading control requires little readjustment once it has been set.

The second dynode is an efficient multiplier consisting of a 32-blade pinwheel with the blades set at an angle of about 30 degrees to the plane of the multiplier. Primary electrons which strike the blades emit secondaries which are drawn through the slots to the next stage. A high-transmission screen is mounted on top of the pinwheel to prevent the secondaries from being pushed back into the surface by the lower voltage of the preceeding stage. Such multipliers will give gains of about 4 per stage at a primary electron velocity of 300 volts. A 5-stage multiplier as used in the 2P23 will give gains of about 1000. The signal output which will be discussed later is about 10 microamperes. This value is considerably higher than the 0.018 microampere output of the 1850-A iconoscope. The gain of the external amplifier can thus be reduced by a value of about 500 permitting the elimination of at least two amplifier stages.

Generally, the recommended voltage per stage of the multiplier is between 200 and 300 volts except for the first dynode which is held at 300 volts. The over-all voltage required by the multiplier stages will then be in the range of 1100 to 1500 volts.

Operation of 2P23

Although the 2P23 has proved very successful for field use because of its high sensitivity, wide light range, and the relative freedom from shading, it has several limitations. Because of the low capacitance of the mosaic, the maximum charge any element can attain is small. This limitation, and the fact that all the beam that approaches a lighted area of the target does not land, limits the signal-to-noise ratio to a relatively low value so that the picture appears somewht "noisy". The type of photocathode used, although it has a high over-all response does not faithfully reproduce colors in black and white. This poor color response is particularly troublesome in studio work. Also, the "white edge" effect gives a somewhat unnatural looking picture which, although it is not too serious for oútside pickup, is very noticeable on high-quality studio scenes.

The effect of beam modulation on the signal-to-noise ratio and its improvement by a change in gun design will be considered first because the results are applicable to both the 2P23 and 5655. In low lighted sections of the target it has been pointed out that the percentage of the beam that lands is low because of the spread in initial velocities at the thermionic cathode. When light is not present, the target is driven to a voltage corresponding to the highest initial velocities. For small illuminations there is only a small percentage of the total beam which can discharge the target. At high lights this limitation is no longer

present and it would be expected that the initial velocities would not be a problem. However, with the original gun design of the 2P23 the percentage of the beam that landed in the highlights was only about 15 per cent. For a maximum signal at the target of 0.005 microampere the beam current needed is 0.033 microampere. The beam noise given by the expression $(2e\,i\,\Delta f)^{1/2}$ is 0.0002 microampere. The maximum signal-to-noise ratio is, therefore, about 25 to 1. The type of noise, because it is due to the beam, is not "peaked channel noise" but is spread over the entire bandwidth so that long noise pulses in the form of streaks come through. This ratio is less favorable than the 60-to-1 ratio of the 1850-A iconoscope with a "peaked channel noise" in which the noise pulses are all short and appear only as small dots.

Development of an improved gun

The original gun of the 2P23 consisted of a thermionic cathode and a control grid with a large aperture spaced at a rather large distance from the cathode. The spacing between the control grid and the accelerating grid (grid No. 2) was also high. This gun could readily be manufactured but the beam current was drawn from a rather large area of the thermionic cathode. Because only the center portion of this beam passes through the small aperture in grid No. 2, it was expected that only the part of the beam that is emitted by the center of the cathode would be used. Extensive study, however, has shown that the center of the beam is not all that is used. The electrons drawn from parts away from the center of the cathode and which would be expected to have a radial component of velocity enter the beam and raise its radial component.

A new gun design has been developed to draw electrons, as far as possible, only from the center of the cathode area. The grid No. 1 aperture was made smaller, the grid No. 1-to-cathode spacing was made as close as possible and an extra accelerating aperture which is also at grid No. 2 potential was added close to the grid No. 1 aperture. The result of these changes is that the cathode is much more heavily loaded; i.e., for a given beam current a much higher percentage of the electrons are drawn from the center of the cathode. Because these electrons have a smaller radial velocity, most of their energy is in the forward direction and they will be more likely to land at the target. When the new gun is used, the percentage of modulation rises to about 30; the signal-to-noise ratio is increased to about 35 to 1. Although this value is still on the low side, it is acceptable for outside pickups. It is interesting to note that the signal-to-noise ratio of good 35-millimeter film is also 35 to 1.

In addition to the improvement in signal-to-noise ratio, this new gun provides an improvement in resolution due probably to the smaller radial velocities which make the final spot smaller. (The presence of radial velocities cause a point source to be imaged as a spot of measurable magnitude at the target.) With the new gun, the beam itself is at present not a limitation on the usable resolution of the tube unless the magnetic field and grid No. 4 focusing voltages are too low. In general, a field of 75 gauss and a grid No. 4 voltage of 200 volts is a good compromise between good resolution and the need for excessive scanning power. With such operating conditions the beam is able to resolve better than 1000 lines in the roughly one-inch vertical height of the picture, or more than 1000 lines per inch.

Whether the 30 per cent modulation efficiency represents a limit to what can be done with gun design is not known. Initial velocities of electron emission at the thermionic cathode, of course, even at highlights present some limitation. Measurements at a variety of cathode temperatures have shown no definite improvement. The main limitation may be the secondary emission and electron reflection that comes at the target.

The new gun was originally developed in connection with the new 5655 studio image orthicon. However, it is equally useful in the 2P23 and has been adopted there. The 5655 now differs from the 2P23 only in the target to mesh spacing and in the photocathode surface. Why these changes give a tube (the 5655) which is superior for studio use but which is not so versatile for remote pickup will be discussed next.

Use of closer target-to-mesh spacings

In discussing target-to-mesh spacing for the 2P23 tube, the spacings were arbitrarily divided into two groups: wide-spaced where the spacing is much greater than the size of a target element; and close-spaced where it is much less. Wide spacing is not used because the low capacitance results in an unusable signal-to-noise ratio and annoying white edges around lighted areas. The 2P23 has a spacing of 0.003 inch which is in the intermediate range where the signal-to-noise ratio is usable and the white edges are not particularly annoying. The question of what occurs as the spacing becomes closer is an important one.

If the spacing is reduced to 0.001 inch, the capacitance rises by a factor of about 3. The signal output will also be three time as high and the signal-to-noise ratio is improved by a factor of $\sqrt{3}$ or about 1.7, provided the modulation for the higher beam currents required

does not change. Numerous experimental tubes have been made with this reduced target-to-mesh spacing in which the signal-to-noise ratio is definitely improved but is still borderline for high-quality studio work. The white edges have disappeared and the half-tone response is improved. This improvement is due to the much longer straight-line portion of the curve of target charge vs. illumination which is shown in curve A of Figure 6. If these tubes are operated so that the highlights are at a point somewhat over the knee of the curve, the half tones will have a better signal-to-noise ratio than the 2P23. The improved signal-to-noise ratio and the lack of white edges make the picture look more "natural".

The close-spaced assembly, however, is not without its drawbacks. Because an inferior picture is obtained below the knee of the signal-output curve, it is nearly always preferable to operate these tubes at the knee or slightly above it. Although a better picture is obtained at this point with a close-spaced target, for the 0.001-inch spacing three times as much light is required. This requirement makes the sensitivity of the experimental tubes appear to be lower than that of the 2P23. The close spacing is also not satisfactory for low-light scenes because the higher capacitance causes picture "lag". The higher capacitance causes a smaller potential rise at the target for a given amount of light. At these small potentials, the beam modulation is very poor and the target is not completely discharged in one frame time. For outdoor scenes the greatest drawback is probably a lack of versatility in handling a wide range of lighting. This drawback shows up in two ways. The beam current needed in the 2P23 is very small and the multiplier shading is a minor item. If the beam is set for a high-light condition and the camera swung over to a low-lighted scene, the shading is not noticeable and the scene can readily be handled. In the close spaced tubes, the higher beam current causes disproportionally more shading. Thus, when the camera is used on a high-light scene a picture of better quality can be obtained; but when the camera is swung to a low-light scene the shading and beam noise are often troublesome. If the beam current is reduced this trouble disappears. In field use, however, this reduction is not always possible, especially when a scene contains both sunlight and shadow which often happens during sport events. Also, because of the long straight section of the target-charge curve, the highlights have more tendency to cause "blooming" at the kinescope. In a scene with a few high lights the picture is set so that the normally lighted parts appear bright at the kinescope. The signal in the highlights therefore, can be high enough to cause loss of resolution in the kinescope and consequent "blooming".

From a manufacturing standpoint the close spacing also puts a greater demand on the thermionic cathode because of the need for a higher beam current. If the center of the cathode is slightly low in emission, the beam will be insufficient to discharge the highlights completely and loss of resolution will occur. Because of this demand for higher beam currents, grid No. 2 of the close-spaced tubes is operated as near to 300 volts as possible and not near 200 volts which has been satisfactory in some cases for the 2P23.

OPERATION AND CONSTRUCTION OF THE 5655

Target-to-mesh spacing

Because it has not been possible to make a completely universal tube, it was decided to design the close-spaced tube for studio use where the lighting can be controlled. Under such conditions the apparent decrease of sensitivity and inability to handle scenes of widely varying illumination is not important. Because a 0.001-inch spacing does not give too good a signal-to-noise ratio, the question arises as to what happens at closer spacings. For a 500-mesh screen the center-to-center spacing is 0.002 inch. For 60 per cent transmission the hole size is about 0.0016 inch, that is, the center of the target element under each hole is 0.0008 inch from the mesh. One would expect that the capacitance would increase slowly for values of spacing less than 0.001 inch. However, the increase is definitely apparent in tubes with still smaller spacings. The capacitance increases until the target and mesh touch. The gain in capacitance over a 2P23 target is about 4 to 6 to 1 and the gain in signal-to-noise ratio is about 2 to 2.5 to 1. The signal is, of course, about 4 to 6 times higher and the apparent sensitivity ¼ to ⅙ as high. This gain in signal-to-noise ratio is very worthwhile and makes the tubes acceptable for studio application. For such tubes, the signal-to-noise ratio has an average value of about 80 to 1.

Target-mesh structure

The actual manufacture of a target-mesh structure with such a close spacing (the spacings are held between contact and 0.0004 inch) presents many problems. A description of the manufacturing process follows. The thin glass target is sealed at its edges to a metal ring. Before sealing, the surface of this ring is coated with a binder. After the seal is made, there is a measurable thickness of this binder above the glass. Also, at the inner edge of the ring the glass target tends to seal around the edge so that it is slightly depressed below the metal. If

the mesh is then placed against this structure, it will have about the correct spacing for the 2P23. To obtain closer spacing it is necessary to design the structure so higher points on the mesh are actually pushed into contact with the glass target. The tolerances are so small that careful fabrication is needed. Any minor deviation from flatness of either the mesh or the target will also show up much more clearly in the close-spaced target.

Picture sticking

Before leaving the close-spaced structure, it is interesting to note that its "picture sticking" characteristics due to glass resistivity are different from those of the 2P23. It has been mentioned previously that in a cycle of operation the charges, remaining on the target after the beam has scanned it, must be neutralized in a frame time by conduction through the glass. If charge neutralization does not take place, the signal will fade for a fixed scene and return to its full value only when the picture is moved. A picture of opposite polarity will then be left on the target and can be seen if this area is lighted. The point of interest here is that for a given glass thickness and conductivity, fading depends on the target-to-mesh spacing in the region of very close spacings because, with the close-spaced assembly the capacitance and, consequently, the amount of charge to be neutralized are greater. For a 2P23 with a target of average thickness and conductivity, the percentage of fading at 20 degrees centigrade is about 10 per cent. If the temperature is increased to 30 or 35 degrees centigrade, the lowered resistivity makes the fading nearly negligible. For a close-spaced tube, however, the value at 20 degrees is closer to 30 per cent. A higher temperature of operation is needed to reduce fading to a low value. Generally, a temperature in the range of 40 to 45 degrees is sufficient. This need for a higher operating temperature, of course, reduces the operating temperature range of the close-spaced tube over that of the 2P23 because the 5655 is limited on the high side by lateral leakage in the same way as the 2P23. During tube life the 5655 target also changes more noticeably than that of the 2P23 because of the greater amount of charge that has to be transported through the glass. The change in contact potential, which generally makes the scanned area appear darker, may amount to several volts and requires shifting the mesh potential to more positive values during the life of the tube. In addition during operation the resistivity of the target slowly increases and after several hundred hours a higher temperature of operation may be needed.

Beat pattern

Because the mesh of the 5655 is nearly in contact with the target, the mesh is in better focus and is more visible than in the 2P23. The beat patterns also show up more readily. Some improvement has been made by using higher-transmission mesh with a transmission of 60 per cent or better. This value is equivalent to a wire 0.0004 inch in diameter. At present, however, the mesh limits the resolution of the tube in the highlights. As the techniques for manufacturing meshes improve, it is expected that eventually a finer mesh will be available.

Photocathode

Because the close-spaced tube has been designed for studio work a high sensitivity, especially for incandescent light, is not of prime importance. The spectral response, however, is of importance. Because of the variation in the spectral response of the 2P23 from tube to tube and because of the high infrared sensitivity of many of the tubes, it is very difficult to light the scene properly and get reproducible results. For these reasons, a different photosurface has been developed for the close-spaced 5655 tube.

The well-known photosensitive surfaces are those of cesium, silver-oxide, and silver, and those of cesium-antimony. Both can be made in the form of semi-transparent surfaces. It has already been shown that the first is not satisfactory for the 5655. The cesium-antimony surface gives a high response to both incandescent and fluorescent sources which is quite reproducible from tube to tube. It has no infra-red response but, unfortunately, also very little red response. Even with incandescent illumination its red response is too low to be satisfactory. A photosurface that overcomes this objection, however, has been developed. It consists of a silver-antimony surface sensitized with cesium. The silver and antimony are made into an alloy in the proportions that give best results. This alloy is evaporated onto the face plate at exhaust and then sensitized. The surface as shown in the spectral response curve of Figure 7 has the high blue response of the cesium-antimony (S4) surface plus an added red response. The over-all sensitivity to incandescent light is only about one-third of that of the 2P23 surface. For fluorescent light and sunlight, the surface compares very favorably with the 2P23. Under certain conditions such as near sunset when considerable blue light is scattered, the 5655 surface is more sensitive.

Operation

Because of the greater capacitance and different photocathode

SPECTRAL SENSITIVITY CHARACTERISTIC
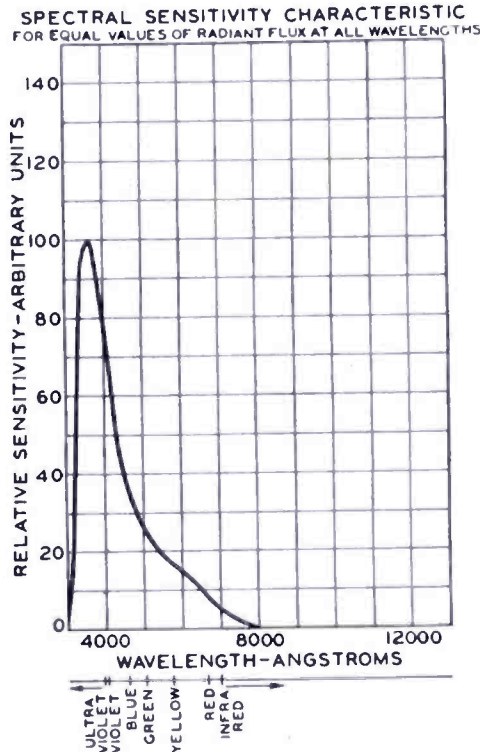FOR EQUAL VALUES OF RADIANT FLUX AT ALL WAVELENGTHS

Fig. 7—Approximate spectral sensitivity characteristics of image orthicon types 5655 and 5769.

surface, the signal-output of the 5655 differs from the 2P23. The signal output curve is given in Figure 8. Because the maximum output is 4 to 6 times that of the 2P23, a two-fold or better increase in the signal-to-noise ratio results although more light is needed to obtain this higher value. As the curve indicates, the illumination is of the order of 0.2 foot-candle at the photocathode. In order to obtain good depth of focus, a minimum of 100 foot-candles should be used on a scene, with 200 to 300 a better choice.

The type of lighting needed to get a good spectral response is fairly well met with a mixture of fluorescent and incandescent sources. In general fluorescent lamps of 3500 or 4500 degrees Kelvin

color temperature are most suitable for obtaining a good level of lighting. However, when only fluorescent lighting is used, the red response is somewhat lower than the yellow or blue. The use of incandescent flood lights will help this condition and at the same time permit high lighting of various scenes. Although the 5655 is able to handle a wide range of light it is more restricted than the 2P23. For this reason care should be taken to eliminate very brightly lighted
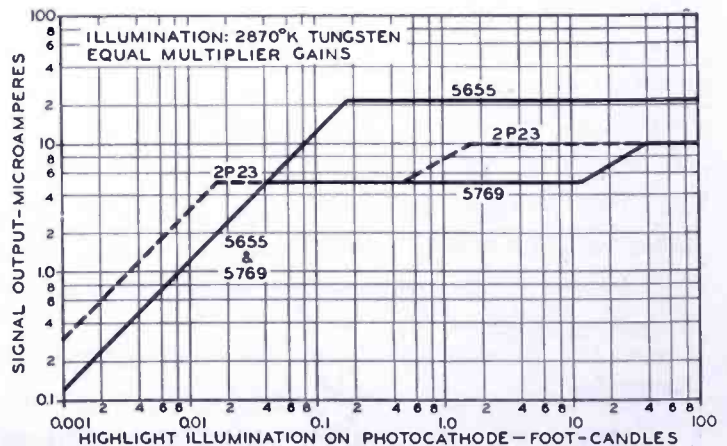

Fig. 8 — Simplified signal output characteristics for image orthicon types 2P23, 5655, and 5769.

areas such as can be caused by highly reflecting objects or by the use of intense spot lighting.

OPERATION AND CONSTRUCTION OF THE 5769

As has been discussed, the 2P23 has the advantages of fair signal-to-noise ratio, good ability to handle a wide range of scenes, and good sensitivity particularly for incandescent lighting. However, because of its high red and infrared response, it does not portray colors faithfully and resolution suffers particularly for the colors near the blue. The 5655, on the other hand, has a good color response. The 5769 is a new tube which is identical with the 2P23 except that it has the 5655 photocathode surface and color response. Its sensitivity for incandescent light is only about one third that of the 2P23 but for fluorescent and daylight it is nearly the same. For a large majority of outdoor pickups it is superior to the 2P23 because of its color response. In addition, operating experience has shown the 5769 to be more stable. Because the photocathode surface of the 2P23 demands an excess of cesium for best sensitivity, it is difficult to prevent migration of the cesium around the tube while it is on the shelf or in operation. If the excess cesium migrates to the target the resolution and signal output of the tube will be lowered, and the tube will fail because of "target leakage". The 5655 and 5769 have, in general, proved less susceptible to this condition and, consequently, are more stable. Because of its good color response, the 5769 can also be used for studio operation. In this use it is somewhat easier to handle because of its wide light range. The 5655, however, is superior in its signal-to-noise ratio and rendition of grays.

OVER-ALL OPERATING CHARACTERISTICS

The over-all operating characteristics of image orthicon tubes can best be considered in terms of the curves of signal output versus light. Figure 6 shows curves of the charge built up during a frame time for increasing illumination on the photocathode. If the charge is divided by the frame time of 1/30 second and multiplied by the multiplier gain, the signal output will be obtained. For a gain of 1000, the maximum signal for a 2P23 of average mesh spacing is about 5 micro-amperes. For a photocathode sensitivity of 14 microamperes per lumen and a secondary emission ratio of 2.5 at the target (the ratio of the cesiated glass is probably about 4 at 400 volts but the mesh transmission is 60 per cent), the high light illumination on the photocathode needed to obtain this maximum signal is about 0.02 foot-candle. With this information the signal output curve (Figure 8) for the 2P23 can

be constructed. As in the charge curve, the signal-output curve rises linearly with light until a point is reached which corresponds to the maximum signal output. Above this point it does not rise except for very high values of light where interelement capacitance comes into effect. This curve is extremely simplified. It holds more closely for the case of a small area of light on a dark background, but even under this condition the break at the knee is rounded off because of the initial emission velocities of the secondaries from the target. These velocities range from 0 up to 5 volts with an average value of about 2 volts.

Should there be more than one bright spot, the curve becomes more complicated. Any lighted area tends to preserve its contrast by reducing the charge on the areas with a smaller amount of light by spraying them with secondary electrons. This spray, however, will also tend to discharge the poorly lighted areas which already have a rather low signal. Brightly lighted areas will, consequently, suppress the grays and make the gray parts of the scene appear flat and noisy. Gray suppression can be reduced by keeping the mesh potential high so that more of the electrons are collected and not redistributed. However, this expedient is of the most help when the highlights are just above the knee of the curve.[9]

In its present state the image orthicon can handle a scene containing very bright high lights and grays better than an orthicon. In outdoor work many such scenes will be encountered. Inferior results in the grays will always occur, however, so that where lighting is under control such as in the studio, every attempt should be made to avoid extreme highlights. Not only do the secondary electrons redistributed directly from the highlight parts of the target suppress the grays, but also secondary electrons from the mesh have the same effect. Internal reflection of the highlights inside the lens and tube add to this limitation. Very poor results are obtained if a direct light gets into the lens from the sun or other sources.

A simplified signal output curve is also shown in Figure 8 for the 5655. Because of its high capacitance, the maximum signal output of the 5655 is higher than that of either the 2P23 or 5769. This advantage leads to a higher possible signal-to-noise ratio and a better gray scale because of the longer straight part of the curve. For the same photosensitivity, however, more light is needed to reach these improved conditions. In addition, more beam current is necessary to discharge

9 O. H. Schade, "Electro-Optical Characteristics of Television Systems", RCA Review, Vol. IX, No. 4, pp. 663-665, December, 1948.

the highlights. For any given scene, the 5655 can produce, in general, a picture as good or better than that produced by a wide-spaced tube. It also has about the same ability to hold down highlights. However, because of the greater beam current needed for a strongly illuminated picture, when the camera is turned to a low light scene, the high beam current produces more noise and shading than is produced by the 2P23 or 5769. If the beam current is reduced for the low-light scene, the picture is again good. Because a continual shifting of the beam current is not practical, the 5655, in general, is not recommended when high-light and low-light scenes must be picked up in quick succession.

CONCLUSION

This paper has discussed in some detail the limitations and operating problems as well as the advantages of the image orthicon. As a result of a continuous program of development, many of the limitations of this tube have been minimized and the image orthicon has evolved from a laboratory device to its present status of being the work horse of television. With continued development, the possibilities of which have by no means been exhausted, the image orthicon can be expected to show further steady improvement.

The operating problems show a measure of the complexity of the image orthicon. This complexity, however, makes it possible for this tube to do what no other camera tube can do. An outstanding advantage of the image orthicon is its exceptional sensitivity which enables the tube to pick up scenes illuminated at very low light levels—only a few foot-candles—and greatly extends the range of outdoor subjects which can be televised. In addition, the image orthicon can reproduce scenes having great depth of field—a valuable advantage which provides flexibility of operation. Both in outdoor and studio pickups, the use of image orthicons has resulted in steady improvement in picture quality. The tube has earned its place today as the best choice for a universal camera tube.

ACKNOWLEDGMENT

REVERSIBLE-BEAM ANTENNA
FOR TWELVE-CHANNEL TELEVISION RECEPTION*

By

O. M. WOODWARD, JR.

Research Department, RCA Laboratories Division,
Princeton, N. J.

Summary—This paper describes a unidirectional receiving antenna which is effective over all twelve of the presently assigned channels without adjustment.

The array is made up of dipole elements which themselves maintain desirable characteristics over the entire television range. These elements are united by a simple transmission line network to yield a directive pattern.

The antenna maintains a high front-to-back ratio over all channels, and is particularly useful in fringe areas where it is necessary to reduce co-channel interference.

The directional beam is reversed on any channel by a simple switch which transposes a single transmission line.

INTRODUCTION

THE rapid growth of television during the last few years has created new problems in securing satisfactory fringe-area reception. Several of these problems are directly related to the antenna system at the receiving location.

The television transmitters in a given region generally locate somewhat closely together in metropolitan areas to obtain the greatest population coverage. Therefore multi-channel reception of the stations at a distant point is restricted to a fairly narrow azimuth angle in direction, requiring a receiving antenna with a beam orientation that remains fixed in direction for all television channels. As the presently assigned twelve channels cover the widely separated bands of 54 to 88 and 174 to 216 megacycles, very broad-band response characteristics are necessary for efficient operation. Many of the simpler types of antennas in current use exhibit widely varying radiation properties in the higher television band. While a compromise may be effected by rotating the antenna for maximum signal or by the use of both low and high band antennas, a single antenna array having a fixed beam orientation is the more desirable solution.

Another difficulty confronts the viewer situated between co-channel stations. In many such instances the signal strength from one of the

---

* Decimal Classification: R125 × R326.61.

stations is sufficient to mar the otherwise good reception from the other. This interference is generally characterized by a "Venetian blind" effect of dark horizontal shadows moving up or down with the relative drift of the stations' carrier frequencies. Tests have shown that the interfering signal amplitude need only be a very small fraction of the desired signal to cause this interaction. Hence the receiving antenna should have a unidirectional beam throughout the television ranges to reduce the objectionable interference as well as to improve the power gain and signal-to-noise ratio.

Many of these viewers are located in regions where multi-channel reception is possible from opposite directions. For example, in the Princeton, New Jersey area, usable signals are received from six stations serving the New York City area and three Philadelphia stations at the present time. This requires an antenna with a unidirectional beam capable of being reversed in direction at will on any television channel.

Unidirectivity is quite easily obtained electrically by means of surface reflectors such as parabolic and plane screens. However, to secure an appreciable suppression of the backward lobe at the lower channels, their size becomes impractically large.

Arrays using sharply tuned parasitic elements have not been found to provide good front-to-back field ratios over a wide frequency band. Also such antennas are not suited for beam-reversing.

Long wire antennas, such as rhombics, are fairly broad-band and also electrically reversible in direction, but the large area needed for installation rejects their application for the average set owner.

On considering the limitations of these various types of antennas it was concluded that an array made of phased dipoles presented a better solution.

The simplest system of this type consists of the familiar two-dipole end-fire antenna producing a cardioid unidirectional pattern. However, a four-dipole phased array was chosen for its broad-band properties as the better system satisfying the outlined requirements.

This paper describes such an array constructed without the mechanical and electrical difficulties of reflectors, parasitic elements, or tuning adjustments.

GENERAL PRINCIPLES OF ARRAY

The reciprocal relationship between transmitting and receiving antennas makes it possible, for purposes of explanation, to consider the simplified array of four point source radiators (Figure 1). The

four sources are arranged in the form of a square and equally spaced one-quarter wavelength from the center (O) of the array. The cur-

Fig. 1 — Simplified four-radiator array.

rents are assumed to be equal in amplitude and phased with respect to the center as indicated in Figure 1.

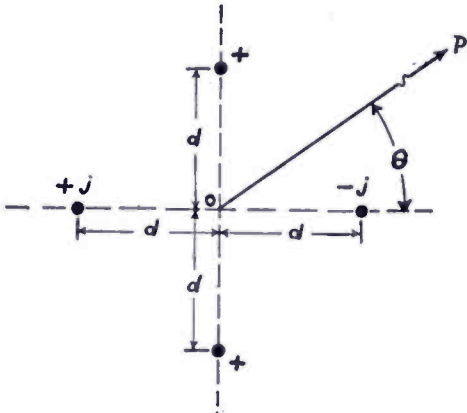The system is seen to be a combination of a broadside array superimposed upon and fed in quadrature with an end-fire array. Both arrays have bi-directional properties. Relative field patterns in the elevation plane of each array taken separately with respect to point O are, respectively:

$$F \text{ (broadside)} = K \cos (90° \sin \theta) \tag{1}$$

and
$$F \text{ (end-fire)} = K \sin (90° \cos \theta) \tag{2}$$

where $F =$ field strength at a distant point, P.

$K =$ a proportionality constant.

$\theta =$ elevation angle, degrees.

Figures 2-A and 2-B show these field distributions graphically in polar form.

Simultaneous operation of both arrays permits direct addition of the lobes on one side and subtraction on the other side, resulting in the unidirectional pattern given by:

$$F \text{ (combination)} = K \left[\cos (90° \sin \theta) + \sin (90° \cos \theta) \right] \tag{3}$$

and plotted in Figure 2-C.

The elevation field pattern of Equation (3) will remain unchanged if the point source radiators are replaced by four horizontal dipoles parallel to one another. However, the dipole field distribution becomes a factor in the relative azimuth field patterns as follows:
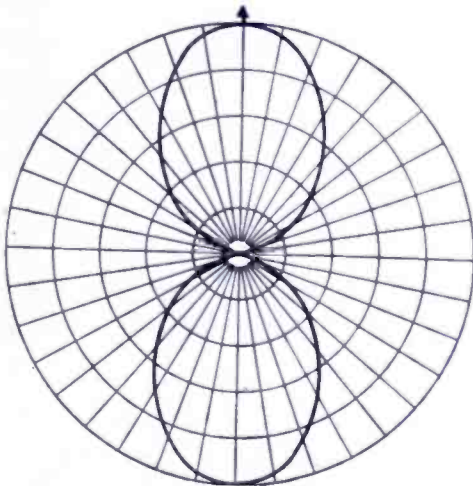
$$F \text{ (broadside)} = K f(\phi), \tag{4}$$

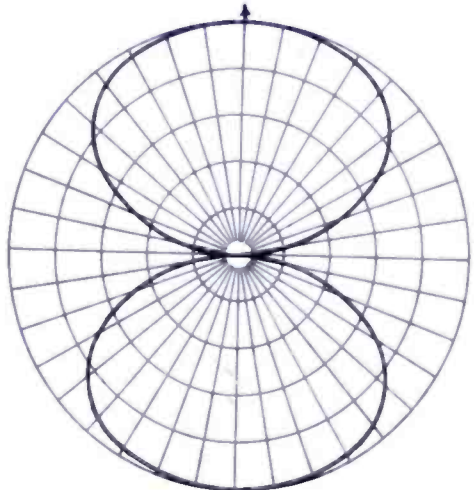$$F \text{ (end-fire)} = K f(\phi) \sin (90° \cos \phi) \tag{5}$$

and $$F \text{ (combination)} = K f(\phi) [1 + \sin (90° \cos \phi)] \qquad (6)$$

where $f(\phi) =$ the relative field pattern of individual dipole.

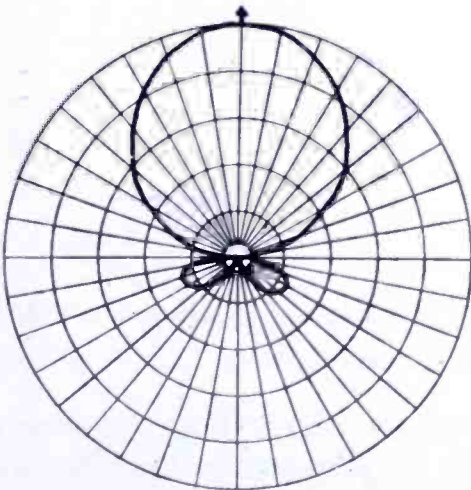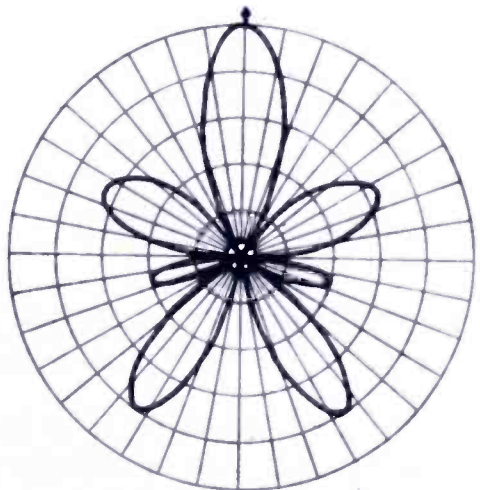$\phi =$ azimuth angle, degrees.

A. Broadside array.　　　　　B. End-fire array.

C. Combination array, $d = 90°$.　　D. Combination array, $d = 270°$.

Fig. 2—Relative elevation field patterns.

Several important points become apparent from inspection of Equations (3) and (6). Under the previously assumed conditions of feed, the dipole spacing (d) from the center of the array may depart considerably from one-quarter wave length without seriously affecting the front-to-back field ratio, thus permitting a coverage equivalent in percentage frequency variation to the lower television band. Furthermore, unidirectivity may be obtained with the dipole spacing (d) made

odd multiples of one-quarter wave length. Since the higher television band bears a three-to-one frequency ratio with a portion of the lower band, satisfactory operation is assured at the higher band. In this case, however, the beam is reversed in direction, (Figure 2-D).

Azimuth field patterns for dipole spacings of 90 and 270 electrical degrees, respectively, are shown in Figures 3-A and 3-B. The function $f(\phi)$ was taken to be that of a simple half-wave dipole in both instances.

It is evident, also, that a 180-degree phase reversal of the currents in either the broadside or the end-fire arrays will reverse the direction of the unidirectional pattern. This property is independent of frequency variation and dipole spacing.

Finally, since the field distribution of the individual dipole is a multiplying factor in Equation (6), it is observed that $f(\phi)$ should maximize at $\phi = 0$ degrees. Stated in other words, this means that the
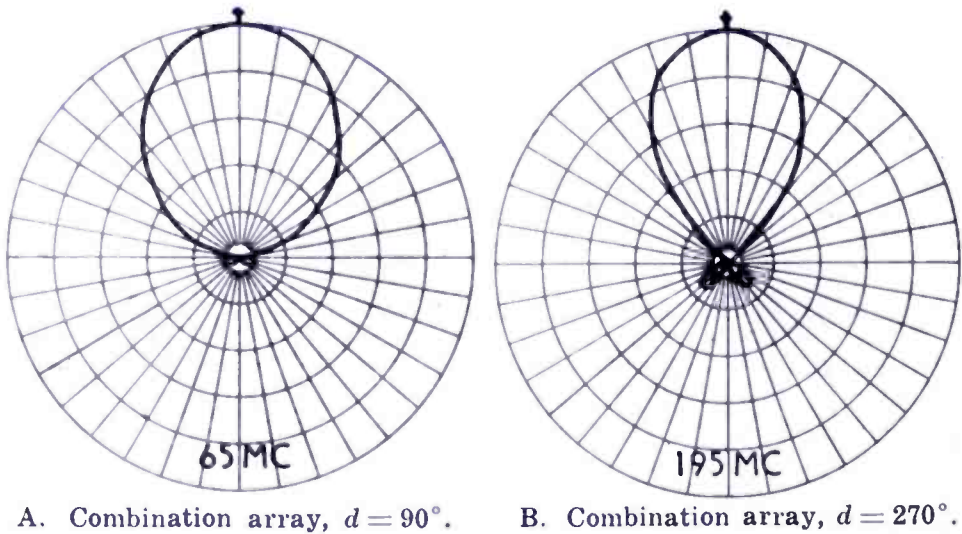
A. Combination array, $d = 90°$.   B. Combination array, $d = 270°$.

Fig. 3—Relative azimuth field patterns.

individual dipole pattern must be oriented in the same direction as the array and have essentially the same radiation characteristics throughout the required frequency ranges.

It is desirable at this point to describe the dipole modifications required to fulfill this latter condition.

MODIFIED DIPOLE

In order to prevent the efficiency from falling off too rapidly at the lower frequencies, the dipoles are made one-half wave in length in that region. Azimuth field patterns taken at representative frequencies in the lower television band of such a dipole are shown in Figure 4-A. The arrows shown on all of the field patterns indicate the direction
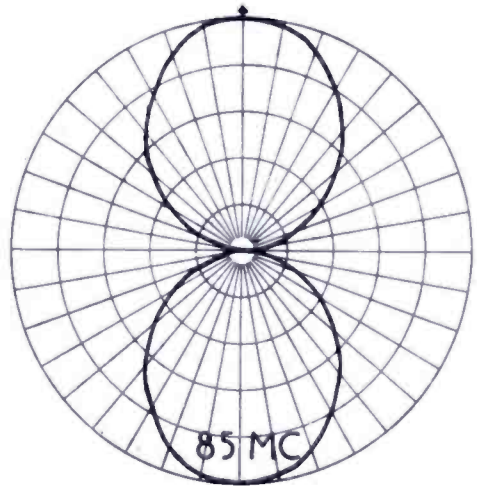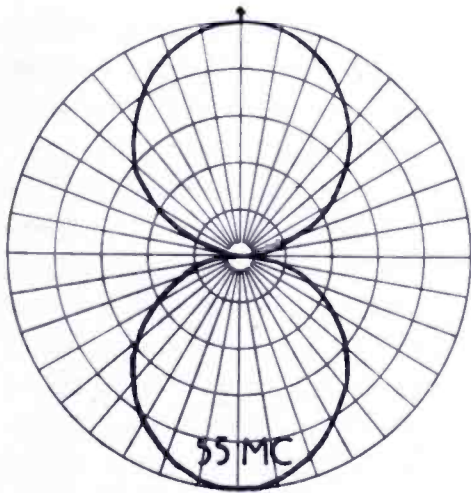
A. At lower band frequencies;
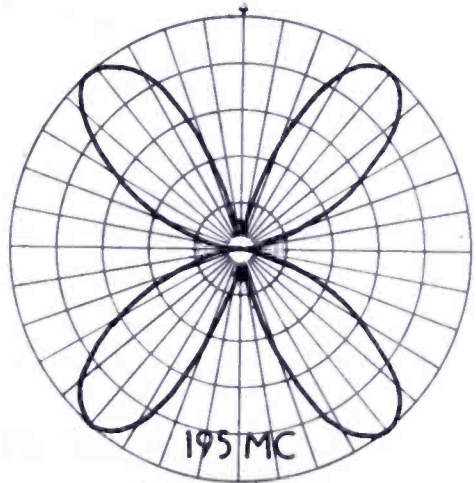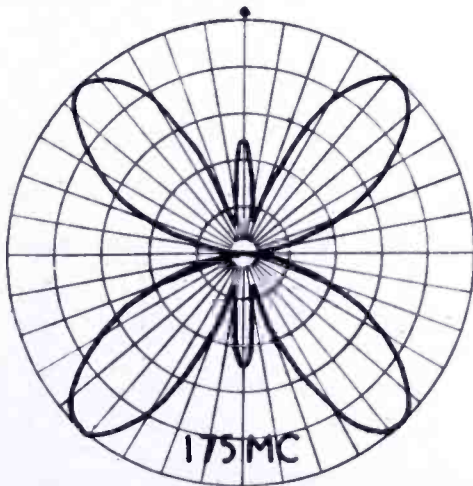
B. At higher band frequencies.

Fig. 4 — Measured azimuth field patterns of simple dipole.
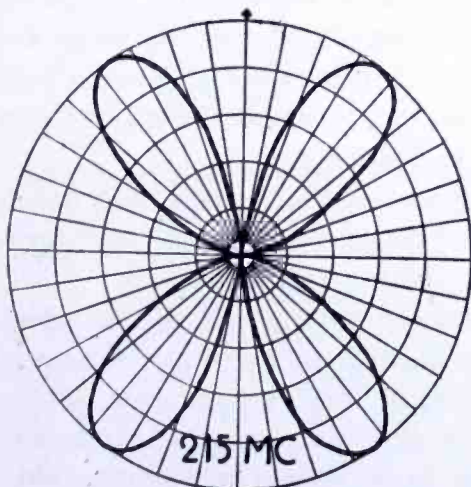
normal to the dipole axis. In the higher band of 174 to 216 megacycles, however, the dipole becomes in the order of 1½ wave lengths long, producing multi-lobe configurations with little radiation broadside to the dipole axis (Figure 4-B).

The desired bi-directional characteristics may be obtained at the higher frequencies by altering the current distribution along the dipole legs. One manner of accomplishing this result is by the use of the well-known "sectionalizing" method of inserting a series reactance at the proper position in each of the dipole legs as diagrammed in Figure 5-A. A coaxial sleeve element shorted at one end, (Figure 5-B), offers a practical means of securing this series reactance at the television frequencies.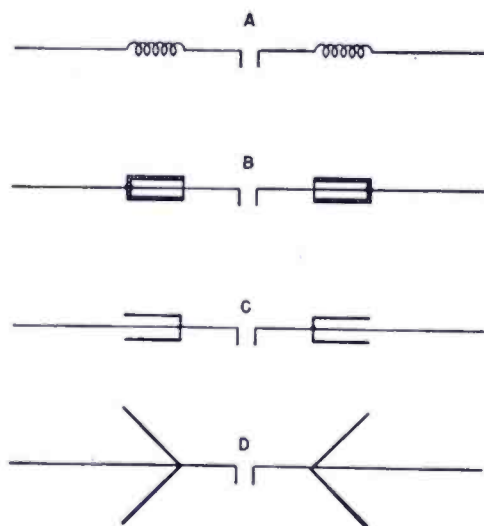 Tests, however, have shown this type of dipole to be rather narrow in band width, due partially to the low characteristic impedance obtainable with the coaxial-sleeve element.

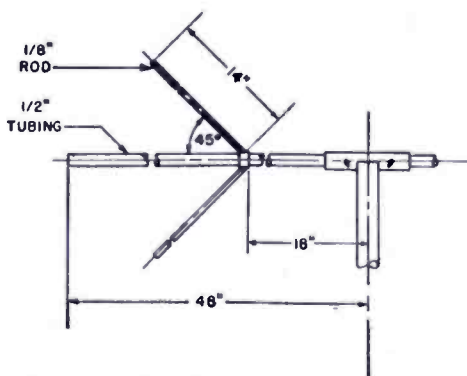Fig. 5—Development of high frequency "vees".

Fig. 6—Modified dipole details.

A higher characteristic impedance and correspondingly increased band width is obtained by replacing the coaxial sleeves with open-wire "hairpin" loops as shown in Figure 5-C. As a final step, the loops are straightened out into right-angle "vees," Figure 5-D. Numerous field measurements were made to arrive at the optimum dimensions and placement of the "vees" as indicated in Figure 6.

While the evolution of the "vee" design outlined above was developed from a nonradiating, sectionalizing reactance, the final "vee" form may be considered also as part of the radiating system.

Installation of the "vees" was found to have practically no effect upon the dipole patterns in the lower band of frequencies. Measured azimuth field patterns of the dipole with "vee" attachments at the higher band of frequencies are given in Figure 7. The multi-lobe patterns of the simple dipole are seen to be altered to "figure-eight"

patterns with fixed orientation by the addition of the "vees." The elevation field distribution was found to be very slightly elliptical, with the maximum intensity normal to the plane of the "vees."

It will be noted that such a modified dipole by itself is well suited as a receiving antenna for many receiver locations where a "figure-eight," bi-directional pattern suffices for interference-free reception on all twelve channels.
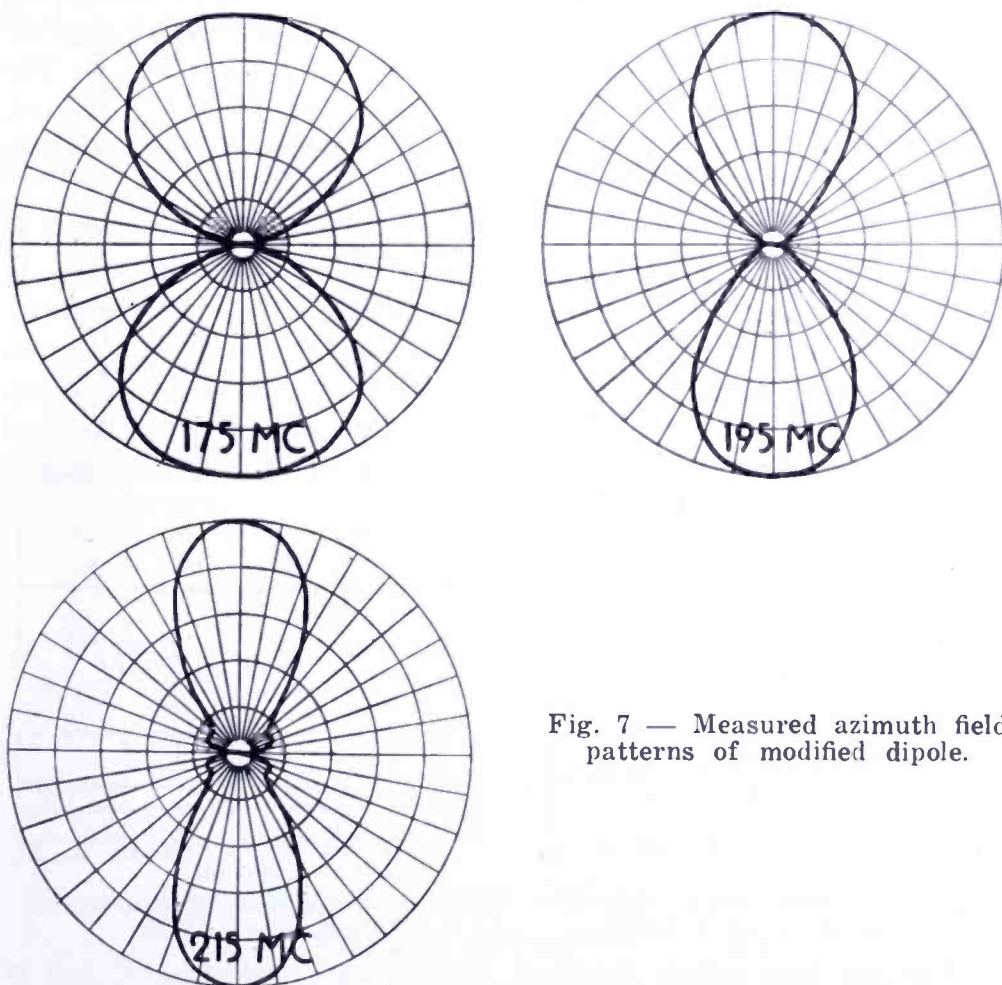
Fig. 7 — Measured azimuth field patterns of modified dipole.

Other field tests were made on the modified dipole constructed as in Figure 6 to determine its performance as a television receiving antenna. The standing-wave characteristics versus frequency, measured on a 300-ohm balanced transmission line, are plotted in Figure 8. The standing-wave ratio is given in terms of the ratio of minimum voltage to maximum voltage. The measured relative power gain, compared to a matched simple dipole one-half wave in length at each frequency of operation, is shown as the solid curves in Figure 9. The relative power gain as calculated from the measured field patterns and

standing-wave characteristics is plotted as the dashed curves. Part of the discrepancy between the curves in the higher band may be due to dielectric losses in the dipole mounting not considered in the calculated curves.

DIPLEXER NETWORK

Means must now be considered for securing the desired feed conditions of the array. Referring to the wiring diagram of Figure 10, the two dipoles of the broadside array are joined for in-phase feed by a length of balanced transmission line fed at its midpoint, A. The two dipoles of the end-fire array are similarly connected to midpoint, B, with the exception of a transmission line transposition as shown to provide for out-of-phase feed.

An important advantage is gained with this arrangement. As the broadside array is symmetrically located in the electrically neutral plane of the end-fire array, independent operation of the two arrays is assured at all frequencies.
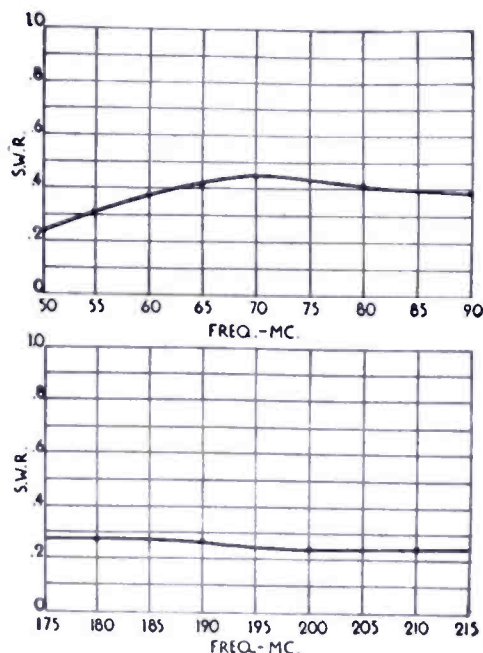
Fig. 8—Standing-wave characteristics of modified dipole.
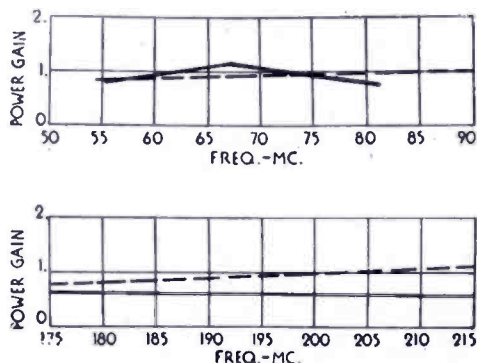
Fig. 9—Power-gain measurements of modified dipole.

The two feed points, A and B, are joined to terminals C and D of a four-terminal network called a diplexer. One of the two lines is made one-quarter wave length longer than the other to provide for the necessary quadrature phasing between the broadside and end-fire arrays as previously described.

The diplexer consists of a bridge made of four one-quarter wavelength lines, one of which is transposed. An absorbing resistor and the television receiver are connected, respectively, to the remaining two bridge terminals.

The explanation of the array in connection with the diplexer may

be described most simply by tracing the paths of the incident and reflected waves throughout the system, rather than on a more rigid mathematical basis.

Assume that an incoming signal approaches the array as indicated by the arrow in Figure 10. The two resulting main waves traveling down the lines from points *A* and *B* in quadrature phasing arrive at
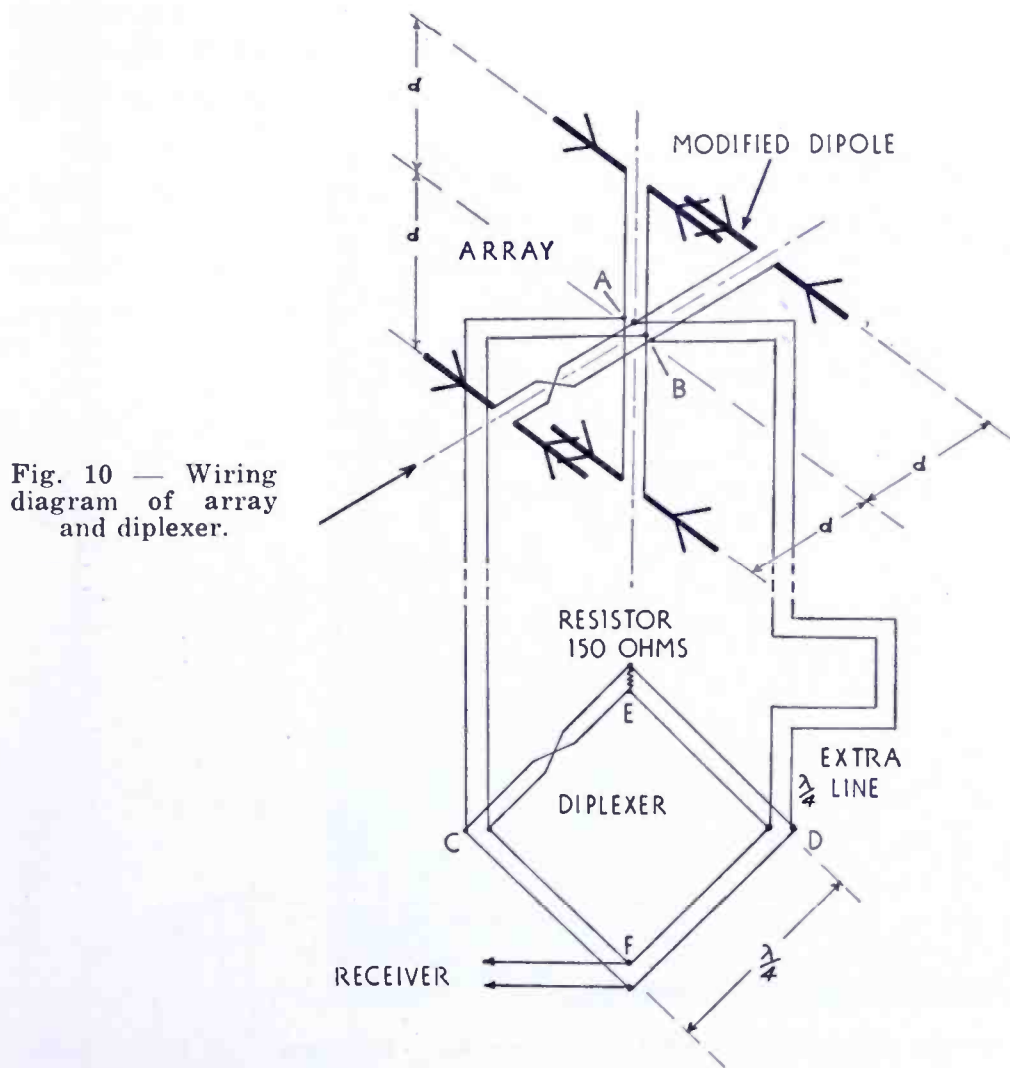
Fig. 10 — Wiring
diagram of array
and diplexer.

points *C* and *D* in-phase due to the quarter-wave difference in line lengths.

The in-phase voltages at *C* and *D* transfer to point *E* in opposite polarity because of the line transposition in one of the diplexer legs. Hence point *E* is at zero potential, and the resistor takes no power. It will be observed that this action is independent of frequency as the lengths of the legs are equal. At frequencies other than that at which

the legs are one-quarter wave length, the legs act as identical reactances attached at points C and D, respectively.

The two main waves arrive in-phase at point F and on to the receiver. In case the receiver input is mismatched, a reflected wave is propagated back to the antenna, where part of the energy is re-radiated and part is re-reflected back down the two lines.

These reflected waves, which left the receiver in-phase, now arrive at points C and D out-of-phase, since one of the waves has traveled over the extra quarter-wave phasing section twice. As the lower legs of the diplexer are not transposed, point F will now be at zero voltage
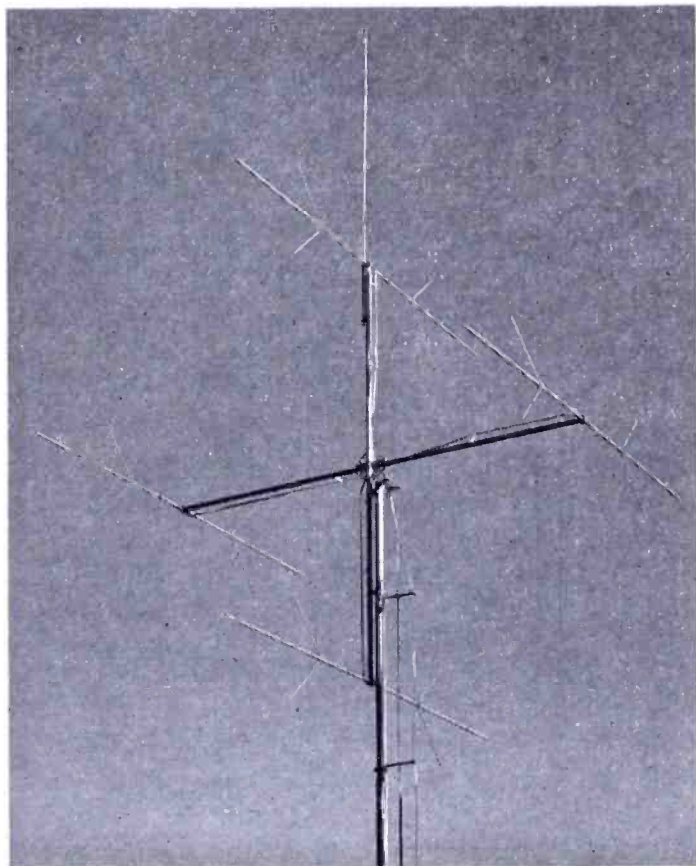
Fig. 11—Reversible-beam array.

and no energy delivered to the receiver. However, the out-of-phase voltages at C and D will now arrive at point E in-phase and be absorbed by the resistor. For complete absorption the value of the resistance should be one-half of the transmission line characteristic impedance, assuming that all lines in the system are identical.

Hence, it is seen that the reflected waves produced by the receiver and antenna mismatches are absorbed in the resistor only. As the diplexer may be installed quite close to the receiver, "ghost" images caused by transmission line reflections can thereby be eliminated.

Assuming now that the signal approaches the array from the opposite direction, a relative phase reversal occurs between the main waves leaving points A and B, and points C and D now become out-of-phase. Under this condition, all of the energy is absorbed

Fig. 12—Diplexer assembly.

by the resistor and none will pass to the receiver.

Thus the resistor serves a dual purpose; absorbing the undesired signal from the backward direction as well as the reflections caused by mismatches in the system. The small reduction in power gain of the array due to this loss in the resistor is more than offset by the broadband, unidirectional properties gained.
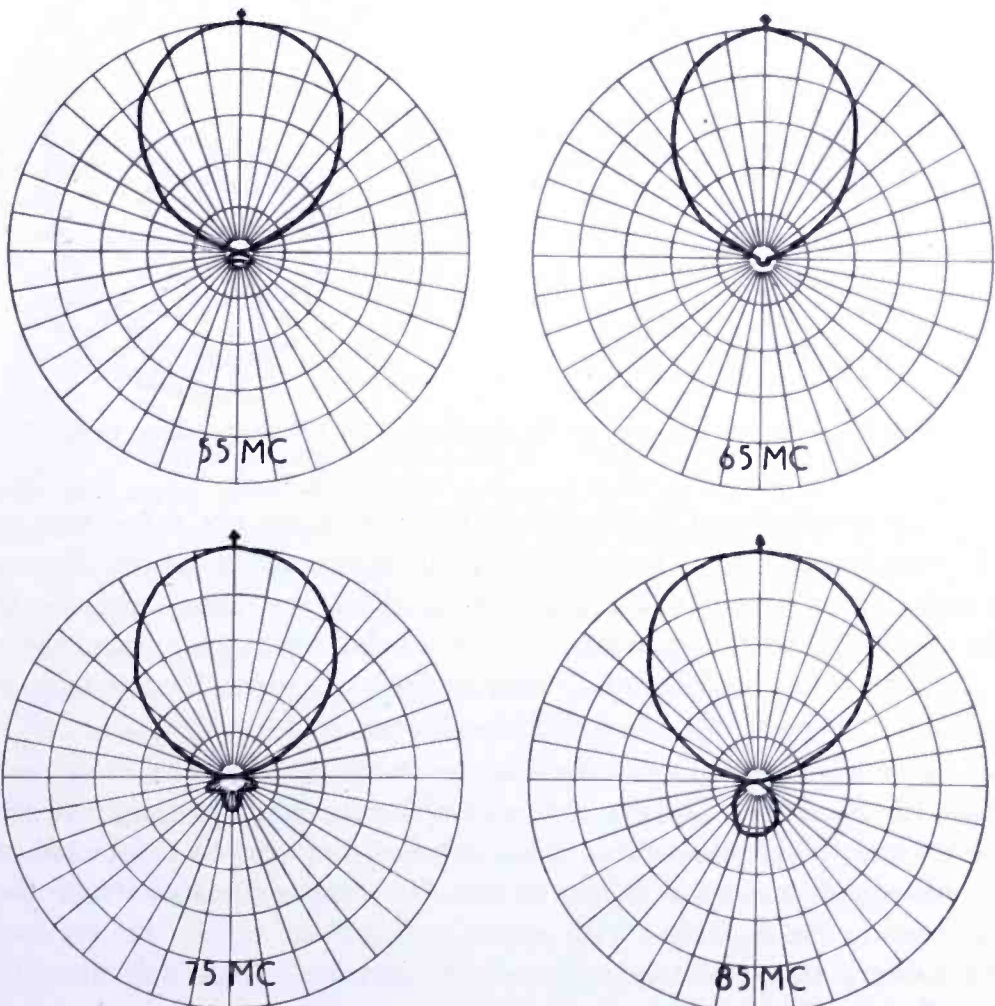
Fig. 13—Measured azimuth field patterns of array in lower band.
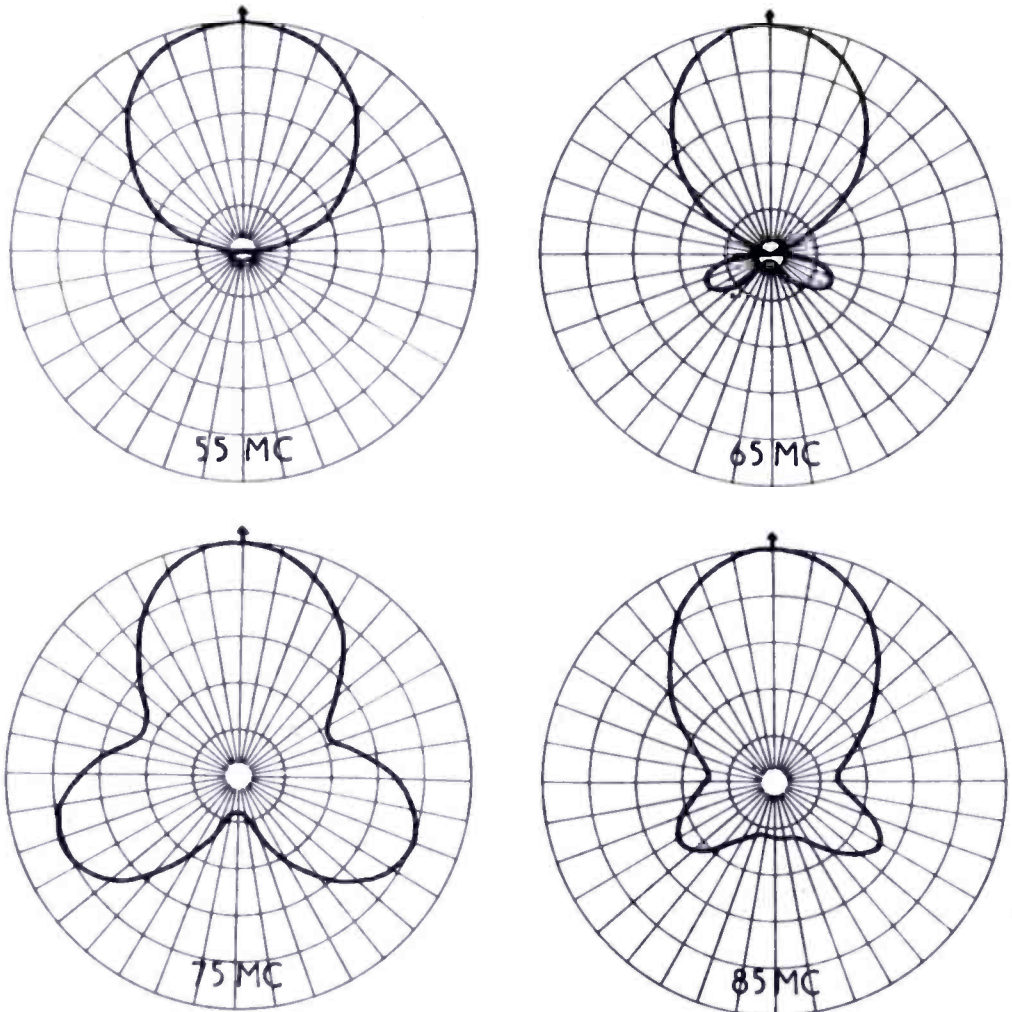
Fig. 14—Measured elevation field patterns of array in lower band.

The amplitudes of the main and reflected waves are a function of the impedances looking back into each of the two-dipole arrays. Hence, for the above action to take place as described, the impedances should be identical. By using arrays of two dipoles each, their impedances vary approximately together, being altered somewhat by the mutual coupling between individual dipoles of each array.

As the undesired signal is absorbed in the resistor, it is evident that the beam may be reversed in direction by interchanging the resistor and the receiver. This beam reversal may also be accomplished by merely transposing either of the two lines extending from the antenna to the diplexer. With either method, best results are secured by using a transposition switch which introduces little discontinuity on the transmission line.

175 MC

195 MC

215 MC
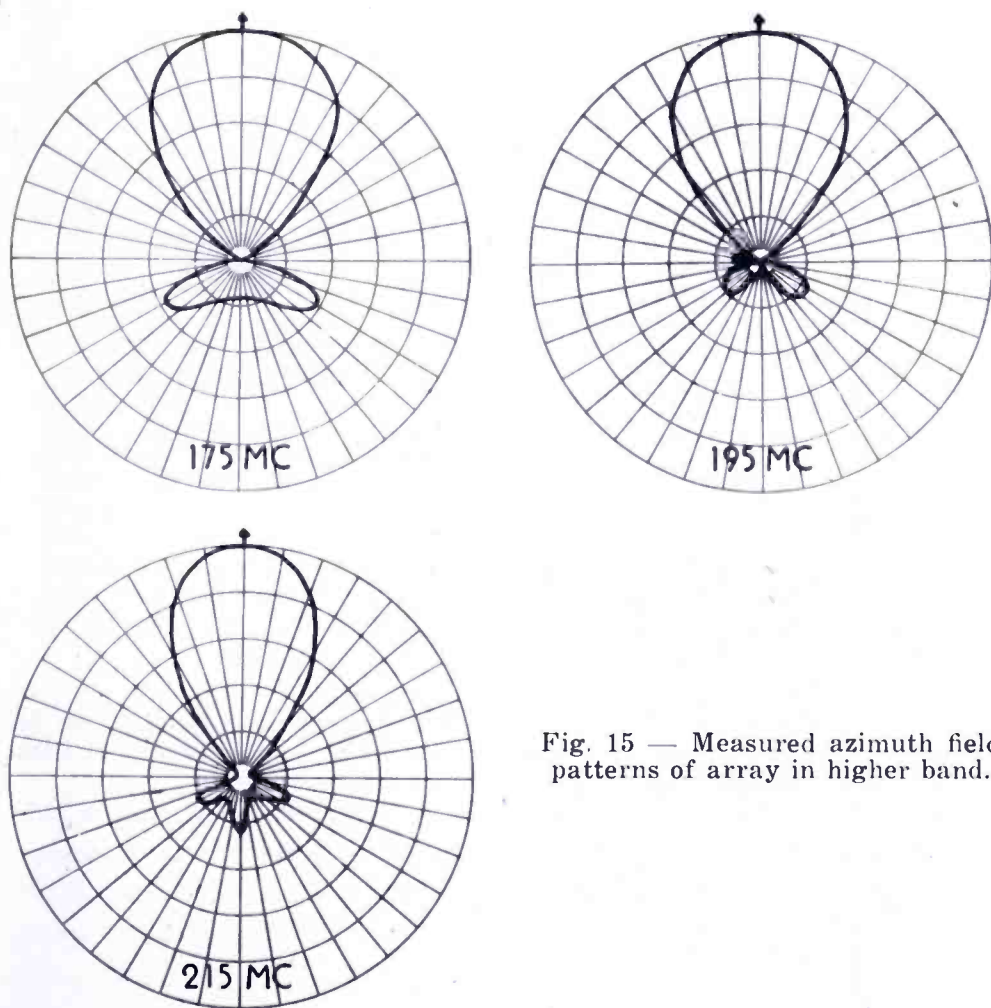
Fig. 15 — Measured azimuth field patterns of array in higher band.

The bridge legs, dipole spacing (*d*), and phasing line in the constructed array were chosen to be one-quarter wave length at a frequency of 65 megacycles. While some error occurs at other frequencies where the phasing line is not one-quarter wave length, overall measurements have shown it not to be serious. These dimensions become three-quarter wavelength at a frequency of 195 megacycles, the midband frequency of the higher band. Thus, proper operation of both the diplexer and dipole pairs is assured at the higher channels also. It will be noticed that the additional half-wavelength effectively added to the phasing line at the higher band compensates for the beam reversal in the higher band previously described, so that the beam remains in the same direction for all twelve channels with a given switch position.

CONSTRUCTION OF THE ARRAY

A photograph of the complete array is shown in Figure 11. The
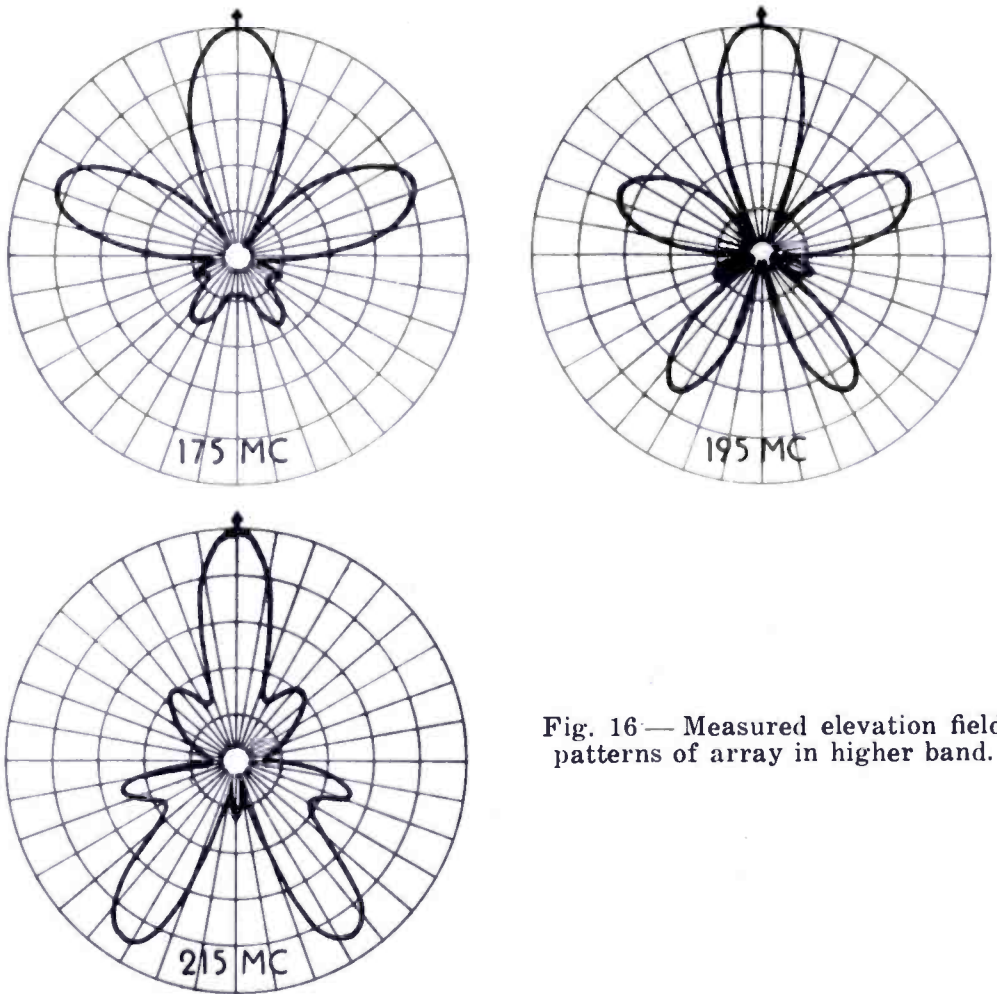
Fig. 16 — Measured elevation field patterns of array in higher band.

vertical rod extending above the antenna affords lightning protection and is not part of the array. The individual dipoles are mounted at the ends of tubular metal arms clamped at right angles at their mid-points. The array is attached on the mast by clamps to the lower portion of the vertical arm. Standard 300-ohm transmission line is used throughout. The lines are carefully supported with stand-off insulators to prevent undesired discontinuities.

The diplexer, (Figure 12), may be strung on spreaders to permit compact installation behind the television receiver. The resistor is an ordinary ½-watt carbon type with a resistance of 150 ohms. A double-pole, double-throw toggle switch (not shown), connected as a trans-position switch in one of the feed lines, may be mounted conveniently near the front of the receiver.

Other variations are possible for certain requirements. For viewers desiring reception from opposite directions, the beam switching may be done automatically with the use of a relay and a tap switch ganged
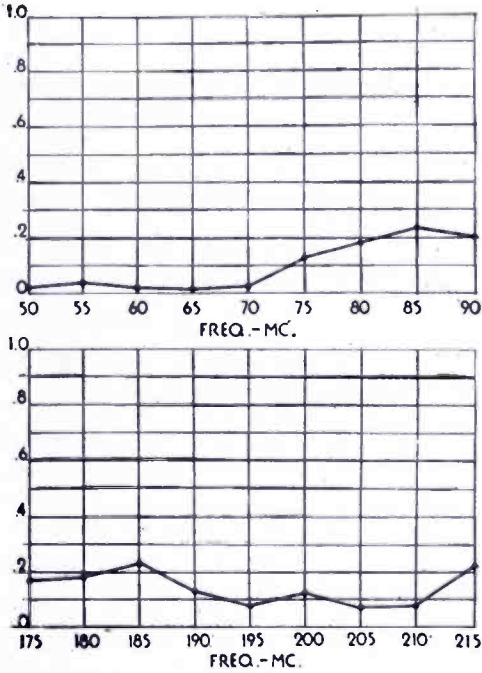
Fig. 17—Backward-to-forward field
ratios of array.
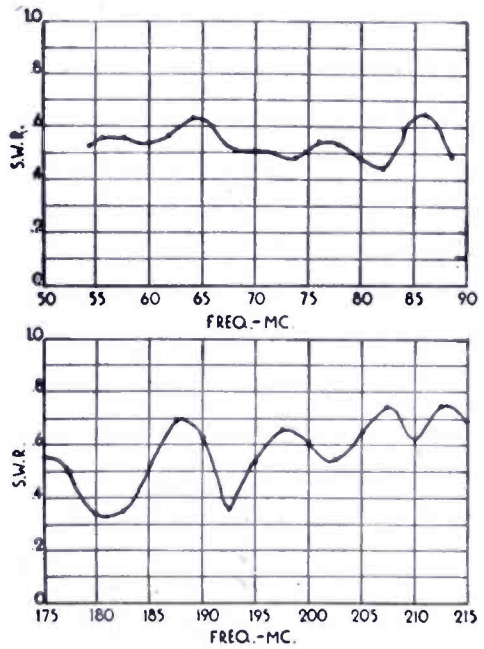
Fig. 18—Standing-wave character-
istics of array.

to the station selector shaft of the receiver. For installations requiring
reception from only one direction, the diplexer may be mounted near
the array without the transposition switch and only one line extended
down to the receiver.
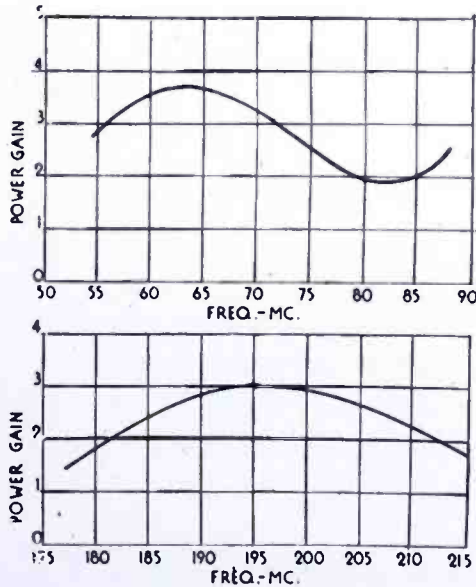
Fig. 19—Power-gain measurements
of array.

FIELD TESTS

Measured azimuth and elevation field patterns of a typical array at representative frequencies throughout both bands are shown in Figures 13, 14, 15 and 16. The backward-to-forward field ratios taken from the measured field patterns are plotted in Figure 17. Slight changes in the length of the quarter-wave phasing line will alter the shape of this curve considerably. For example, a reduction in length of the phasing line to favor Channel six will cause an increase in the backward radiation on Channel two. In addition, the pattern will be changed in the higher band. In some installations minor corrections in this line length may be necessary to compensate for transmission line discontinuities.

The measured input standing-wave characteristics (Figure 18) show approximately a 2:1 standing-wave ratio throughout both bands.

Averaged results of several power gain tests are given in Figure 19. In making the power gain measurements, the array was compared to a matched 300-ohm dipole one-half wave in length at each test frequency.

TRACING DISTORTION IN PHONOGRAPH RECORDS*

By

Murlan S. Corrington

Home Instrument Department, RCA Victor Division,
Camden, N. J.

Summary—The results of Lewis and Hunt for the amount of tracing distortion produced when a spherical stylus traces a groove in a phonograph record have been extended by considering more terms of the series. The extended formulas are more accurate when there is considerable distortion, and permit an estimate of the errors by an examination of the rate of convergence of the series.

Introduction

SOME recent problems in the design of phonograph equipment have made it necessary to extend the results of Lewis and Hunt[1] for the amount of tracing distortion produced when a spherical stylus traces a lateral-cut groove. The explicit results which they gave were obtained by expanding the functions in a power series and using three terms of the series. For large amounts of distortion this degree of approximation is inadequate because of the slow convergence of the series; and since only one term of the resulting series for the distortion is given, there is no estimate of the resulting error in the approximation. The analysis which follows will be equivalent to theirs, but will include more terms of the series. Because of the enormous amount of analytical work required to obtain these results, some of the intermediate results will also be given.

Derivation of Equations

Let one cylindrical wall of the record groove be $Y = a \psi(x + v t)$ where a is an amplitude factor, x is the distance along the groove, v is the velocity of the groove in the $-x$ direction, and t is the time as shown by Figure 1. Let the displacement of the stylus be $Y = S + \phi(x)$, where $\phi(0) = 0$, $\phi'(0) = 0$ and $\phi''(0) > 0$. Assume that the relative curvatures are such that there is always a single point of contact. Then at the point of contact P,

---

$$Y = S + \phi(\Delta x) = a\,\psi(\Delta x + v\,t) \tag{1}$$

and the slopes of the two curves are equal.

$$Y' = \phi'(\Delta x) = a\,\psi'(\Delta x + v\,t). \tag{2}$$

Expand Equation (2) in a power series about $x = 0$.

Fig. 1—Stylus and groove wall.
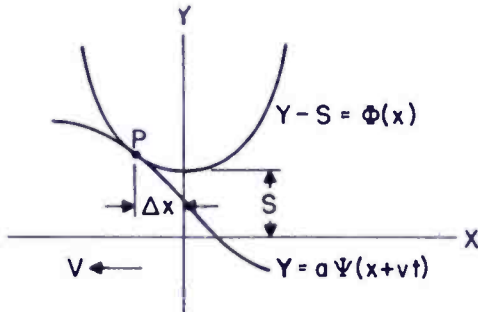
$$\sum_{r=1}^{\infty} \frac{1}{r!}(\Delta x)^r \phi^{r+1}(0) =$$

$$\sum_{s=0}^{\infty} a\,\frac{1}{s!}(\Delta x)^s \psi^{s+1}(v\,t). \tag{3}$$

Assume a series for Δx in powers of a

$$\Delta x = \sum_{t=1}^{\infty} a_t\,a^t \tag{4}$$

$$(\Delta x)^2 = a_1{}^2 a^2 + 2a_1 a_2 a^3 + (2a_1 a_3 + a_2{}^2)\,a^4 + 2(a_1 a_4 + a_2 a_3)\,a^5$$
$$+ (2\,a_1 a_5 + 2\,a_2 a_4 + a_3{}^2)\,a^6 + \cdots \tag{5}$$

$$(\Delta x)^3 = a_1{}^3 a^3 + 3\,a_1{}^2 a_2 a^4 + (3\,a_1{}^2 a_3 + 3\,a_1 a_2{}^2)\,a^5$$
$$+ (3\,a_1{}^2 a_4 + 6\,a_1 a_2 a_3 + a_2{}^3)\,a^6 + \cdots \tag{6}$$

$$(\Delta x)^4 = a_1{}^4 a^4 + 4\,a_1{}^3 a_2 a^5 + \cdots \tag{7}$$

etc.

Substitute Equations (4), (5), (6), (7), etc. in (3), and equate coefficients of like powers of a. This leads to a series of equations.

$$s_2\,a_1 - r_1 = 0 \tag{8}$$

$$s_2\,a_2 + \tfrac{1}{2}\,s_3\,a_1{}^2 - r_2\,a_1 = 0 \tag{9}$$

$$s_2\,a_3 + s_3\,a_1 a_2 + \tfrac{1}{6}\,s_4\,a_1{}^3 - r_2\,a_2 - \tfrac{1}{2}\,r_3\,a_1{}^2 = 0 \tag{10}$$

$$s_2 a_4 + \tfrac{1}{2} s_3 (2 a_1 a_3 + a_2{}^2) + \tfrac{1}{2} s_4 a_1{}^2 a_2 + \frac{1}{4!} s_5 a_1{}^4$$

$$- r_2 a_3 - r_3 a_1 a_2 - \frac{1}{3!} r_4 a_1{}^3 = 0 \qquad (11)$$

etc., where $\psi^n(vt) = r_n$ and $\phi^n(0) = s_n$.

Solving simultaneously for the a's,

$$a_1 = \frac{r_1}{s_2} \qquad (12)$$

$$a_2 = \frac{r_1}{s_2{}^2} \left[r_2 - \frac{1}{2!} \frac{r_1 s_3}{s_2} \right] \qquad (13)$$

$$a_3 = \frac{r_1}{s_2{}^3} \left[- \frac{3}{2!} \frac{r_1 r_2 s_3}{s_2} + \frac{s_3{}^2 r_1{}^2}{2! \, s_2{}^2} \right.$$

$$\left. - \frac{1}{3!} \frac{s_4 r_1{}^2}{s_2} + r_2{}^2 + \frac{1}{2!} r_1 r_3 \right] \qquad (14)$$

$$a_4 = \frac{r_1}{s_2{}^4} \left[r_2{}^3 + \frac{3}{2!} r_1 r_2 r_3 + \frac{1}{3!} r_1{}^2 r_4 - \frac{6}{2!} \frac{r_1 r_2{}^2 s_3}{s_2} - \frac{r_1{}^2 r_3 s_3}{s_2} \right.$$

$$- \frac{4}{3!} \frac{r_1{}^2 r_2 s_4}{s_2} - \frac{1}{4!} \frac{r_1{}^3 s_5}{s_2} + \frac{10}{(2!)^2} \frac{r_1{}^2 r_2 s_3{}^2}{s_2{}^2}$$

$$\left. + \frac{5 r_1{}^3 s_3 s_4}{2! \, 3! \, s_2{}^2} - \frac{5 r_1{}^3 s_3{}^3}{(2!)^3 s_2{}^3} \right] \qquad (15)$$

etc. The expressions become exceedingly complicated very rapidly. Using the relation

$$S(t) = a \psi(\Delta x + v t) - \phi(\Delta x) \qquad (1)$$

$$= a r_0 + \frac{a}{1!} \Delta x \, r_1 + \frac{1}{2!} (\Delta x)^2 (a r_2 - s_2)$$

$$+ \frac{1}{3!} (\Delta x)^3 (a r_3 - s_3) + \cdots$$

$$= b_1 a + b_2 a^2 + b_3 a^3 + b_4 a^4 + \cdots \tag{16}$$

Substituting Equations (4), (5), (6), etc., and (12), (13), (14), etc., in Equation (16), collecting terms and simplifying leads to the values for the b's.

$$b_1 = r_0 \tag{17}$$

$$b_2 = \frac{r_1{}^2}{2\, s_2} \tag{18}$$

$$b_3 = \frac{r_1{}^2}{2\, s_2{}^2} \left[r_2 - \frac{r_1\, s_3}{3\, s_2} \right] \tag{19}$$

$$b_4 = \frac{r_1{}^2}{2\, s_2{}^3} \left[r_2{}^2 + \frac{1}{4}\, \frac{r_1{}^2\, s_3{}^2}{s_2{}^2} - \frac{r_1\, r_2\, s_3}{s_2} - \frac{r_1{}^2\, s_4}{12\, s_2} + \frac{1}{3}\, r_1\, r_3 \right] \tag{20}$$

$$b_5 = \frac{r_1{}^2}{2\, s_2{}^4} \left[r_2{}^3 - \frac{2\, r_1\, r_2{}^2\, s_3}{s_2} + \frac{5}{4}\, \frac{r_1{}^2\, r_2\, s_3{}^2}{s_2{}^2} - \frac{r_1{}^3\, s_3{}^3}{4\, s_2{}^3} \right.$$

$$\left. + r_1\, r_2\, r_3 - \frac{r_1{}^2\, r_2\, s_4}{3\, s_2} - \frac{r_1{}^2\, r_3\, s_3}{2\, s_2} + \frac{r_1{}^3\, s_3\, s_4}{6\, s_2{}^2} + \frac{r_1{}^2\, r_4}{12} - \frac{r_1{}^3\, s_5}{60\, s_2} \right] \tag{21}$$

etc.

Equation (16) can be used to compute the distortion for various groove modulations and arbitrary stylus shape.

APPLICATION TO SINGLE-TONE MODULATION, VERTICAL-CUT RECORD

To derive formulas valid for a spherical stylus of radius r tracing a sinusoidal cylindrical wall, or a vertical groove, let

$$\psi\, (v\, t) = r_0 = \sin k\, x$$

$$r_1 = k \cos k\, x$$

$$r_2 = - k^2 \sin k\, x$$

$$r_3 = - k^3 \cos k\, x, \text{ etc.}$$

where $x = v\, t$ and $k = \dfrac{2\, \pi\, f}{V} = \dfrac{2\pi}{\lambda}$, f is the frequency, v is the velocity

of the groove, and λ is the wave length along the groove.

For a spherical stylus of radius r

$$s_0 = 0 \qquad\qquad s_4 = 3/r^3$$

$$s_1 = 0 \qquad\qquad s_5 = 0$$

$$s_2 = 1/r \qquad\qquad s_6 = 45/r^5$$

$$s_3 = 0 \qquad\qquad s_7 = 0, \text{ etc.}$$

Substituting these values into Equations (17), (18), (19), etc., collecting terms and simplifying,

$$b_1 = \sin k x \tag{22}$$

$$b_2 = \frac{1}{4} r k^2 (1 + \cos 2 k x) \tag{23}$$

$$b_3 = -\frac{1}{8} r^2 k^4 \sin k x - \frac{1}{8} r^2 k^4 \sin 3 k x \tag{24}$$

$$b_4 = -\frac{3}{64} r k^4 - \left(\frac{1}{12} r^3 k^6 + \frac{1}{16} r k^4 \right) \cos 2 k x$$

$$- \left(\frac{1}{12} r^3 k^6 + \frac{1}{64} r k^4 \right) \cos 4 k x \tag{25}$$

etc.

Introduce the dimensionless quantities.

$$A = k a$$

$$R = k r$$

Substitute Equations (22), (23), (24), etc. into Equation (16) and collect terms. This gives the series for each harmonic amplitude, where each term has been normalized by multiplying by k.

$$\text{D-C Term} = \frac{1}{4} RA^2 \left\{ 1 - \frac{3}{16} A^2 + \frac{5}{64} A^4 - \cdots \right\} \tag{26}$$

Fundamental Amplitude $= A - \dfrac{1}{8} R^2 A^3 \left\{ 1 - \dfrac{1}{2} A^2 + \dfrac{5}{16} A^4 - \cdots \right\}$

$$+ \dfrac{1}{192} R^4 A^5 \left\{ 1 - \dfrac{5}{4} A^2 + \cdots \right\} - \dfrac{1}{9216} R^6 A^7 \{ 1 - \cdots \} + \cdots \qquad (27)$$

Second Harmonic Amplitude

$$= \dfrac{1}{4} R A^2 \left\{ 1 - \dfrac{1}{4} A^2 + \dfrac{15}{128} A^4 - \cdots \right\}$$

$$- \dfrac{1}{12} R^3 A^4 \left\{ 1 - \dfrac{15}{16} A^2 + \cdots \right\} + \dfrac{1}{96} R^5 A^6 \{ 1 - \cdots \} - \cdots \qquad (28)$$

Third Harmonic Amplitude

$$= - \dfrac{1}{8} R^2 A^3 \left\{ 1 - \dfrac{3}{4} A^2 + \dfrac{9}{16} A^4 - \cdots \right\}$$

$$+ \dfrac{9}{128} R^4 A^5 \left\{ 1 - \dfrac{3}{2} A^2 + \cdots \right\} - \dfrac{81}{5120} R^6 A^7 \{ 1 - \cdots \} + \cdots \qquad (29)$$

Fourth Harmonic Amplitude

$$= - \dfrac{1}{64} R A^4 \left\{ 1 - \dfrac{3}{4} A^2 + \cdots \right\}$$

$$- \dfrac{1}{12} R^3 A^4 \left\{ 1 - \dfrac{3}{2} A^2 + \cdots \right\} + \dfrac{1}{15} R^5 A^6 \{ 1 - \cdots \} + \cdots \qquad (30)$$

Fifth Harmonic Amplitude

$$= \dfrac{1}{32} R^2 A^5 \left\{ 1 - \dfrac{5}{4} A^2 + \cdots \right\}$$

$$+ \dfrac{25}{384} R^4 A^5 \left\{ 1 - \dfrac{5}{2} A^2 + \cdots \right\} - \dfrac{625}{9216} R^6 A^7 \{ 1 - \cdots \} - \cdots \qquad (31)$$

Sixth Harmonic Amplitude

$$= \frac{1}{512} R A^6 \{1 - \cdots\} + \frac{3}{64} R^3 A^6 \{1 - \cdots\}$$

$$+ \frac{9}{160} R^5 A^6 \{1 - \cdots\} + \cdots \qquad (32)$$

Seventh Harmonic Amplitude

$$= - \frac{1}{128} R^2 A^7 \{1 - \cdots\} - \frac{49}{768} R^4 A^7 \{1 - \cdots\}$$

$$- \frac{2401}{46080} R^6 A^7 \{1 - \cdots\} - \cdots \qquad (33)$$

These formulas must not be used when $RA > 1$ since at that point the stylus will not have single point contact; it will start to "bump" in the groove. An estimate of the error caused by breaking off the double series at the term shown can be made by noting the rate of convergence of successive terms when the numerical values are substituted into the series. *If the pickup used is a velocity responsive device, each formula for the distortion amplitude must be multiplied by the corresponding harmonic number.*

APPLICATION TO A LATERAL-CUT RECORD

A lateral-cut record is equivalent to a push-pull system, so the d-c term and the even-order harmonics produced by the two groove walls cancel.[2] For a 90-degree stylus angle, moving so that its plane is always at right angles to the unmodulated groove, Equations (26) to (33) must be modified[3] by dividing each lateral groove amplitude by $\sqrt{2}$ and multiplying the distortion by $\sqrt{2}$.

$$\text{Fundamental Amplitude} = A - \frac{1}{16} R^2 A^3 \left\{ 1 - \frac{1}{4} A^2 + \frac{5}{64} A^4 - \cdots \right\}$$

$$+ \frac{1}{768} R^4 A^5 \left\{ 1 - \frac{5}{8} A^2 + \cdots \right\} - \frac{1}{73728} R^6 A^7 \{1 - \cdots\} + \cdots \qquad (34)$$

[2] J. A. Pierce and F. V. Hunt, "On Distortion in Sound Reproduction from Phonograph Records", *Jour. Acous. Soc. Amer.*, Vol. 10, pp. 14-28; July, 1938. Also *Jour. Soc. Mot. Pic. Eng.*, Vol. 31, pp. 157-182; August, 1938, Disc. 182-186.

[3] Reference 1, p. 251, Eq. (10).

Third Harmonic Amplitude

$$= -\frac{1}{16} R^2 A^3 \left\{ 1 - \frac{3}{8} A^2 + \frac{9}{64} A^4 - \cdots \right\}$$

$$+ \frac{9}{512} R^4 A^5 \left\{ 1 - \frac{3}{4} A^2 + \cdots \right\} - \frac{81}{40960} R^6 A^7 \{1 - \cdots\} + \cdots \quad (35)$$

Fifth Harmonic Amplitude

$$= \frac{1}{128} R^2 A^5 \left\{ 1 - \frac{5}{8} A^2 + \cdots \right\}$$

$$+ \frac{25}{1536} R^4 A^5 \left\{ 1 - \frac{5}{4} A^2 + \cdots \right\} - \frac{625}{73728} R^6 A^7 \{1 - \cdots\} - \cdots \quad (36)$$

Seventh Harmonic Amplitude

$$= -\frac{1}{1024} R^2 A^7 \{1 - \cdots\} - \frac{49}{6144} R^4 A^7 \{1 - \cdots\}$$

$$-\frac{2401}{368640} R^6 A^7 \{1 - \cdots\} - \cdots \quad (37)$$

where $A = ka = 2\pi \dfrac{a}{\lambda}$, $R = kr = 2\pi \dfrac{r}{\lambda}$, a is the amplitude of the lateral modulation of the groove, measured in the plane of the record, r is the stylus radius (assumed spherical), and λ is the wave length of the sinusoidal modulation measured in the direction of an unmodulated groove. The above formulas must not be used when $RA > \sqrt{2}$ since at this limit single point contact between the stylus and the groove wall no longer exists; the stylus starts to "bump" in the groove. These results are for a reproducing system that responds to the amplitude of the groove motion. *If a velocity responsive pickup is used, each equation should be multiplied by the corresponding harmonic number.* For example, the third harmonic response will be three times as great as shown by Equation (35).

NUMERICAL EXAMPLE

A lateral-cut phonograph record has a tangential groove velocity of 10 inches per second and a lateral groove velocity of 2 inches per second for a pure tone of 4000 cycles per second. The cutting stylus had an included angle of 90 degrees. Find the harmonics in the output from a velocity responsive phonograph pickup having a 2.3-mil spherical stylus.

The variables are determined as follows:

Wavelength $= \lambda = 10/4000 = .0025$ inch.

Amplitude $= a = 2/2\pi(4000) = 1/4000\pi$ inch.

$A = 2\pi a/\lambda = 0.2$.

$R = 2\pi(.0023)(400) = 1.84\pi$.

From Equation (34), the

Fundamental Amplitude $= 0.1839$

$= 91.9$ per cent of true fundamental.

From Equation (35), the

Third Harmonic Amplitude $= -.0113$.

Multiply by 3 because of the velocity pickup.

Per cent third harmonic $= \dfrac{.0113(3)}{.1839} = 18.4$.

From Equation (36), the

Fifth Harmonic Amplitude $= +.0035$.

Multiply by 5 because of the velocity pickup.

Per cent fifth harmonic $= \dfrac{.0035(5)}{.1839} = 9$.

The RMS distortion $= 20$ per cent.

This is somewhat lower than the 30 per cent shown by Pierce and Hunt.[4] Their value was determined by a harmonic analysis with points every 30 degrees of the cycle so is not accurate for large amounts of distortion.

---

[4] Reference 2, page 19, Figure 4.

APPLICATION TO INTERMODULATION TESTS, LATERIAL-CUT RECORD

Assume that two sinusoidal tones are recorded on a lateral-cut record. Then

$$\psi(vt) = r_0 = (a_1/a)\sin k_1 x + (a_2/a)\sin k_2 x \qquad (38)$$

$$r_1 = (a_1 k_1/a)\cos k_1 x + (a_2 k_2/a)\cos k_2 x, \text{ etc.} \qquad (39)$$

where $x = vt$ and $k_n = 2\pi f_n/v = 2\pi/\lambda_n$, f_n is the frequency, v is the velocity of the groove, and λ is the wave length along the groove. Assume a spherical stylus so

$$s_0 = s_1 = s_3 = s_5 = s_7 = 0, \text{ etc.} \qquad (40)$$

$$s_2 = 1/r, \ s_4 = 3/r^3, \ s_6 = 45/r^5, \text{ etc.} \qquad (41)$$

Substituting these values into Equations (17), (19) and (21), collecting terms, simplifying, and applying Equation (16), leads to the equations for the harmonics and intermodulation products. Each term has been modified for the lateral record with 90-degree angle on the cutter, in accord with Reference (3). Terms of seventh and higher orders have been neglected, and from the rate of convergence of the series, when numerical values are used, it can be shown that these higher terms actually are negligible.

$$\text{Coefficient of }\sin k_1 x = a_1 - \frac{k_1 r^2}{16}\{A_1{}^3 + 2A_1 A_2{}^2\}$$

$$+ \frac{k_1 r^2}{64}\{A_1{}^5 + 6A_1{}^3 A_2{}^2 + 3A_1 A_2{}^4\}$$

$$+ \frac{k_1{}^3 r^4}{768}\{A_1{}^5 + 6A_1{}^3 A_2{}^2 + 3A_1 A_2{}^4\} - \cdots \qquad (42)$$

$$\text{Coefficient of }\sin k_2 x = a_2 - \frac{k_2 r^2}{16}\{A_2{}^3 + 2A_1{}^2 A_2\}$$

$$+ \frac{k_2 r^2}{64}\{A_2{}^5 + 6A_1{}^2 A_2{}^3 + 3A_1{}^4 A_2\}$$

$$+ \frac{k_2{}^3 r^4}{768}\{A_2{}^5 + 6A_1{}^2 A_2{}^3 + 3A_1{}^4 A_2\} + \cdots \qquad (43)$$

Coefficient of $\sin 3k_1 x = \dfrac{r^2(3k_1)}{128}\left\{-\dfrac{8}{3}A_1{}^3 + A_1{}^5 + 4A_1{}^3A_2{}^2\right\}$

$$+ \dfrac{r^4(3k_1)^3}{1536}\{A_1{}^5 + 4A_1{}^3A_2{}^2\} + \cdots \qquad (44)$$

Coefficient of $\sin 3k_2 x = \dfrac{r^2(3k_2)}{128}\left\{-\dfrac{8}{3}A_2{}^3 + A_2{}^5 + 4A_1{}^2A_2{}^3\right\}$

$$+ \dfrac{r^4(3k_2)^3}{1536}\{A_2{}^5 + 4A_1{}^2A_2{}^3\} + \cdots \qquad (45)$$

Coefficient of $\sin 5k_1 x = \dfrac{r^2(5k_1)}{640}A_1{}^5 + \dfrac{r^4(5k_1)^3}{7680}A_1{}^5 + \cdots \qquad (46)$

Coefficient of $\sin 5k_2 x = \dfrac{r^2(5k_2)}{640}A_2{}^5 + \dfrac{r^4(5k_2)^3}{7680}A_2{}^5 + \cdots \qquad (47)$

Coefficient of $\sin\,(k_1 \pm 2k_2)\,x =$

$$\dfrac{r^2}{64}(k_1 \pm 2k_2)\{-4A_1A_2{}^2 + 2A_1A_2{}^4 + 3A_1{}^3A_2{}^2\}$$

$$+ \dfrac{r^4}{768}(k_1 \pm 2k_2)^3\{2A_1A_2{}^4 + 3A_1{}^3A_2{}^2\} + \cdots \qquad (48)$$

Coefficient of $\sin\,(2k_1 \pm k_2)\,x =$

$$\dfrac{r^2}{64}(2k_1 \pm k_2)\{-4A_1{}^2A_2 + 2A_1{}^4A_2 + 3A_1{}^2A_2{}^3\}$$

$$+ \dfrac{r^4}{768}(2k_1 \pm k_2)^3\{2A_1{}^4A_2 + 3A_1{}^2A_2{}^3\} + \cdots \qquad (49)$$

Coefficient of $\sin\,(k_1 \pm 4k_2)\,x = \dfrac{r^2A_1A_2{}^4}{128}(k_1 \pm 4k_2)$

$$+ \dfrac{r^4A_1A_2{}^4}{1536}(k_1 \pm 4k_2)^3 + \cdots \qquad (50)$$

Coefficient of sin $(4k_1 \pm k_2)x = \dfrac{r^2 A_1{}^4 A_2}{128} (4k_1 \pm k_2)$

$$+ \dfrac{r^4 A_1{}^4 A_2}{1536} (4k_1 \pm k_2)^3 + \cdots \qquad (51)$$

Coefficient of sin $(2k_1 \pm 3k_2)x = \dfrac{r^2 A_1{}^2 A_2{}^3}{64} (2k_1 \pm 3k_2)$

$$+ \dfrac{r^4 A_1{}^2 A_2{}^3}{768} (2k_1 \pm 3k_2)^3 + \cdots \qquad (52)$$

Coefficient of sin $(3k_1 \pm 2k_2)x = \dfrac{r^2 A_1{}^3 A_2{}^2}{64} (3k_1 \pm 2k_2)$

$$+ \dfrac{r^4 A_1{}^3 A_2{}^2}{768} (3k_1 \pm 2k_2)^3 + \cdots \qquad (53)$$

NUMERICAL EXAMPLE

The curves of Figure 2 show how the intermodulation varies with record diameter when two tones, one at 400 cycles per second, and the other at 4000 cycles per second, with the customary velocities shown on the figure, are cut on a lateral record. A velocity-responsive pick-up was used, and a band-pass filter extending from 3200 to 4800 cycles per second assumed in the measuring equipment. The per cent inter-modulation is defined as the output at 3200 cycles per second plus the 4800 cycle-per-second output, divided by the output at 4000 cycles per second.

Since experimental tests show that a trained observer does not detect less than ten per cent inter-modulation, it is evident that the limiting inside diameter of the records shown can be read off the curves. If the recording level is changed, other curves could be computed.

RPM	R MILS	U₁ IN/SEC	U₂ IN/SEC
33-1/3	1	4.44	1.11
45	1	4.44	1.11
78.26	3	7.04	1.76

F₁ · 400 CPS
F₂ · 4000 CPS
LATERAL-CUT RECORD
VELOCITY PICKUP
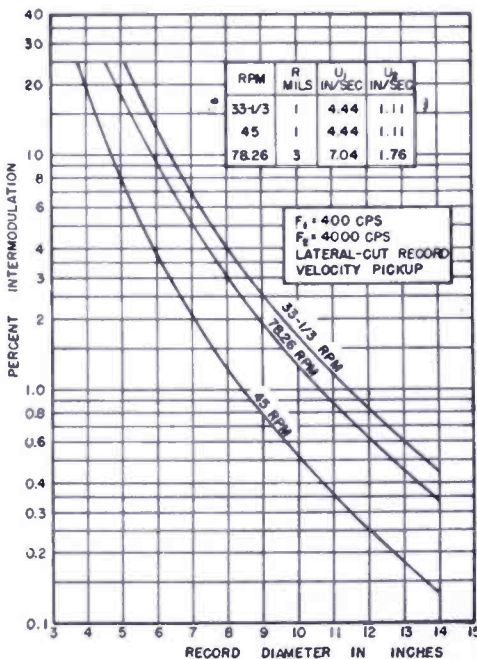
Fig. 2—Variation of intermodulation distortion with record diameter.

CONCLUSIONS

Series approximations have been derived for the first seven harmonics produced when a reproducing stylus traces a sinusoidal groove in a vertical-cut record, and for the corresponding odd-order harmonics produced by a lateral-cut record. For large amounts of distortion the series are more accurate than the schedule analysis used by Pierce and Hunt, and give results somewhat lower. For small amounts of distortion the agreement is better.

Formulas are given for the intermodulation products which occur when two sine waves are recorded simultaneously on a lateral-cut record. A set of curves for 400 and 4000 cycles per second modulation is given for three typical records.

No attempt was made to correct for the error introduced by yield of the record material caused by the pressure of the stylus or cold flow, for the spurious vertical response of a lateral pickup, or for "rattle" of the stylus in the groove.

ANALYSIS BY THE TWO-FREQUENCY INTERMODULATION METHOD OF TRACING DISTORTION ENCOUNTERED IN PHONOGRAPH REPRODUCTION*

BY

H. E. ROYS

Engineering Products Department, RCA Victor Division,
Camden, N. J.

Summary—A form of distortion encountered in record reproduction known as tracing distortion due to the physical size of the reproducing tip, the recorded signal level, and groove velocity has been studied by means of the two-frequency intermodulation method of distortion analysis. Frequencies of 400 and 4000 cycles per second that have been used before have shown such good correlation with listening tests that calculations have been continued. Existing home and transcription records have been evaluated and calculations have also been made to show what improvement can be expected with reproducers having small tip radii. Test frequencies other than 400 and 4000 cycles per second have been considered and found to require different interpretations. Calculations have also been made for single frequency third harmonic components.

INTRODUCTION

ABOUT five years ago, the two-frequency method of distortion testing was investigated as a means of studying tracing and other forms of distortion prevalent in disk recording. The correlation between measurements, theory, and listening tests was so good and the method found to be such a powerful tool that theoretical investigation of tracing distortion, which is the inability of the reproducing stylus to exactly retrace the path of the recording stylus, has been continued.

It is the purpose of this paper to show how the intermodulation method of evaluating tracing distortion can be used to establish limits with respect to linear groove speed, tip size and recording level, the observance of which will keep tracing distortion below objectionable magnitudes. The results can be used either to improve an existing system or to determine the parameters for a new system.
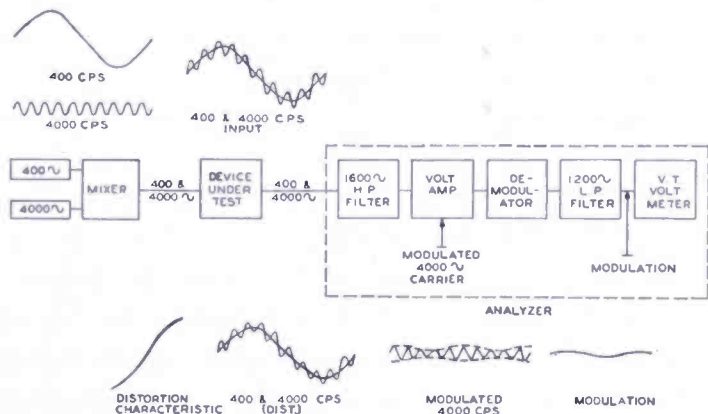
METHOD

In the intermodulation method of distortion testing, two frequencies, preferably one low and the other high, are combined in a linear

---

* Decimal Classification: 681.843.

network to form the test signal.[1,2] The usual practice is to have the higher frequency 12 decibels below the level of the low frequency and to maintain this relation for all tests. According to Frayne and Scoville,[1] with a 12-decibel difference in level, the sensitivity of the intermodulation method, as applied to measurement of distortion in variable-density photographic tracks, is somewhere between 3.2 and 3.8 times greater than the single-frequency harmonic method. Warren and Hewlett[3] in a more recent article have also shown that a simple relationship exists in amplifiers and systems where the transfer characteristic that causes distortion is independent of frequency. However, a more complicated relationship exists in mechanical recording systems, as will be shown, and a simple factor cannot be used for expressing the difference between intermodulation and harmonic values.

Fig. 1 — Intermodulation equipment, 400 and 4000 cycles combined in a linear n e t w o r k with the 4000-cycle signal 12 decibels l o w e r in level than the 400-c y c l e signal. The combined signal is passed to the device under test and from there to the analyzer.

In using this method, the two-frequency signal is applied to the device being tested, and the output is fed to an anlyzer (see Figure 1) which consists of high-pass filter that eliminates the low-frequency component, and passes only the high frequency and the side frequencies which are generated if there is non-linearity in the device. The passed signal is rectified and measured, the carrier is filtered out, and the modulation measured and expressed as a per cent of the magnitude of the high-frequency carrier.

The equipment used utilizes 400 and 4000 cycles as the test frequencies. At one time it was thought that 100 cycles might constitute a better choice of low frequency, but in the mathematical analysis of tracing distortion it will be noted (Equation (7), Appendix A) that the

[1] J. G. Frayne and R. R. Scoville, "Analysis and Measurements of Distortion in Variable-Density Recording", *Jour. Soc. Mot. Pict. Eng.*, Vol. 32, p. 648, June, 1939.

[2] J. K. Hilliard, "Distortion Tests by the Intermodulation Method", *Proc. I.R.E.*, Vol. 29, No. 12, pp. 614-620, December, 1941.

[3] W. J. Warren and W. R. Hewlett, "An Analysis of the Intermodulation Method of Distortion Measurement", *Proc. I.R.E.*, Vol. 36, No. 4, pp. 457-466, April, 1948.

velocity of the low-frequency signal appears as a squared term and with the normal recording characteristic (constant amplitude below 400 cycles) a full amplitude 100-cycle tone would have only one-fourth the velocity of a 400-cycle tone. With a 100-cycle tone the intermodulation term would be one-sixteenth of that obtained with 400 cycles. Such a low frequency, therefore, does not appear to be as significant as the higher frequency for tracing distortion study.

Intermodulation Frequencies of 400 and 4000 Cycles per Second

Since such good agreement was obtained in the earlier work[4] between measurements and calculations, the theoretical investigation was continued. Calculations based upon the work of Lewis and Hunt[5], were made at different recording levels and groove velocities to determine the intermodulation tracing distortion resulting when various tip sizes are used during playback. The results of these calculations are shown in the following curves. The curves are plotted with groove velocity as the abscissa and distortion as the ordinate. The term "groove velocity" is used in the sense of the linear speed of the record past the reproducing device. This is a function of recording diameter and turntable speed, whereas the terms "stylus velocity" and "recording level" are used to designate the transverse velocity of the cutting stylus which depends upon amplitude and frequency of the signal being recorded. In order to correlate groove velocity with recording diameter, three inclined lines drawn from the axis and marked "78", "45" and "33$\frac{1}{3}$ R.P.M." are used in conjunction with the ordinate scale on the right-hand side marked "recording diameter". The groove velocity for any recording diameter can be found by noting the point at which a horizontal line from the selected recording diameter intersects the sloping line of the turntable speed. Additional lines of the proper inclination may be drawn for other turntable speeds.

Figure 2 shows the results for a recorded stylus velocity of 2 inches per second for the 400-cycle tone and 0.5 inches per second for the 4000-cycle frequency when using reproducing tips of 2.8, 2.3, 1.25, and .75 mils radii. The smallest tip size was at that time being used for the 45-r.p.m. (revolution-per-minute) phonograph system. The velocity of 2 inches or approximately 5 centimeters per second is the

---

[4] H. E. Roys, "Intermodulation Distortion Analysis as Applied to Disk Recording and Reproducing Equipment", *Proc. I.R.E.*, Vol. 35, No. 10, pp. 1149-1152, October, 1947.

[5] W. D. Lewis and F. V. Hunt, "A Theory of Tracing Distortion in Sound Reproduction from Phonograph Records", *Jour. Acous. Soc. Amer.*, Vol. 12, pp. 348-365, January, 1941.

recommended NAB normal recording level (peak levels may be 10 or 12 decibels higher) for 33⅓-r.p.m. transcriptions, but the normal level for the 78-r.p.m. phonograph record is known to be somewhat higher. The reproducing stylus tip radius for 78-r.p.m. phonograph disks ranges from 2.5 to 3.2 mils, and the recommended size for 33⅓-r.p.m. transcriptions is 2.3 mils*.

The minimum inside recording diameter for 78-r.p.m. recordings is 3.75 inches, and if, in Figure 2, we project a horizontal line from this recording diameter to the sloping line marked "78 R.P.M.", we find that the resulting groove velocity is 15.5 inches per second. At this groove velocity, the intermodulation distortion for a 2.8-mil reproducer tip is about 6 per cent. For a 33⅓-r.p.m. transcription, the minimum recording diameter is 7.5 inches, and the groove velocity at this diameter is 13 inches per second. The intermodulation distortion for a 2.3-mil playback tip is about 7 per cent.
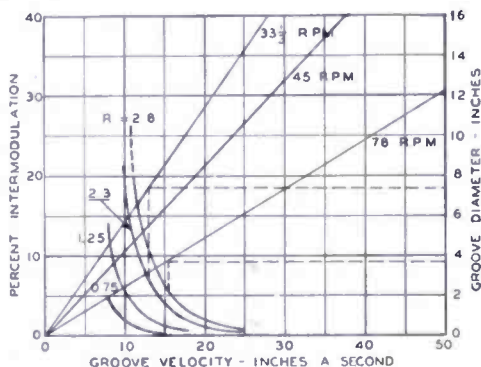

Fig. 2—Calculated intermodulation for frequencies of 400 and 4000 cycles. Stylus velocity 2 inches per second for 400 cycles and .5 inches per second for 4000 cycles. The stylus tip radius is indicated.

Listening tests over a widerange system by persons accustomed to hearing direct studio programs, have indicated that 10 per cent intermodulation, as based upon test frequencies of 400 and 4000 cycles is a good practical acceptance limit. Below 10 per cent the distortion is not readily detectable unless compared directly with the material being recorded. Therefore the calculated values of 7 per cent and less for a recording level of 2 inches per second appear to be acceptable. An allowance must be made for peak values, and, it was thought when the first calculations were made that these peak values may be 10 or 12 decibels greater than the assumed normal level of 2 inches a second. A more recent study has indicated that the peak values may be somewhat lower.

Calculations were therefore made as before except that the recording level was increased 12 decibels, resulting in a stylus velocity of 8 inches (approximately 20 centimeters) per second for the 400-cycle frequency. These results appear in Figure 3, and if we select 10 per cent intermodulation distortion as the acceptable value, we find that the minimum recorded diameter of the 78-r.p.m. phonograph record

---

* NAB has recently recommended a stylus radius of 2.0 mils for transcriptions.
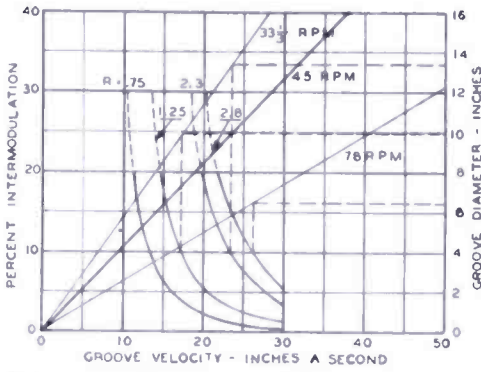
Fig. 3 — Same conditions as for Figure 2, except the levels have been increased 12 decibels.
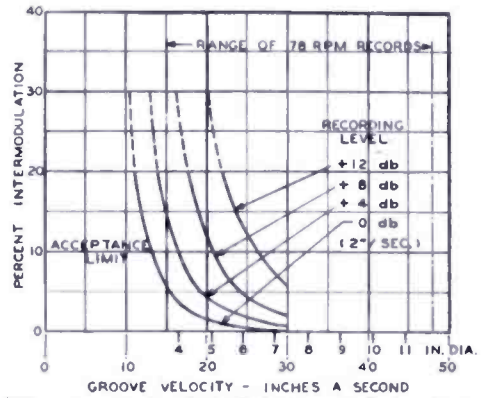

Fig. 4—Calculated intermodulation for a 2.8-mil tip radius and for different recording levels. The diameter range of the 78-r.p.m. records is shown.

should be about 6.5 inches instead of 3.75. The minimum diameter for the 33⅓-r.p.m. transcription when using a 2.3-mil playback tip radius should be 13½ inches or only 2 inches less than the starting diameter. Persons making phonograph demonstrations often use only the outside portion of the recording, a practice which tends to confirm the results of our calculations.

Calculations were also made at recording levels 4 and 8 decibels above the initial level of 2 inches per second in order to determine what peak level would be satisfactory for the present reproducer tip sizes. The curves of Figure 4 show for 78-r.p.m. recordings, when using a playback tip radius of 2.8 mils, that the plus 3-decibel level should not be exceeded, in order to keep the intermodulation distortion below 10 per cent. The calculations for transcriptions at 33⅓ r.p.m.

Fig. 5 — Intermodulation encountered with a 2.3-mil tip, as normally used for transcription, for different recording levels.

and 2.3-mil tip radius, Figure 5, show that the maximum recording level should not greatly exceed a level of plus 2 decibels.

FINE GROOVE RECORDING
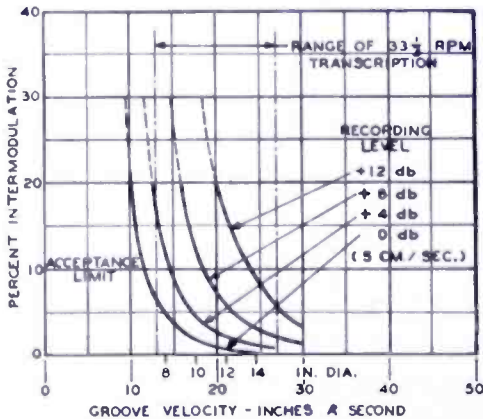
It is obvious from the preceding curves that improvements can be obtained by resorting to grooves with small bottom radii and pickups with appropriately small reproducing tips. Such method of reducing tracing distortion has been advo-

cated by a number of authors[5-7] and a public demonstration of high quality recordings was given by F. C. Barton[8] in 1933 in which a reproducer having a stylus tip radius of 1.0 mil was used.

Recently the new RCA 45-r.p.m. phonograph system[9] was announced and prior to that a fine groove long playing record[10] was made available to the public. Both of these new systems use a 1.0-mil tip and require a turntable speed other than the conventional 78 r.p.m.

Figure 6 shows the improvements obtained with a 1-mil tip when using a new value of recording level. A peak recording level for the combined frequencies of about 14 centimeters per second, was used since it is believed to be more representative of present day practices. Calculations were also made at the above level for transcriptions. For 78-r.p.m. records a tip radius of 3 mils was chosen instead of 2.8, and the recording level was changed to 22 centimeters per second, which is believed to be in better accord with present day practices. A minimum diameter of 4.89 inches has been selected for the 45.-r.p.m. record in order not to exceed 10 per cent intermodulation.

It is of interest to consider the use of fine groove records for transcription services. Using a 1.0-mil radius reproducing tip, it is possible to obtain better than 15 minutes of recording time with a disk 12 inches in diameter at either 45 or 33⅓ r.p.m. Based upon the acceptance limit of 10 per cent intermodulation for test frequencies of 400 and 4000 cycles, the innermost diameter should be 6.6 inches for 33⅓ and 4.89 inches for 45 r.p.m., which corresponds to a minimum groove velocity of 11.5 inches per second.

Another means of expressing the results of Figure 6, is illustrated by Figure 7, in which intermodulation is plotted with respect to per cent of maximum playing time. It is assumed that the recordings extend to their innermost diameters which would be 6.6 inches for 33⅓-r.p.m., 4.89 inches for 45-r.p.m. fine groove transcriptions, and 7½ inches for regular transcriptions, and 3¾ inches for 78-r.p.m. records.

[6] J. A. Pierce and F. V. Hunt, "On Distortion in Sound Reproduction from Phonograph Records", *Jour. Acous. Soc. Amer.*, Vol. 10, pp. 14-28, July, 1938.

[7] L. W. Sepmeyer, "Tracing Distortion in the Reproduction of Constant Amplitude Recordings", *Jour. Acous. Soc. Amer.*, Vol. 13, pp. 276-280, January, 1942.

[8] F. C. Barton, "High-fidelity Lateral Cut Disk Records", *Jour. Soc. Mot. Pict. Eng.*, Vol. 22, pp. 179-182, March, 1934. Demonstration before the New York Section, December 13, 1933.

[9] B. R. Carson, A. D. Burt and H. I. Reiskind, "A Record Changer and Record of Complementary Design", pp. 173-190 of this issue.

[10] P. C. Goldmark, R. Snepvangers and W. S. Bachman, "A New Long-Playing Disk Recording System", paper delivered by Goldmark before the New York Section of I.R.E., September 8, 1948.

Figure 8 shows recommended groove dimensions for fine groove transcriptions having 224 grooves per inch which would actually permit 16.5 minutes of undistorted playing time. This sketch is for an unmodulated groove and contact between side walls and stylus is shown well below the surface of the record. Such a wide groove permits variations due to changes in depth of cut and included angle due to

I.T. RPM	TIP SIZE MILS	STYLUS VEL. INCHES/SEC.	
		400 ∿	4000 ∿
33⅓	1.0	4.44	1.11
33⅓	2.3	4.44	1.11
45	1.0	4.44	1.11
78	3.0	7.04	1.76
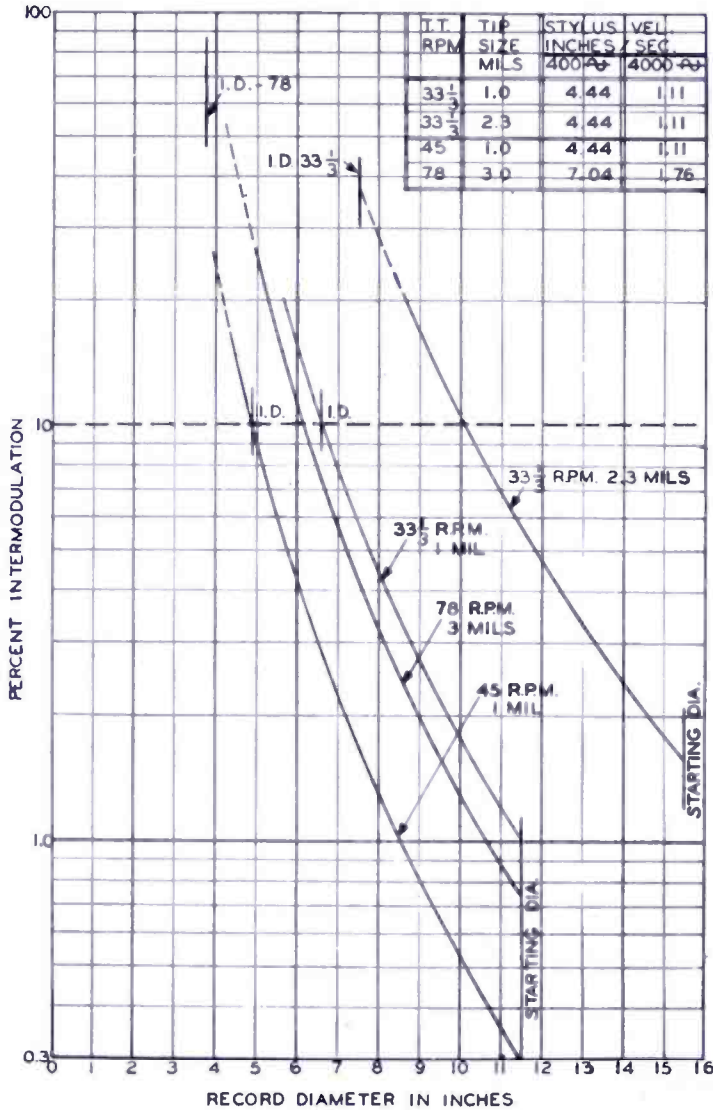
Fig. 6 — Intermodulation calculations for existing phonograph and transcription recordings and for fine groove records at 45 and 33⅓ r.p.m.

heavy modulation (resulting in pinch effect during playback) without causing the reproducing stylus to ride the rough top surfaces of the groove and produce considerable noise.

INTERMODULATION FREQUENCIES OF 100 AND 7000 CYCLES PER SECOND

Intermodulation equipment is on the market which uses frequencies other than 400 and 4000 cycles. As can be seen by the mathematical

expression of intermodulation (Equation (7), Appendix A) different test frequencies result in different values of intermodulation while the other parameters are held the same. Figure 9 shows the calculated intermodulation for the same parameters as used for Figure 2 except that frequencies of 100 and 7000 cycles were used. The voltage applied to the recording amplifier was assumed to be the same in both cases with the high-frequency signal 12 decibels lower in level. The recorded amplitude for 100 and 400 cycles is equal due to the constant amplitude recording characteristic for the lower frequencies but the

Fig. 7 — Results of Figure 6 expressed in per cent maximum playing time assuming innermost diameters of 3¾ inches for 78 r.p.m., 7.5 inches for 33⅓ r.p.m. transcriptions, and 4.9 inches and 6.6 inches for 45 and 33⅓-r.p.m. fine groove transcriptions.

resulting velocity for 100 cycles is one-fourth the 400-cycle value.

Examining the results of Figure 9 it is seen that for a minimum diameter of 3¾ inches for 78-r.p.m. records the intermodulation is approximately 1 per cent instead of 6. For 33⅓-r.p.m. transcriptions and a minimum diameter of 7.5 inches, the resulting intermodulation is about 1.5 per cent instead of 7 per cent as obtained with frequencies of 400 and 4000 cycles.

Increasing the recording level 12 decibels and again assuming an acceptable limit of 10 per cent intermodulation we find from Figure 10 that the minimum diameters for home and transcription recordings

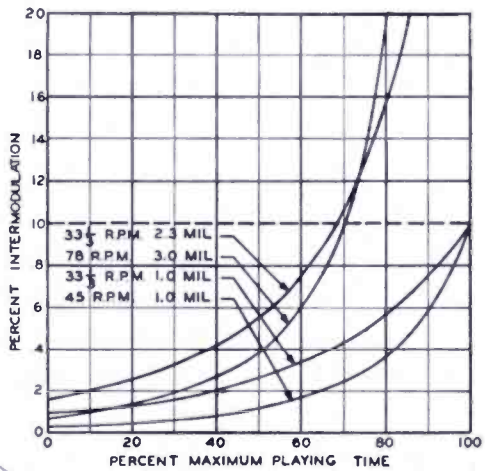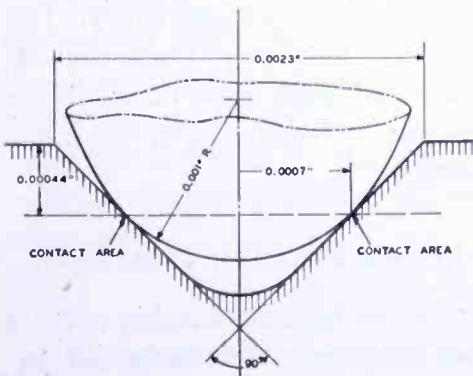Fig. 8 — Cross section of groove with 0.0005-inch bottom radius showing playback stylus contacting the side walls in an ideal manner.
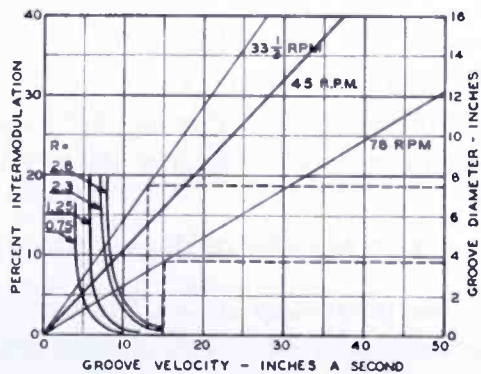
Fig. 9 — Intermodulation calculations for frequencies of 100 and 7000 cycles for different tip sizes and 0-decibel recording level.

should be about 4 and 8.7 inches respectively instead of 6.5 and 13½ inches. Thus it is evident that different intermodulation frequencies require a different interpretation of results. A higher low frequency such as 400 cycles offers the advantage that the tracing distortion will be greater and hence easier to detect where cutter distortion is appreciable. For cutter distortion as introduced by the magnetic system is essentially independent of wavelength and so unaffected by the choice intermodulation frequencies. Cutter distortion masks low values of tracing distortion and hence should be several times less than tracing distortion for accurate analysis.

INTERMODULATION FREQUENCIES OF 400 AND 8000 CYCLES PER SECOND

As a matter of interest, calculations were also made for a frequency of 8000 cycles instead of 4000 cycles while using 400 cycles as the lower
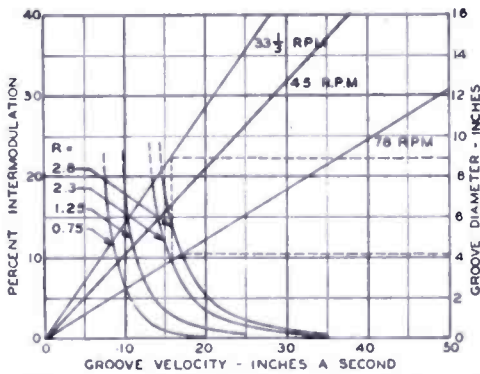
Fig. 10—Calculations for 100 and 7000 cycles for a + 12-decibel recording level.
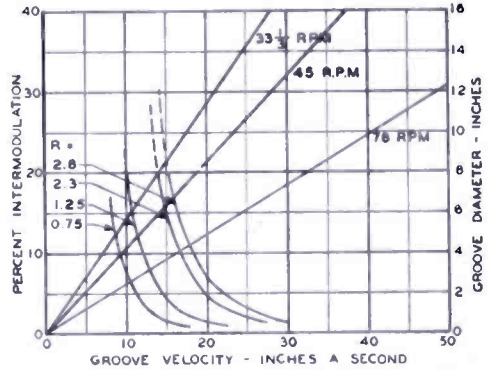
Fig. 11 — Calculated intermodulation for 400 and 8000 cycles at 0-decibel recording level.

frequency. These were made at the normal recording level of 2 inches per second and for the same playback tip sizes as used previously. The results are illustrated in Figure 11. The significance of these calculations is not known, as listening tests have not been made on the basis of 400 and 8000 cycles so that an acceptable intermodulation value has not been established for these frequencies.

COMPARISON OF HARMONIC AND INTERMODULATION RESULTS

As previously stated, the sensitivity of the intermodulation method as compared with the single-frequency harmonic method is not expressible as a simple ratio but depends on the test frequencies in a rather complicated manner. Using the equations developed by Lewis and Hunt, Appendix B, the third harmonic distortion was calculated

for 400 cycles at the normal recording level of 2 inches per second, for 4000 cycles at the same velocity, and for 4000 cycles at a reduced level of 12 decibels. These curves, Figure 12, show that the third harmonic distortion for 4000 cycles at a normal level of 2 inches per second, results in tracing distortion 1.5 times greater than the calculated intermodulation. For 400 cycles at the same level the third harmonic distortion is approximately one-hundredth of the intermodulation value and for 4000 cycles at the reduced level of 12 decibels, the third harmonic distortion is approximately one-fortieth the calculated intermodulation distortion. Listening tests indicate that the intermodulation distortion, as measured here, is a far more reliable index of the impairment of quality than harmonic measurements.
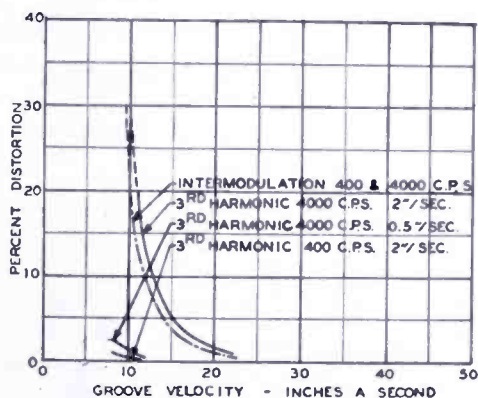
Fig. 12—Comparison of intermodulation and harmonic calculations for 400 and 4000 cycles.
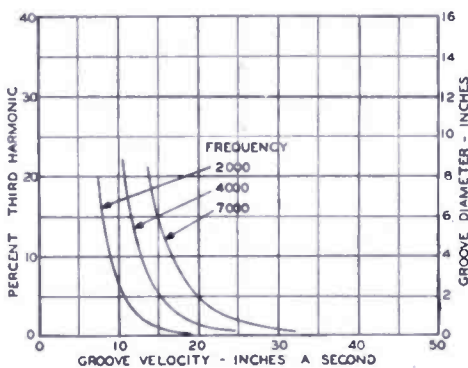
Fig. 13—Third harmonic calculations for frequencies of 2000, 4000, and 7000 cycles when reproduced with a 2.3-mil tip. A recording level of 2 inches per second was assumed.

THIRD HARMONIC CALCULATIONS

Single-frequency third harmonic calculations were made for frequencies of 2000, 4000 and 7000 cycles per second and the results are shown in Figure 13 for a recorded velocity of 2 inches per second, and a reproducer tip radius of 2.3 mils. As might be expected, tracing distortion increases as the frequency is increased and the wavelength becomes shorter and more directly comparable in magnitude to the stylus tip.

EFFECT OF YIELD OF RECORD MATERIAL

The equations derived by Lewis and Hunt do not take into account yield of record material due to the force at the stylus tip. It has been observed in one particular case that the effect of yield was to reduce the predicted distortion. Measurements made with a vinyl pressing of

a frequency record showed much less third harmonic tracing distortion than anticipated by calculations. The loss in response due to record yield was measured and the distortion recalculated for the level obtained when the playback loss was subtracted from the recorded level, as indicated of the optical pattern method of calibration. The agreement between measured and calculated results was then found much better (Table I). It is probable that in many cases the yield of record material, resulting in an apparent loss of level, accounts for the fact that the distortion heard is much less than that indicated by calculations based upon the actual recorded level.

Table I—Effective Reduction in Recorded Level Due to Playback Loss Results in Reduced Distortion

| Frequency Cycles | Per cent 3rd Harmonic Distortion | | | Playback Loss Decibels |
| | Measured | Calculated | | |
		No Loss	With Loss	
6000	3.0	12	4.4	3.7
4000	2.5	7.0	3.8	2.1
2000	1.8	2.0	1.4	.7
1000	1.5	.6	.6	0.

ACCURACY OF CALCULATION

M. S. Corrington upon reviewing the work of Lewis and Hunt concluded that more terms of the series were necessary for greater accuracy[11]. His analysis of single-frequency harmonic distortion results in less distortion, whenever high values of distortion are encountered, but where the distortion is low, the difference is less. His more recent analysis of intermodulation results in the same conclusion.

In view of Corrington's work, the high values of intermodulation distortion (above 15 or 20 per cent) given in this report are probably in error; however, this does not necessarily greatly alter the results, for once distortion is encountered the rate of increase is so great, as the groove velocity is decreased, that changes in magnitude will not greatly shift the "breaking point," and hence alter the conclusions.

CONCLUSIONS

1. Present disk recording standards and practices permit objec-

---

[11] M. S. Corrington, "Tracing Distortion in Phonograph Records", pp. 241-253 of this issue.

tionable amount of tracing distortion during playback, especially when high recording levels are maintained at the inside of the disk. This is true for both 78-r.p.m. phonograph records and $33\frac{1}{3}$-r.p.m. transcriptions used in radio broadcasting.

2. The magnitude of the tracing distortion is normally low for the high groove velocities encountered at the outside of the disk, but at the inside where the groove velocities are low it becomes great and overshadows distortion due to other causes.

3. Tracing distortion might be eliminated by forming the groove with a stylus similar to the playback stylus, but this amounts to adopting the embossing system of recording. No satisfactory high-quality embossing means has so far been found.

4. In order to reduce tracing distortion while using the present type of sharp-edged cutting tool, it is necessary to have the curvature of the groove, due to modulation, much less than the curvature of the reproducing tip. There are three possible ways of accomplishing this:

  a. Decreasing the recorded level, which will result in relatively higher background noise.

  b. Increasing the turntable speed. This will decrease the playing time.

  c. Decreasing the radius of the reproducer tip (using an appropriate smaller tip radius for recording).

ACKNOWLEDGMENT

APPENDIX A

INTERMODULATION DISTORTION

In the article on the "Theory of Tracing Distortion", Lewis and Hunt give the following equation for the displacement of the stylus tip during playback:

$$S_{lateral}(t) = q(Vt) + \tfrac{1}{2}r^2 q'^2 q'' \cos^2 B + \ldots\ldots$$

<div align="right">(Equation (10′), p. 351)   (1)</div>

This is a general equation where $q(Vt)$ represents the fundamental tone and $\tfrac{1}{2}r^2 q'^2 q''$ is an expression of a distortion term.

The distortion term, when two different tones are combined, is developed and is expressed as follows:

$$\frac{r^2}{2}(q'^2 q'') = -\tfrac{1}{2}r^2\,(\tfrac{1}{4}A_1{}^3 k_1\,(\sin 3k_1 Vt + \sin k_1 Vt)$$

$$+ \tfrac{1}{4}A_2{}^3 k_2\,(\sin 3k_2 Vt + \sin k_2 Vt) + \tfrac{1}{4}A_1{}^2 A_2\,[\,(2k_1 + k_2)\sin (2k_1 + k_2)\,Vt$$

$$+ (2k_1 - k_2)\sin (2k_1 - k_2)\,Vt + 2k_2 \sin k_2 Vt\,]$$

$$+ \tfrac{1}{4}A_1 A_2{}^2\,[\,(k_1 + 2k_2)\sin (k_1 + 2k_2)\,Vt$$

$$+ (-k_1 + 2k_2)\sin (-k_1 + 2k_2)\,Vt + 2k_1 \sin k_1 Vt\,]).$$

$$\text{(Equation (30), p. 356)} \qquad (2)$$

This equation is in terms of displacement of the stylus and must be differentiated with respect to time if we wish to have an expression in terms of stylus velocity.

Table II—Separating into Frequency Terms and Differentiating with Respect to Time.

Frequency	Displacement	Velocity
f_1	$(a_1 - \tfrac{1}{8}\,r^2 A_1{}^3 k_1 - \tfrac{1}{4}\,r^2 A_1 A_2{}^2 k_1)\sin k_1 Vt$	$(a_1 k_1 V - \tfrac{1}{8}\,r^2 k_1{}^2 A_1{}^3 V - \tfrac{1}{4}\,r^2 k_1{}^2 A_1 A_2{}^2 V)\cos k_1 Vt$
$3f_1$	$(-\tfrac{1}{8}\,r^2 A_1{}^3 k_1)\sin 3k_1 Vt$	$(-\tfrac{3}{8}\,r^2 k_1{}^2 A_1{}^3 V)\cos 3k_1 Vt$
f_2	$(a_2 - \tfrac{1}{8}\,r^2 A_2{}^3 k_2 - \tfrac{1}{4}\,r^2 A_1{}^2 A_2 k_2)\sin k_2 Vt$	$(a_2 k_2 V - \tfrac{1}{8}\,r^2 A_2{}^3 k_2{}^2 V - \tfrac{1}{4}\,r^2 A_1{}^2 A_2 k_2{}^2 V)\cos k_2 Vt$
$3f_2$	$(-\tfrac{1}{8}\,r^2 A_2{}^3 k_2)\sin 3k_2 Vt$	$(-\tfrac{3}{8}\,r^2 A_2{}^3 k_2{}^2 V)\cos 3k_2 Vt$
$(2f_1 + f_2)$	$-\tfrac{1}{8}\,r^2 A_1{}^2 A_2\,(2k_1 + k_2)\sin (2k_1 + k_2)Vt$	$-\tfrac{1}{8}\,r^2 A_1{}^2 A_2\,(2k_1 + k_2)^2 V\cos (2k_1 + k_2)Vt$
$(2f_1 - f_2)$	$-\tfrac{1}{8}\,r^2 A_1{}^2 A_2\,(2k_1 - k_2)\sin (2k_1 - k_2)Vt$	$-\tfrac{1}{8}\,r^2 A_1{}^2 A_2\,(2k_1 - k_2)^2 V\cos (2k_1 - k_2)Vt$
$(f_1 + 2f_2)$	$-\tfrac{1}{8}\,r^2 A_1 A_2{}^2\,(k_1 + 2k_2)\sin (k_1 + 2k_2)Vt$	$-\tfrac{1}{8}\,r^2 A_1 A_2{}^2\,(k_1 + 2k_2)^2 V\cos (k_1 + 2k_2)Vt$
$(-f_1 + 2f_2)$	$-\tfrac{1}{8}\,r^2 A_1 A_2{}^2\,(-k_1 + 2k_2)\sin (-k_1 + 2k_2)Vt$	$-\tfrac{1}{8}\,r^2 A_1 A_2{}^2\,(-k_1 + 2k_2)^2 V\cos (-k_1 + 2k_2)Vt$

Taking the values of the constants as given by Hunt and Lewis and making the following substitutions,

$$A = ka \qquad (3)$$

where a = amplitude of stylus motion

$$k = \frac{w}{V}$$

$$w = 2\pi f$$

and V = groove velocity (not stylus velocity).

Therefore $$A = \frac{wa}{V} \tag{4}$$

$$= \frac{2\pi fa}{V} \tag{5}$$

$$= \frac{u}{V} \tag{6}$$

where u = stylus-velocity.

To take into account the included angle between the groove side walls, the expression for the distortion terms must be multiplied by

$$\cos^2 B,$$

where $B = \frac{1}{2}$ the included angle between the groove side walls.

For 90 degrees included angle between the side walls

$$B = 45 \text{ degrees}$$

and $\cos^2 B = .5.$

Substituting the above expression for stylus velocity and multiplying by $\cos^2 B$ gives the coefficients shown in Table III.

The intermodulation distortion analyzer, see Figure 1, has a high-pass filter in the input circuit which passes everything above 1600 cycles. This filter excludes the 400-cycle fundamental tone and the first three harmonics. The 4000-cycle carrier and side frequencies are transmitted through to the rectifier. In practically all measurements, an additional filter of the low-pass type, having a cut-off frequency of 6000 cycles, was used in the input circuit, in order to minimize the effects of surface noise, and as a result only frequencies between 1600 and 6000 cycles were passed through to the rectifier. The only terms to be concerned with then are the velocity terms for the side frequencies, $2f_1 + f_2$ or 4800 cycles, $2f_1 - f_2$ or 3200 cycles, and the 4000-cycle carrier. In stating the modulation, the ratio of the sum of the velocities

of the side frequencies to the carrier frequency velocity is expressed as a percentage.

Table III

Frequency	Velocity Coefficients
f_1	$u_1 - \dfrac{\pi^2 r^2 f_1^2}{2V^4}\left(\dfrac{u_1^3}{2} + u_1 u_2^2\right)$
$3f_1$	$-\tfrac{3}{4}\dfrac{\pi^2 r^2 f_1^2 u_1^3}{V^4}$
f_2	$u_2 - \dfrac{\pi^2 r^2 f_2^2}{2V^4}\left(\dfrac{u_2^3}{2} + u_1^2 u_2\right)$
$3f_2$	$-\tfrac{3}{4}\dfrac{\pi^2 r^2 f_2^2 u_2^3}{V^4}$
$(2f_1 + f_2)$	$-\dfrac{\pi^2}{4}\dfrac{r^2 u_1^2 u_2}{V^4}(2f_1 + f_2)^2$
$(2f_1 - f_2)$	$-\dfrac{\pi^2}{4}\dfrac{r^2 u_1^2 u_2}{V^4}(2f_1 - f_2)^2$
$(f_1 + 2f_2)$	$-\dfrac{\pi^2}{4}\dfrac{r^2 u_1 u_2^2}{V^4}(f_1 + 2f_2)^2$
$(-f_1 + 2f_2)$	$-\dfrac{\pi^2}{4}\dfrac{r^2 u_1 u_2^2}{V^4}(-f_1 + 2f_2)^2$

$$\frac{\pi^2}{2} = 4.93483; \qquad \frac{\pi^2}{4} = 2.46741; \qquad \frac{3\pi^2}{4} = 7.40224; \qquad \frac{\pi^2}{8} = 1.2337$$

The expression for the percentage intermodulation is

Per Cent Intermodulation =

$$\frac{\dfrac{\pi^2}{4}\dfrac{r^2 u_1^2 u_2}{V^4}\left[(2f_1 + f_2)^2 + (2f_1 - f_2)^2\right]}{u_2 - \dfrac{\pi^2}{2}\dfrac{r^2 f_2^2}{V^4}\left(\dfrac{u_2^3}{2} + u_1^2 u_2\right)} \times 100 \qquad (7)$$

where

$u_1 = $ low frequency (400-cycle) velocity,

$u_2 = $ high frequency (4000-cycle) velocity, down 12 decibels,

$f_1 = 400$ cycles per second,

$f_2 = 4000$ cycles per second,

$r = $ radius of playback stylus tip,

$V = $ groove velocity.

APPENDIX B

THIRD HARMONIC DISTORTION

In order to calculate the third harmonic distortion for a single frequency, set u_2 equal to zero in the expressions for the stylus velocity which were derived in Appendix A. For the fundamental frequency term for the velocity coefficient

$$u_1 - \frac{\pi^2 r^2 f_1^2}{2V^4} \left(\frac{u_1^3}{2} + u_1 u_2^2 \right). \tag{1}$$

Setting $u_2 = 0$

$$u_1 - \frac{\pi^2}{4} \cdot \frac{r^2 f_1^2 u_1^3}{V^4}. \tag{2}$$

The third harmonic velocity coefficient term is

$$- \frac{3}{4} \frac{\pi^2 r^2 f_1^2 u_1^3}{V^4}. \tag{3}$$

Per Cent Third Harmonic Distortion $= \dfrac{-\dfrac{3}{4} \dfrac{\pi^2 r^2 f_1^2 u_1^3}{V^4}}{u_1 - \dfrac{\pi^2}{4} \dfrac{r^2 f_1^2 u_1^3}{V^4}} \times 100 \tag{4}$

where

$f_1 = $ frequency,

$u = $ recorded velocity of f_1,

$r = $ radius of playback stylus tip,

$V = $ groove velocity.

THE ELECTRON COUPLER — A DEVELOPMENTAL TUBE FOR AMPLITUDE MODULATION AND POWER CONTROL AT ULTRA-HIGH FREQUENCIES*†

PART I. PHYSICAL THEORY

By

C. L. CUCCIA

Research Department, RCA Laboratories Division,
Princeton, N. J.

Summary—The Electron Coupler is a new type of electron tube, using spiralling electrons, which is installed between an ultra-high-frequency power generator and its load and permits modulation and control of the power reaching the load.

This paper discusses the physical theory of the basic tube which consists of an electron gun, an input cavity which is connected to a power source, an output cavity which is connected to a load, and a collector. These cavities are adjacent and are tuned to the cyclotron frequency of a magnetic field which is parallel to the axis of alignment of the two cavities; they have the property, when excited, of introducing an alternating electric field normal to the magnetic field. The electron beam passes through both cavities, absorbing the radio-frequency power in the input cavity in the form of rotational energy, and delivering this power to the output cavity and load or to the collector. The power transfer may be controlled by varying either the beam current or the electron transit time in the output cavity.

INTRODUCTION

THE Electron Coupler** is a fundamentally new type of electronic ultra-high-frequency and microwave tube, using a beam of spiralling electrons, which is installed as shown in Figure 1, between a power generator and its load and permits effective and complete control of the power reaching the load. Its development is an outgrowth of the extensive work on spiral beam tubes for both

---

* Decimal Classification: R385.4.

† This is the first of two papers describing the Electron Coupler. The second paper, by C. L. Cuccia and J. S. Donal, Jr. will describe the engineering of the Electron Coupler.

** "The Electron Coupler—A Developmental Tube, Utilizing New Principles, for the Modulation and Control of Power at the Ultra-High Frequencies" by C. L. Cuccia and J. S. Donal, Jr., which was presented at the 1949 National I.R.E. Convention in New York.

frequency and amplitude modulation which has been done at these laboratories.[1-4]

The Electron Coupler is essentially a modulator tube and may be utilized for high-power, rapid-rate amplitude modulation. With one of the two methods of power-transfer control which will be shown to be possible in the basic tube, the Electron Coupler will display the characteristics of a unilateral impedance such that the output circuit, which includes the load, is isolated from the input circuit which includes power source thereby eliminating frequency pulling of the power source during a modulation cycle. No amplification is possible with the Electron Coupler—its use being confined to its properties as a control impedance for the high power which is easily obtained at the ultra-high frequencies using such tubes as magnetrons.
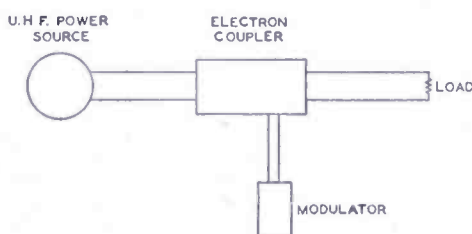

Fig. 1—Block diagram of an Electron Coupler circuit showing the Electron Coupler as the control impedance between the power source and the load. The modulator controls the amount of power which reaches the load.

The following treatment will discuss the physical principles and electron optics involved in the transfer of power using a beam of spiralling electrons, and will be a theoretical development based on an idealized set of conditions.

DESCRIPTION OF THE FUNDAMENTAL OPERATION OF THE ELECTRON COUPLER

Before embarking on a description of the physical theory of the Electron Coupler, it is convenient to state the basic principles of operation involved.

The Electron Coupler is a power transfer device which is capable of efficiently transferring high power from a generator to a load. By using a signal from a modulating wave source to control the transfer, amplitude modulation of the generator, as seen by the load, may be achieved.

[1] Lloyd P. Smith and Carl I. Shulman, "Frequency Modulation and Control by Electron Beams," *Proc. I.R.E.*, Vol. 35, No. 7, pp. 644-657, July, 1947.

[2] G. R. Kilgore, C. I. Shulman, and J. Kurshan, "A Frequency Modulated Magnetron for Super-High Frequencies," *Proc. I.R.E.*, Vol. 35, No. 7, pp. 657-664, July, 1947.

[3] J. S. Donal, Jr., R. R. Bush, C. L. Cuccia, and H. R. Hegbar, "A 1-Kilowatt Frequency-Modulated Magnetron for 900 Megacycles," *Proc. I.R.E.*, Vol. 35, No. 7, pp. 664-669, July, 1947.

[4] J. S. Donal, Jr., and R. R. Bush, "A Spiral-Beam Method for the Amplitude Modulation of Magnetrons," *Proc. I.R.E.*, Vol. 37, No. 4, pp. 375-382, April, 1949.

A basic but not definitive structure utilizing a beam of spiralling electrons for the transfer and control of power is shown in Figure 2. Two suitable resonant cavities are seen to be adjacent and in a magnetic field which is parallel to the axis of alignment of the two cavities. These cavities have the particular property, when excited, of introducing an alternating electric field normal to the magnetic field. An electron beam passes successively through the cavities and is then collected.

The mechanism of power transfer may be described qualitatively as follows in terms of the interactions in three regions.
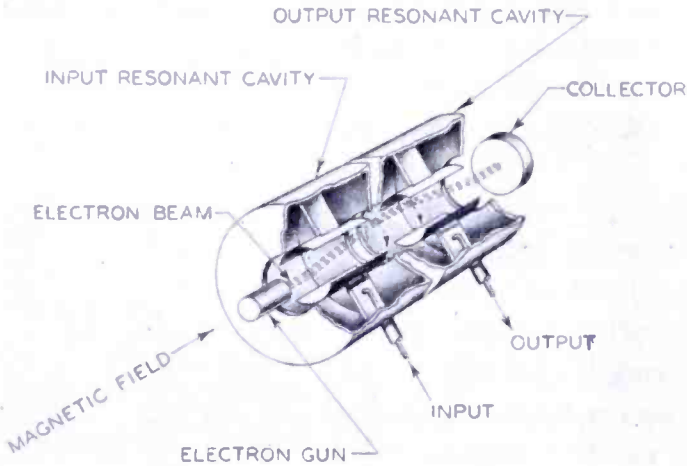

Fig. 2—Diagram of a basic Electron Coupler structure showing the adjacent cavities each of which produces a transverse electric field when excited—and the rotating coupling beam. The rotating beam configuration in the output cavity is illustrated for the case when all of the rotational energy is given up to the output load (see Figure 6). In an operable Electron Coupler of this design, the output cavity would be rotated 90 degrees with respect to the position shown here, in order to prevent electromagnetic coupling between this cavity and the input cavity.

Region I—The Input Cavity

When microwave power is transmitted into the input cavity, an alternating electric field is produced which is transverse to the path of the electrons. As the electrons enter the cavity due to an accelerating potential, interaction with the combined transverse electric field and axial magnetic field will cause the electrons to spiral with increasing radius as they proceed through the cavity. For a cylindrical beam of small cross-sectional area and for a particular magnetic field which is related to the frequency of the input energy, all of the electrons, as they spiral, will lie on the line directrix of a cone whose base radius will be a function of the energy absorbed by the rotating beam. The rotating beam will display the characteristics of a pure resistance and the total power absorbed will be a function of the parameters involved.

Region II—The Inter-Cavity Space

In the inter-cavity space, the rotating electrons will not acquire or give up any energy due to the absence of transverse electric fields and thus the electrons, as they pass through this space, will form a rotating line directrix of a cylinder whose radius will be equal to that of the base of the cone formed by the directrix beam in the input cavity.

Region III—The Output Cavity

As the rotating-directrix electron beam enters the output cavity whose resonant frequency* is the same as that of the input cavity, currents will be induced in the output circuit of this cavity and a transverse alternating electric field will be produced due to these induced currents which will extract the rotational energy from the rotating beam.

To clearly visualize the operation of the Electron Coupler, the electron energies must be identified. The electron receives energy from the accelerating beam potential which causes it to proceed axially to the collector. This energy will determine the transit time. It receives rotational energy from the transverse electric field in the input cavity and it is this rotational energy only which can be given up to the output system. In this way the Electron Coupler is a true power transfer device and may be regarded as a variable-coupling electronic power transformer.

If all of the rotational energy is extracted from the beam by the output cavity, the electron beam will arrive at the collector with only axial velocity and no rotational velocity. For this case the directrix beam in the output cavity will form a cone whose base radius (at the entrance to the output cavity) is equal to the radius of the entering rotating beam and whose apex is at the exit of the output cavity. This is a special case. In general, however, any rotational energy which is not extracted by the output cavity, will go to the collector.

The power transfer may be varied either by controlling the beam current or by controlling the transit time in the output cavity which will control the ratio of the rotational energy extracted by the secondary cavity system to the rotational energy reaching the collector. When the beam current is varied, the input impedance of the input cavity changes. However, during transit time control, no reaction

---

* If a cavity of the cavity-magnetron type is used for the output system and if its frequency is tuned to some integral multiple of the frequency of the input cavity, frequency multiplication will take place. Aspects of spiral-beam frequency multipliers were presented to the I.R.E. Electron Tube Conference at Syracuse University in June 1947 by C. L. Cuccia and H. Johnson. Acknowledgment was made at that time of the independent work on spiral beam frequency multipliers by R. Jepson at the Columbia Radiation Laboratory.

back to the input cavity is experienced—the tube thereby functioning as a unilateral control impedance.

THEORY OF THE ELECTRON COUPLER

The following discussion is concerned with the electron optics and interactions in each of the three regions previously defined. The theory will be idealized with particular regard to the use of fringeless, truly transverse electric fields which will be confined to the regions in which they are produced. No electromagnetic coupling is assumed to exist between the input and the output systems.

ELECTRON BEHAVIOR AND POWER CONSIDERATIONS IN REGION I (INPUT CAVITY)

Consider the case of an electron with charge, e, and mass, m, which enters the input cavity with axial velocity (in the z direction) due to a constant accelerating potential V_{b_1}. In this input cavity, an axially directed magnetic field of density, H, and an alternating, transverse, x-directed electric field described by $E_1 e^{j\omega_c t}$, due to the driving generator, shall be produced in addition to the potential, V_{b_1}. The equations determining the motion of the electron in this space are

$$m\ddot{x} = -|e| E_1 e^{j\omega_c t} - |e| H\dot{y}$$
$$m\ddot{y} = +|e| H\dot{x}$$
$$m\ddot{z} = 0 \tag{1}$$

where $|e|$ is the absolute value of the charge on the electron. Let the frequency of the alternating transverse electric field be related to the magnetic field such that

$$f_c = \frac{\omega_c}{2\pi} = \frac{1}{2\pi} \frac{|e|}{m} H. \tag{2}$$

This is the cyclotron frequency and all frequencies in the text will conform to this relation.

Equations (1) and (2) may be combined to form the following pair of differential equations:

$$\ddot{v}_x + \omega_c^2 v_x = j \frac{|e|}{m} \omega_c E_1 e^{j\omega_c t} \tag{3}$$

$$\ddot{v}_y + \omega_c^2 \, v_y = -\frac{|e|}{m} \, \omega_c E_1 e^{j\omega_c t} \qquad (4)$$

If the electron enters the input cavity at $t = t_1$, then the entrance conditions may be specified as follows:

$$\text{at } t = t_1 \qquad v_x = 0 \qquad \dot{v}_x = 0$$

$$v_y = 0 \qquad \dot{v}_y = 0. \qquad (5)$$

Solving for v_x yields

$$v_x = \frac{1}{2} \frac{|e|}{m} \frac{E_1}{j\omega_c} \cos \omega_c \, (t - t_1) \, e^{j\omega_c t_1} + \frac{1}{2} \frac{|e|}{m} \, (t - t_1) \, E_1 e^{j\omega_c t}. \qquad (6)$$

The first term of Equation (6) is of importance only near the entrance to Region I where it describes the initial gyrations of the electron until it becomes properly phased with respect to the transverse electric field. If the transit time through Region I is made sufficiently large, this term may be neglected.

The cone-directrix nature of the beam, as previously mentioned, may be verified as follows: The particular-integral solutions for v_x and v_y may be integrated to yield the expressions

$$x = \frac{1}{2} \frac{|e|}{m} \, E_1 \frac{(t - t_1)}{\omega_c} \, e^{j\omega_c t}, \qquad (7)$$

$$y = -\frac{j}{2} \frac{|e|}{m} \, E_1 \frac{(t - t_1)}{\omega_c} \, e^{j\omega_c t}. \qquad (8)$$

By referring to Figure 3, it is seen that since the azimuthal angle, φ, of an electron may be expressed as

$$\varphi = \tan^{-1} \frac{x}{y} \qquad (9)$$

the substitution of Equations (7) and (8) into Equation (9), shows that the angle, φ, of any electron traveling through the input cavity at any instant of time is the same regardless of its transit time. If the electron source is of vanishingly small cross section, then as the transit time increases, both x and y will increase linearly and it is

evident that the electrons lie on a line directrix of a cone and that this directrix beam rotates with an angular velocity equal to ω_c. Each individual electron, however, will actually spiral as it proceeds through the cavity.

The radius of rotation of the cone-directrix beam may be found by taking the absolute magnitude of Equation (7) such that

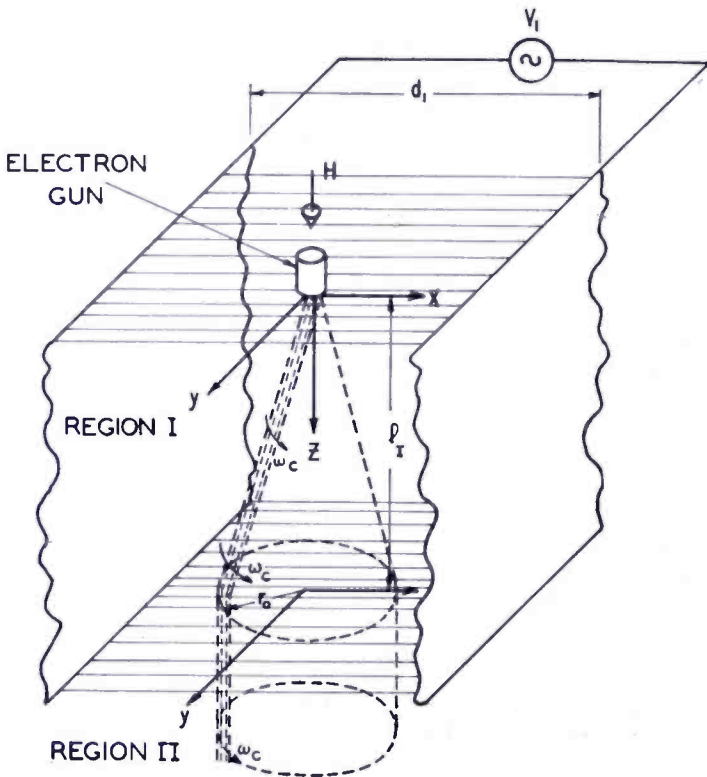$$|x| = \frac{1}{2} \frac{|e|}{m} \frac{(t - t_1)}{\omega_o} E_1. \tag{10}$$

Fig. 3 — Diagram showing the cone-directrix beam in Region I and the cylinder directrix beam in Region II. The effect due to the initial gyrations of the electrons as they enter Region I is not shown.

Equation (10) may be written in practical units as follows:

$$x = 2.36 \frac{E_1 l_1}{V_{b_1}^{1/2} f_c} \text{ centimeters} \tag{11}p*$$

where f_c is the frequency in megacycles, E_1 is in peak volts per centimeter, l_1 is the distance in centimeters, and V_{b_1} is in volts. The transit time, $t - t_1$, is related to V_{b_1} such that

---

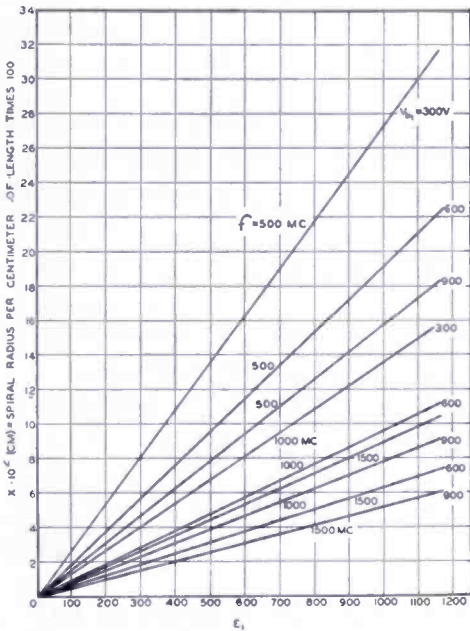* p used in this manner denotes an equation in practical units.

Fig. 4—Chart of the spiral beam radius per centimeter length of travel in Region I as a function of E_1 for $f = 500$, 1000, and 1,500 megacycles and $V_{b_1} = 300$, 600, and 900 volts as derived from Equation (11).

$$(t - t_1) = \frac{l_1\, 10^{-7}}{6 \sqrt{V_{b_1}}} \text{ seconds.} \qquad (12)\text{p}$$

Equation (11) is charted in Figure 4 in terms of radius per centimeter of axial travel by the electrons for the frequency range between 500 and 1500 megacycles and beam potentials from 300 to 900 volts. The fact that the radius increases as the beam potential decreases is, of course, due to the fact that the electron transit-time is reduced and the electron remains in a particular region of field longer.

The power which will be absorbed by a number of electrons which constitute a current I_0, will be

$$P = \frac{v_x^2}{2 \dfrac{|e|}{m}} I_0. \qquad (13)$$

Substituting the second term of Equation (6) into Equation (13) gives

$$P = E_1^2 \frac{(t - t_1)^2}{8} \frac{|e|}{m} I_0. \qquad (14)$$

Using Equation (12), Equation (14) may be written in practical units as follows:

$$P = \frac{1}{16} E_1^2 l_I^2 \frac{I_0}{V_{b_1}} \text{ watts} \qquad (15)\text{p}$$

where I_0 is the beam current in amperes. If the total length of Region I is l_I, the maximum power which can be absorbed by the beam* is

---

* When the frequency of the input power is not equal to the cyclotron frequency, the electron beam will twist into a spiral or corkscrew shape to an extent depending upon the deviation from the cyclotron frequency. A reactive component of the impedance presented by the electron beam will
(Continued on next page)

$$P = \frac{1}{16} E_1^2 l_I^2 \frac{I_0}{V_{b_1}}. \tag{15-a)p}$$

For a particular spiral radius at a particular frequency and current, the power absorbed by the directrix beam will be the same for any transit time. Substituting Equation (11) into Equation (15), results in

$$P = 1.122 \times 10^{-2} f_c^2 I_0 x^2 \text{ watts} \tag{16)p}$$

which shows that the power absorbed is proportional to the square of the radius of rotation and is independent of the beam potential.

If the boundaries of the transverse electric field are a distance d_1 apart, where d_1 is measured in centimeters, then the voltage, V_1, producing the field is

$$V_1 = d_1 E_1 e^{j\omega_c t} \tag{17)p}$$

and the electronic resistance presented by the beam is found to be

$$R_1 = \frac{d_1^2 E_1^2}{2P} = 8 \left[\frac{d_1}{l_I} \right]^2 \frac{V_{b_1}}{I_0} \tag{18)p}$$

where R_1 is the beam resistance in ohms.

LIMITATIONS IN ULTRA-HIGH-FREQUENCY POWER ABSORPTION BY THE ELECTRON BEAM IN THE INPUT CAVITY

A. Space Charge Limitations

If space charge is introduced into a region where an electrostatic potential exists, this potential will be depressed in the region of the charge. For a particular geometry and potential, there will correspond a maximum amount of charge or current which can be sustained. If this value is exceeded, the potential at some point in the vicinity of the charge will suddenly drop to zero and some of the charge will turn back. This will be a condition of instability which will place a major

appear. This is caused by the fact that as the electrons proceed through the input cavity, they will first absorb energy thereby spiralling with increasing radius to some maximum radius and then a decrease in radius will occur thereby withdrawing energy from the field in accordance with the nature of reactance. This will decrease the rotational energy available to the output cavity—in fact, if $(\omega - \omega_o) \tau_I = 2\pi$, where ω is the angular frequency of the input power, the rotational energy possessed by the beam as it emerges from the input cavity will be equal to zero. A corkscrew action of the beam will also take place in the output cavity. It is therefore evident that as a result of this beam behavior in both the input and output cavities for $\omega \neq \omega_c$, a decrease in power transfer efficiency will take place.

limitation on the amount of microwave power which can be absorbed by the electron beam.

A. V. Haeff[5] has investigated this instability for the case of a rectangular electron beam, of thickness, w, in the x direction which is flowing parallel to a magnetic field, H, in the z direction midway between two plates which are separated by a distance d and on which is placed a potential, V_b. The maximum current per centimeter of length in the y direction, which the region will sustain in a stable condition, is

$$I_{max} = 9.35 \times 10^{-6} V_b{}^{3/2} \frac{F_{max}}{d} \tag{19}p$$

where I is in amperes, V_b is in volts, d is in centimeters and F_{max} is related to w and d by the expressions

$$\frac{d}{w} - 1 = \frac{3}{2} \frac{2p-1}{(1-p)(1+2p)} \tag{20}$$

$$F_{max} = \frac{(1-p)(1+2p)^2 + 3/2(2p-1)(2p+1)}{(4p-1)^{3/2}}. \tag{21}$$

The parameter p may be shown to be the ratio, $\left[\dfrac{V_0}{V_b}\right]^{1/2}$, where V_0 is the potential minimum which is equal to zero for the unstable case.

The preceding discussion of space charge limitation has been derived from a theory involving an electron beam with no rotational velocity. Actually, for a rectangular beam in an Electron Coupler in which the electron spiral radii, x, are comparable to the dimension, $\dfrac{d-w}{2}$, some improvement in the ability of Region I to sustain charge is realized*, thereby raising slightly the value of current at which instability will take place. This is due to the fact that as the rotating charge approaches first one field boundary and then the other as each electron spirals, the amount of lowering of space potential will be less near the electric field boundaries than half way between them and the electrons pass through this midway potential region with maximum

---

[5] A. V. Haeff, "Space-Charge Effects in Electron Beams," *Proc. I.R.E.*, Vol. 27, No. 9, pp. 586-602, September, 1939.

* In several experimental Electron Couplers in which the ratio, $\dfrac{w}{d} = \dfrac{1}{3}$, was used, an improvement of about 10 per cent was measured.

x-directed velocity. Some further improvement may be achieved by resorting to the use of a cylindrical beam in a space bounded by arcuate field boundaries. Such boundaries are illustrated in Figure 2. It is well known that a cylindrical beam of electrons, coaxial with respect to an enclosing cylindrical conductor, is capable of sustaining higher currents without instability than the equivalent parallel-plane rectangular-beam case. When arcuate field boundaries are used to simulate approximately the completely enclosed cylindrical case,[6] the electron trajectories, when a transverse electric field is present, will bring the rotating beam to a region of almost constant proximity to the field boundaries thus avoiding the center of the region.

If a cylindrical electron beam is used, the spiralling electrons will describe a hollow cone whose thickness is equal to the beam diameter. This cone will be formed by a finite-thickness, cone-directrix electron beam, which rotates with an angular velocity corresponding to the cyclotron frequency. The position of the electrons in the beam will vary as the beam rotates since the electrons which are closest (outermost) to a field boundary at some transit angle, will be innermost or farthest from the other field boundary a half cycle later.

The power handling capabilities of the Electron Coupler can be demonstrated by substituting Equation (19) into Equation (15). The maximum space-charge-limited power is found to be

$$P = 5.84 \times 10^{-7} \, V_1{}^2 \, V_{b_1}{}^{\frac{1}{2}} \left[\frac{l_1}{d_1} \right]^2 \frac{b}{d_1} F_{\max} \qquad (22)\,\text{p}$$

where b is the distance in centimeters in the y direction such that cross sectional area of the electron beam is equal to bw. Equation (22) is plotted in Figure 5 as a function of the parameter $\dfrac{l_1}{d_1}$ for the case where $\dfrac{b}{d_1} = 1$ and $\dfrac{w}{d} = \dfrac{1}{3}$. Curves are shown for values of V_{b_1} from 300 to 900 volts and for values of V_1 from 200 to 1000 peak volts. Electron grazing considerations which will be discussed in the next section are not included here.

An aspect of particular interest which is demonstrated by Figure 5 is the large amount of power which can be absorbed by the beam. Thousands of watts can be handled by a properly engineered input

[6] L. P. Smith and P. L. Hartman, "Formation and Maintenance of Electron and Ion Beams," *Jour. Appl. Phys.*, Vol. 11, No. 3, pp. 220-229, March, 1940.

region and since it is this input power which is to be transferred to the load, it is evident that the Electron Coupler is capable of serving as a system parameter for a wide range of applications.

If a rectangular beam is used, the concept of a cone-directrix beam must be replaced by a concept of rotating charge. Each incremental emitting surface, when considered individually, will be the source of a cone-directrix beam but the total effect produced by all of the emitting surfaces can be accurately described only in terms of the

Fig. 5—Chart of the space-charge limited power which can be absorbed in Region I as a function of $\dfrac{l_1}{d_1}$ for $\dfrac{b}{d_1}=1$, $\dfrac{w}{d}=\dfrac{1}{3}$, and $F_{max}=1.1$ as derived from Equation (22).
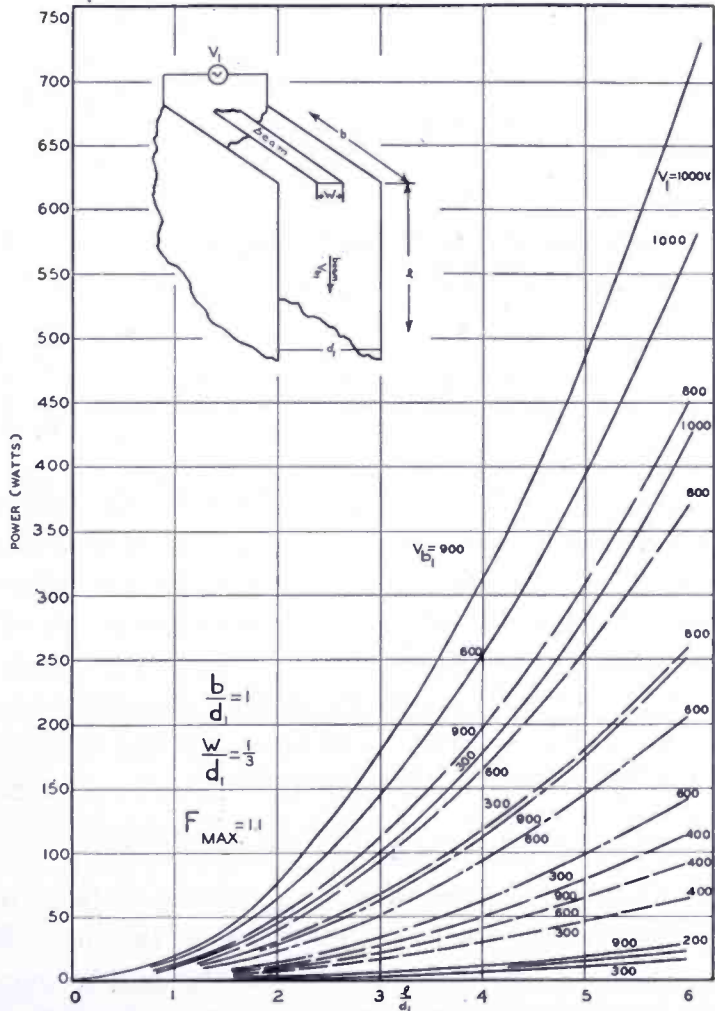
x-directed velocity of the charge which will be the same for all charge which has attained a certain spiral radius. This will be seen to be of importance in the interactions in Region III.

B. *Power Limitation due to Grazing*

It has been seen in Equation (16) that the power absorbed will be proportional to the square of the spiral radius of the electrons. This will place a limitation on the power since at some power, certain elec-

trons in the beam will graze on the transverse electric field boundaries. This will take place when, for a beam of thickness or diameter, w, in a field whose boundaries are separated by a distance, d, the electrons at the edge of the beam attain the spiral radius

$$x = \frac{1}{2} d_1 \left[1 - \frac{w}{d_1} \right]. \qquad (23)\,\text{p}$$

Substituting this value into Equation (16) yields

$$P = 2.8 \times 10^{-3} f_c^2 I_0 d_1^2 \left[1 - \frac{w}{d_1} \right]^2. \qquad (24)\,\text{p}$$

In the space charge limited case for a rectangular beam in parallel boundaries, the maximum power is found to be

$$P \approx 2.618 \times 10^{-8} V_{b_1}{}^{3/2} f_c^2 b \, d_1 \left[1 - \frac{w}{d_1} \right]^2 F_{\max}. \qquad (25)\,\text{p}$$

Equations (24) and (25) are specifically applicable to the Electron Coupler since no grazing can be tolerated in the primary cavity—the energy absorbed by the grazing electrons being lost to the output cavity. In an absorption tube,[4] more power can be absorbed since the electrons in the center of the electron beam can be made to absorb more power before they graze than the electrons at the edge of the beam. For a beam of large cross section, this may represent a substantial increase in absorption alone.

C. *Power Limitation due to Current Density*

At the lower microwave frequencies (L band to S band) the chief limitations on power into the beam in the input cavity are those due to grazing and space charge. At the higher microwave frequencies, the limitation becomes one of current density. Since, for example, an attempt to achieve a current density of more than 200 milliamperes per square centimeter from an oxide coated cathode will in general materially shorten the life of the cathode, it is evident that as the frequency is increased with a commensurate reduction in size of the tube geometry, the power into the beam is governed by the amount of current which can be safely drawn from the emitter.

For a beam of cross-sectional area A, the current density, J, is

$$J = \frac{I_0}{A} \tag{26}$$

where $A = w\,b$ for a beam of thickness w and width b. The power absorbed by the beam per square centimeter of emitter area may be found using Equations (26) and (15).

For a rectangular beam, the space-charge-limited power per square centimeter of beam-emitter area may be found to be

$$\frac{P}{A} \approx 2.618 \times 10^{-8}\, V_{b_1}^{3/2} f_c^2 \left[1 - \frac{w}{d_1} \right]^2 \frac{1}{.w/d_1} F_{\max}. \tag{27}p$$

Equation (27) is derived on the basis that the electrons at the beam edge just barely graze and that all electrons attain a maximum spiral radius described by Equation (23). It is evident, then, that optimum design requires $\dfrac{w}{d_1}$ to be as small as possible and that its choice will be governed chiefly by the characteristics of the emitter surface.

ELECTRON BEHAVIOR IN REGION II (THE INTER-CAVITY SPACE)

Region II is the intercavity space and the following discussion is intended to describe the behavior of the electron beam as it passes through this space on its way to Region III.

After each electron enters Region II, its trajectory will be determined by the axial magnetic field, H, during the transit of the electron through this space. The transit time will be a function of the direct-current beam potential V_{b_2}. No transverse electric fields are encountered however and so the equations of motion in Region II may be written as follows:

$$\begin{aligned}
m\ddot{x} &= -H\,|e|\,\dot{y} \\
m\ddot{y} &= +H\,|e|\,\dot{x} \\
m\ddot{z} &= 0
\end{aligned} \tag{28}$$

If the electron enters the region at time, $t = t_2$, let its motion be determined by the following set of initial conditions: at $t = t_2$

$$\begin{array}{ll}
v_x = -\omega_c\, r_0 e^{j\omega_c t_2} & v_y = j\omega_c r_0 e^{j\omega_c t_2} \\
\dot{v}_x = -j\omega_c^2\, r_0 e^{j\omega_c t_2} & \dot{v}_y = -\omega_c^2 r_0 e^{j\omega_c t_2}
\end{array} \tag{29}$$

where

$$r_0 = \sqrt{x^2(l_1) + y^2(l_1)} \tag{30}$$

and is, specifically, the maximum spiral radius attained by the electron in the primary space after it has traversed the total distance, l_1, in this space.

The expressions in (28) may be combined to yield the following homogeneous differential equations:

$$\ddot{v}_x + \omega_c^2 v_x = 0, \qquad \ddot{v}_y + \omega_c^2 v_y = 0 \tag{31}$$

which, when solved using the boundary conditions listed in (29), yield the expressions

$$v_x = - \omega_c r_0 e^{j [\omega_c l_2 + \omega_c (t - t_2)]}$$

$$v_y = j \omega_c r_0 e^{j [\omega_c l_2 + \omega_c (t - t_2)]} \tag{32}$$

These expressions are in terms of the entrance phase, $\omega_c t_2$, and the transit angle, $\omega_c (t - t_2)$, through the region where $(t - t_2)$ is the transit time described by

$$(t - t_2) = \frac{l_2 \times 10^{-7}}{6 V_{b_2}} \text{ seconds.} \tag{33} p$$

l_2 is the distance in the z direction. It is evident that the angular velocity or the x- or y-directed velocities of the electron do not change in Region II. Integration of (32) shows that the electrons pursue a helical path about the axis. All of the electrons with entering radius r_0 will form a line directrix of a cylinder with radius r_0 as illustrated in Figure 3. This action of the electron is due to the fact that although each electron enters with a certain kinetic energy due to the angular velocity ω_c, and the rotational radius r_0, no energy is given up or absorbed since there are no accelerating or decelerating electric fields present. Each electron will therefore retain the spiral or rotational energy imparted to it in the input cavity and will travel through the intercavity space to Region III at a velocity which is determined by the potential, V_{b_2}.

ELECTRON BEHAVIOR IN REGION III (THE OUTPUT CAVITY)

Before the electron beam arrives at the collector, it must pass through Region III which actually consists of an output cavity coupled

to a load. This cavity, as in the case of the input cavity, resonates at a frequency f_c, and, when excited, produces a transverse electric field.

When electrons with no spiral energy are passing through this cavity, no transverse electric field will be produced. When electrons with spiral energy pass through, however, circulating currents are induced in the output in a manner to be described and a decelerating transverse electric field is produced which extracts the spiral energy from the beam and transfers it to the load.

If microwave energy is imparted to the electron beam by a transverse electric field $E_1 e^{j\omega_c t}$, in the first cavity, physical reasoning based on the interactions in this cavity would lead one to believe that if an alternating transverse electric field were to be present in the output cavity, and if this field were to be 180 degrees out of phase with respect to $E_1 e^{j\omega_c t}$, the output cavity would extract energy from this beam. For the special case where the input and output cavities are identical with respect to geometry and beam potentials, if the transverse fields were equal in magnitude, but 180 degrees out of phase with respect to each other, the electron configuration in the output cavity would be an image of that in the input cavity; i.e., a cone whose apex is at the exit of the output cavity. For this case, *all* of the energy absorbed in the input cavity would be extracted from the beam in the output cavity.

For the present, assume a transverse electric field in the output cavity which may be expressed as $-E_3 e^{j\omega_c t}$. The equations of motion in this cavity will be

$$m\ddot{x} = |e|\, E_3 e^{j\omega_c t} - |e|\, H\dot{y}$$
$$m\ddot{y} = |e|\, H\dot{x} \tag{34}$$
$$m\ddot{z} = 0$$

which, when the various terms are combined, yield the following differential equation in v_x:

$$\ddot{v}_x + \omega_c^2 v_x = j\omega \frac{|e|}{m} E_3 e^{j\omega_c t} \tag{35}$$

where ω_c is described by Equation (2)

Let the electron enter the output cavity at $t = t_3$ such that at this entrance time

$$v_x = \omega_c r_0 e^{j\omega_c t_3} \qquad \dot{v}_x = \left[\frac{|e|}{m} E_3 + j\omega_c^2 r_0 \right] e^{j\omega_c t_3}$$

$$v_y = -j\omega_c r_0 e^{j\omega_c t}{}_3 \qquad \dot{v}_y = \omega_c^2 r_0 e^{j\omega_c t}{}_3. \tag{36}$$

Using these boundary conditions, the solution of Equation (35) is found to be

$$v_x = \left[\omega_c r_0 - \frac{|e|}{m} \frac{E_3}{2} (t - t_3) \right] e^{j\omega_c t}$$

$$+ \frac{1}{2} \frac{|e|}{m} \frac{E_3}{\omega_c} \sin \omega_c (t - t) \, e^{j\omega_c t}. \tag{37}$$

The last term is a velocity component which, as will be shown in the Appendix, may be neglected if the transit time in Region III is sufficiently long. Consider then the absolute value of the first term such that

$$|v_x| = \left[\omega_c r_0 - \frac{1}{2} \frac{|e|}{m} E_3 (t - t_3) \right] \tag{38}$$

$\omega_c r_0$ is a velocity which is equal to that of the spiralling electron as it leaves Region I since it is assumed that no energy is taken from or imparted to the electron in Region II. It follows that

$$\omega_c r_0 = \frac{1}{2} \frac{|e|}{m} E_1 \tau_I \tag{39}$$

where τ_I is the transit time through the first cavity and is a fixed quantity as far as the interactions in Region III are concerned. Equation (38) may then be rewritten as

$$|v_x| = \frac{1}{2} \frac{|e|}{m} [E_1 \tau_I - E_3 (t - t_3)]. \tag{40}$$

Equation (40) shows that there is a linear decrease in v_x as the electron proceeds through Region III. It will go to zero when

$$(t - t_3) = \tau_I \frac{E_1}{E_3} \tag{41}$$

and will increase linearly as $(t - t_3)$ increases beyond this point.

Integration of the first term of Equation (37) shows that the posi-

tion of the electron in the x plane may be found in terms of $|x|$ to be

$$|x| = r_0 - \frac{|e|\ (t - t_3)\ E_3}{2\ m\ \omega_c}. \tag{42}$$

A similar expression for $|y|$ may be derived from (34) which will be found to be identical to (42) in every way except phase in which it will differ by 90 degrees. $|x|$ and $|y|$ are functions of transit time alone and decrease linearly. They will go to zero when the time relationship specified in Equation (41) is satisfied, after which time, they will increase. Equation (41) may be rewritten in terms of distance as

$$l_{3_c} = l_I \frac{E_1}{E_3} \sqrt{\frac{V_{b_3}}{V_{b_1}}} \tag{43}\text{p}$$

where l_{3_c} represents the distance in the z direction which the beam must traverse in Region III for the zero or crossover point to occur.

As in Equations (7) and (8) for Region I, the general expressions for x and y show that electrons which are injected into Region III will spiral but, at any particular time, will have the same azimuthal angle. The decrease or increase in $|x|$ and $|y|$ is linear for all $(t - t_3)$ and the electrons will lie on the line directrix of any of three geometric figures which are contained in Region III and which are a function of l_{3_c} and l_{III} which is the total length of Region III. These figures are shown in Figure 6 and are identified as follows:

a. When $l_{3_c} = l_{III}$, the electrons in Region III will lie on the line directrix of a cone whose apex is at the exit.

b. When $l_{3_c} > l_{III}$, the electrons will lie on the line directrix of a truncated cone whose base is at the entrance to the region.

c. When $l_{3_c} < l_{III}$, the electrons will lie on the line directrix of a double cone. It will be shown that l_{3_c} can never be less than one half of l_{III}.

Power Extracted from the Electron Beam in Region III

The power due to rotational energy which can be extracted from the beam may be readily deduced from the electron spiral-radius behavior as specified by Equation (42). In Region I (see Equation (16)) it was seen that as the spiral radius increased, power was absorbed by

the beam such that the magnitude of the power was proportional to the square of the radius. It is convenient to describe this absorption in terms of increments of power which are pictured in Figure 7. Each increment pictured for Region I is for a corresponding increment of transit time and does not represent the total power which will be equal to the sum of all of the increments up to the one in question. Note that due to the parabolic nature of the power equation, the magnitude of the increments increases linearly.
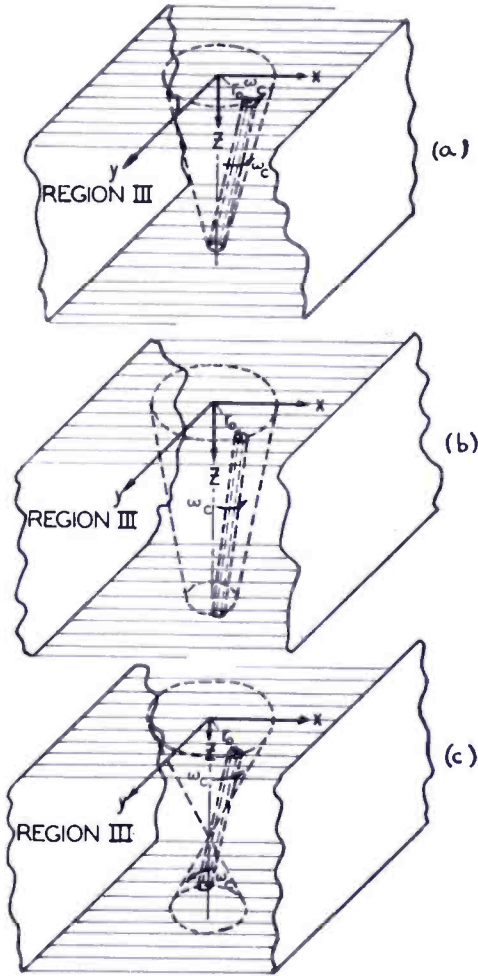
Fig. 6—Directrix-beam configurations in Region III for the case when, (a) $l_{3c} = l_{III}$, (b) $l_{3c} > l_{III}$, and (c) $l_{3c} < l_{III}$. l_{III} is the total length of Region III and l_{3c} is the length at which the spiral radius goes to zero — see Equation (43).
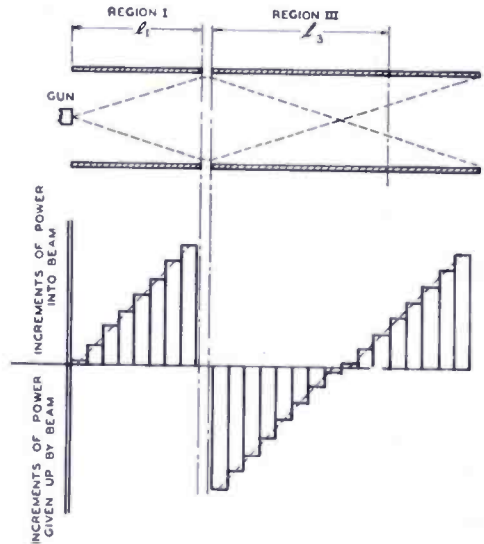
Fig. 7—Diagram which illustrates the process whereby the coupling beam acquires or gives up increments of power as it travels through the Electron Coupler. The total power, corresponding to a particular length, is equal to the *sum* of all of the increments of power contained in that length.

When the rotating beam, I_0, has traversed the entire distance, l_I, in Region I and has passed through Region II into Region III, increments of power will be given up to the transverse field, $-E_3 e^{j\omega_c t}$, of this region in the reverse of the order in which they were acquired. As shown in Figure 7, the largest increment is given up first followed by increments of decreasing amplitude. This extraction of power from the beam is accompanied by a linear decrease in spiral radius as is specified by Equation (42). At the zero or crossover point (Equation

(43)), all of the power absorbed in Region I will have been given up to the fields of Region III. From that point on, power will be absorbed from the transverse electric field, $-E_3 e^{j\omega_c t}$ in the same manner in which it was absorbed in Region I.

It is convenient now to discuss the power considerations resulting from the variation of the crossover distance, l_{3_c} with respect to the fixed length of Region III, which is l_{III}. The ratio of these lengths is found from Equation (43) to be

$$\frac{l_{3_c}}{l_{III}} = \frac{l_I E_1}{l_{III} E_3} \sqrt{\sqrt{\frac{V_{b3}}{V_{b1}}}}. \qquad (44)\text{p}$$

Figure 8 shows a number of positions of l_{3_c}. When $l_{3_c} = l_{III}$, as has already been pointed out, all of the power absorbed in Region I is extracted from the beam in Region III. When $l_{3_c} = l_d$ where, for this example, $l_d = 2l_{III}$, the crossover point is outside of Region III. Since power can only be extracted from the beam in Region III, then the beam spiral-radius will be reduced to one half of its entrance radius which will correspond to a loss of 75 per cent of its power. The remaining 25 per cent of the power in the beam is lost to Region III and goes to a suitable collector. As l_{3_c} increases with respect to l_{III}, a decreasing amount of power is extracted by the fields of Region III with the remaining power going to the collector.
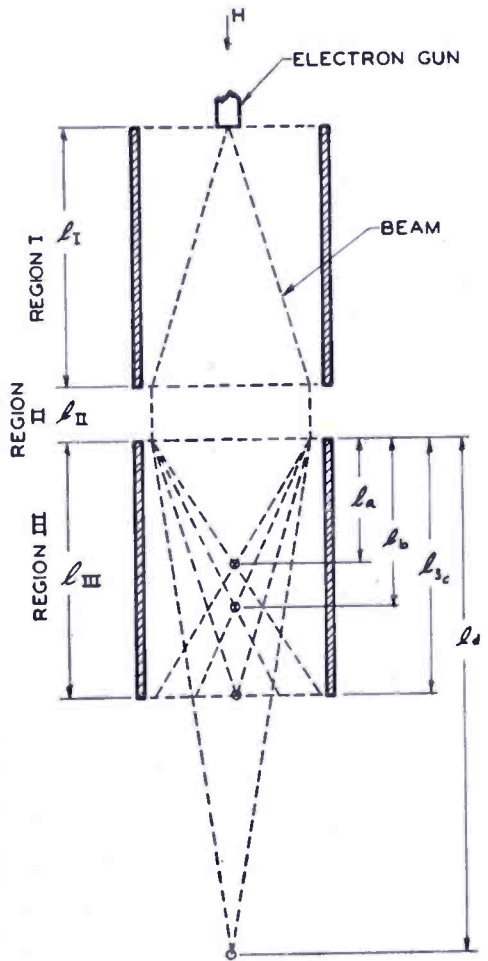

Fig. 8—Diagram illustrating the positions of convergence of the coupling beam in Region III for the cases when $l_3 = l_a = \dfrac{l_{III}}{2}$, $l_3 = l_b = \dfrac{2}{3} l_{III}$, $l_3 = l_{3_c}$ and $l_3 = l_d = 2l_{III}$.

When the crossover distance, l_{3_c}, is made smaller than l_{III}, then the electron beam gives up all of its energy to the field of Region III and reabsorbs it to an extent determined by $\dfrac{l_{3_c}}{l_{III}}$. The net power extracted

from the beam will then be the difference between the input power and the reabsorbed power. When $l_{3c} = l_b$, as is shown in Figure 8, approximately half of the input power has been reabsorbed whereas when $l_{3c} = \dfrac{l_{III}}{2}$, all of the power has been reabsorbed and the net power to the load of Region III is zero. In an Electron Coupler in which the field, $-E_3 e^{j\omega_c t}$, will be produced across an external load, it will be seen that l_{3c} cannot be made smaller than $\dfrac{l_{III}}{2}$. If a generator is to produce the field, then there is no theoretical limit to how small l_{3c} may become with respect to $\dfrac{l_{III}}{2}$.

The power extracted from the beam in Region III may be described as a function of the general distance, l_3, in this region as

$$P(l_3) = P(l_I) - \frac{E_3^2 (l_{3c} - l_3)^2 I_0}{16 V_{b3}} \tag{45}p$$

where $P(l_I)$ is the power absorbed by the beam in Region I.

Substitution of Equations (43) and (15-a) into Equation (45) yields the expression

$$P(l_3) = \frac{I_0 E_3 l_3}{16 \sqrt{V_{b3}}} \left[\frac{2l_I E_1}{\sqrt{V_{b1}}} - \frac{l_3 E_3}{\sqrt{V_{b3}}} \right] \tag{46}p$$

where it is seen that if $l_3 = l_{3c}$, all of the power will be extracted from the beam, while if $l_3 = 2l_{3c}$, no net power will be extracted.

OPTIMUM LOAD CONDITIONS FOR REGION III

In the previous section, the assumption was made that the transverse electric field, $-E_3 e^{j\omega_c t}$, was produced by an electric generator. In an Electron Coupler, this field is actually due to a voltage produced across a load resistor by currents induced by the rotating beam. This load resistance, which will be designated as R_0, will determine the rate at which the energy will be extracted from the rotating beam and will materially determine the position of the crossover point, l_{3c}. It will be assumed to be a pure resistance which is placed in shunt with the field boundaries which, in turn, are assumed to present no capacitance with which to shunt this resistance. This condition is easily met in practice where the transverse field is produced in a resonant cavity

and the resistance previously described is the external load resistance transformed to the field boundaries in the cavity.

The current to the parallel plane boundaries of Region III due to an oscillating charge, dq, between them is

$$dIe^{j\omega_c t} = \frac{dq}{d_3}\, v_x = \frac{-|I_0|\, v_x}{v_0\, d_3}\, dz \qquad (47)$$

where v_0 is the z-directed velocity of the charge. Substituting the expression for v_x, as given by Equation (37) with the third term omitted, into (47) gives

$$dIe^{j\omega_c t} = -\frac{I_0}{d_3}\left[\omega_c r_0 - \frac{1}{2}\frac{|e|}{m}\, E_3\, \tau_3\right] d\tau_3\, e^{j\omega_c t} \qquad (48)$$

where $d\tau_3$ is the z-directed transit time through an incremental distance in Region III. Integrating (48) with respect to the total transit time τ_{III} in Region III, to sum the image currents for each differential increment of charge, the total induced current is found as follows

$$i_{III} = \int_{\tau_3 = 0}^{\tau_3 = \tau_{III}} dIe^{j\omega_c t} = -\frac{I_0}{d_3}\left[\omega_c r_0\, \tau_{III} - \frac{1}{4}\frac{|e|}{m}\, E_3\, \tau_{III}^2\right] e^{j\omega_c t} \qquad (49)$$

i_{III} may be written in practical units and in terms of geometric dimensions as

$$i_{III} = -\frac{I_0}{4}\left[\frac{d_1 E_1}{\sqrt{V_{b_1} V_{b_3}}}\left\{\frac{l_I}{d_1}\right\}\left\{\frac{l_{III}}{d_3}\right\} - \frac{d_3 E_3}{2V_{b_3}}\left\{\frac{l_{III}}{d_3}\right\}^2\right] e^{j\omega_c t}. \qquad (50)\text{p}$$

This current will pass through R_0 and will produce the transverse electric field.

The resistance R_0, can be expressed as follows:

$$R_0 = \frac{-d_3 E_3 e^{j\omega_c t}}{i_{III}}$$

$$= \frac{4}{I_0\left\{\dfrac{l_{III}}{d_3}\right\}\left[\dfrac{d_1 E_1}{d_3 E_3}\left\{\dfrac{l_I}{d_1}\right\}\dfrac{1}{\sqrt{V_{b_1} V_{b_3}}} - \dfrac{1}{2}\left\{\dfrac{l_{III}}{d_3}\right\}\dfrac{1}{V_{b_3}}\right]} \qquad (51)\text{p}$$

As it stands, Equation (51) is of academic interest alone since it contains E_3^*. If, however, it is assumed as a special case that $l_{III} = l_{3c}$, Equation (36) may be rewritten as

$$l_I = l_{III} \frac{E_3}{E_1} \sqrt{\frac{V_{b_1}}{V_{b_3}}} \qquad (52)\text{p}$$

which, when substituted into Equation (51), yields the optimum load resistance, R_{00}, where

$$R_{00} = 8 \left[\frac{d_3}{l_{III}}\right]^2 \frac{V_{b_3}}{I_0} \qquad (53)\text{p}$$

and is the particular load resistance which will absorb *all* of the rotational energy in the electron beam as it passes through Region III. E_3 does not appear and all parameters are geometric or nonoscillatory.

MODULATION CHARACTERISTICS OF THE ELECTRON COUPLER

The preceding section has discussed the loading conditions for optimum transfer of power in the Electron Coupler. The Electron Coupler is theoretically capable of transferring all of the input power to the output but in practice the modulation characteristics of the device into a given load are considerably more important. The power-transfer efficiency, η, may be found from Equations (15) and (45) to be

$$\eta = \frac{P_{\text{out}}}{P_{\text{in}}} \times 100 = 100 \left[1 - \left\{1 - \frac{l_{III} E_3}{l_I E_1} \sqrt{\frac{V_{b_1}}{V_{b_3}}}\right\}^2\right]. \qquad (54)\text{p}$$

Note that when $l_{III} = l_{3c}$, the transfer efficiency will be equal to 100 per cent. The modulation characteristics may be found from Equation (54) by the following graphical analysis which will yield results in terms of load resistances and currents instead of E_3 in addition to clearly illustrating the fundamental concepts of power transfer.

Since the current through the load resistance is

$$i_{III} = \frac{d_3 E_3 e^{j\omega_c t}}{R_0} \qquad (55)\text{p}$$

_____

* A solution presented in the Appendix is based on an equivalent circuit representation in which E_3 does not appear for any R_0.

the following expression for i_{III} from Equations (54) and (15a) may be obtained:

$$i_{III} = \frac{E_1\, l_I\, l_{III}\, I_0}{16\, \sqrt{V_{b_1} V_{b_3}}\, d_3} \left[2 - \frac{l_{III}\, E_3}{l_I\, E_1} \sqrt{\frac{V_{b_1}}{V_{b_3}}} \right] e^{j\omega_c t}. \quad (56)\,\text{p}$$

It is evident from Equations (54) and (56) that the power into the load resistance may be varied by controlling either the ratio $\dfrac{V_{b_1}}{V_{b_3}}$, or the magnitude of the beam current, I_0.

A. Power-Transfer Modulation Using Beam Current Variation

Consider first the power-transfer modulation characteristics when the beam current is varied. In order to avoid complexity, let

$$\sqrt{\frac{V_{b_1}}{V_{b_3}}} = 1 \qquad (57)\,\text{p}$$

and

$$K = \frac{l_{III}\, E_3}{l_I\, E_1}. \qquad (58)\,\text{p}$$

The expression for K may be adapted to any particular Electron Coupler of lengths l_I and l_{III}.

Using Equations (57) and (58), Equation (54) is graphed in Figure 9 where it describes an inverted parabola whose maximum, which corresponds to optimum transfer efficiency, occurs at $K = 1$. η is seen to go to zero at $K = 0$ and $K = 2$. This curve is to be expected since it may be explained in terms of the shifting of the crossover point in Figure 7.

Let Equation (56) be rewritten using (57) and (58) such that
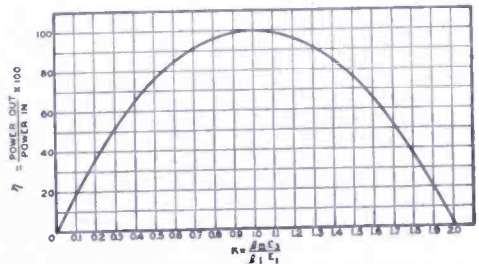
Fig. 9—Chart of the power transfer efficiency versus K where $K = \dfrac{l_{III}}{l_I} \cdot \dfrac{E_3}{E_1}$. E_1 and E_3 are the peak values of the alternating-current transverse electric field in Regions I and III, respectively.

$$i_{III}' = \alpha\, [-K + 2] \qquad (59)\,\text{p}$$

where

$$i_{III}' \; i_{III} \frac{16 \, d_3 \sqrt{V_{b_1} V_{b_3}}}{E_1 \, l_I \, l_{III} \, I_{00}} e^{-j\omega_c t} \qquad (60)\,\text{p}$$

and

$$I_{00} = \frac{I_0}{\alpha} = \left. \frac{8 \, V_{b_3}}{R_{00}} \; \frac{d_3}{l_{III}} \right\}^2 \qquad (61)\,\text{p}$$
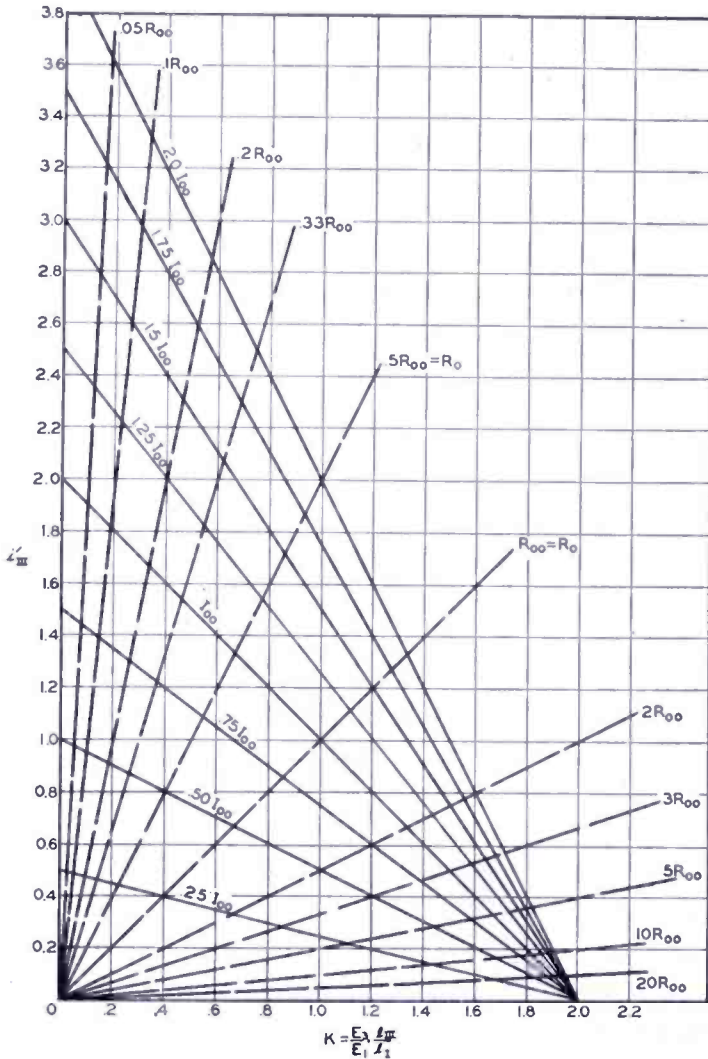

Fig. 10—Characteristic curves and load lines which yield i_{III}' as a function of K.

I_{00} is the beam current which yields R_{00} for a particular d_3, l_{III}, and V_{b3}. α is a factor which expresses I_{00} in terms of the general beam current, I_0.

As the ratio, K, is varied from $K = 0$ to $K = 2$, it is seen in Figure 10 that the curve for I_{00} is a straight line such that $i_{III}' = 2$ when $K = 0$ and $i_{III}' = 0$ when $K = 2$. A family of beam current lines for values of α from $\alpha = 0.25$ to $\alpha = 2.0$ are depicted and it is seen that these lines have a common intercept on the abscissa at $K = 2$.
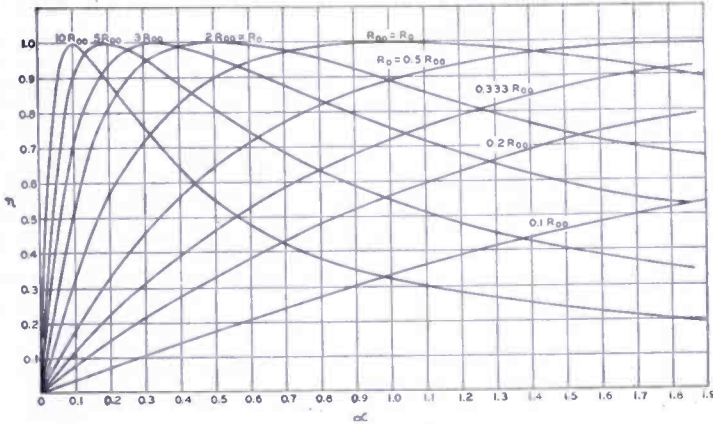
Fig. 11 — Chart of the power transfer efficiency, η, versus α for values of γ from 0.1 to 10. α and γ are factors which relate the beam current, I_0, and the output load, R_0 to the optimum beam current, I_{00}, and load, R_{00}, respectively; i.e. $I_0 = \alpha I_{00}$ and $R_0 = \gamma R_{00}$.

A set of load lines are added to Figure 10 and are positioned with respect to the load line corresponding to R_{00}. This optimum load-resistance line will start from zero and pass through the point, $i_{III}' = K = 1$. It has a slope of 45 degrees which is a consequence of the fact that as E_1 is kept contant and E_3 is varied, i_{III}' will vary linearly due to the straight-line characteristics of a pure resistor. If values of load resistance other than the optimum are used, the slopes of the load lines corresponding to these resistances will vary accordingly. The load resistance, R_0, may be related to R_{00} by the factor γ such that

$$R_0 = \gamma R_{00}. \tag{62}p$$

Load lines for values of γ from $\gamma = 20$ to $\gamma = 0.05$ are pictured in Figure 10.

The intersections of the beam current lines and the load lines will correspond to particular values of i_{III}' and K which are in turn related to values of η by Figure 9. These values of i_{III}' and η are plotted in Figures 11 and 12 as a function of α. Figure 11 shows that for any γ,

Fig. 12 — Chart of i_{III}' versus α for values of γ from 0.05 to 10.
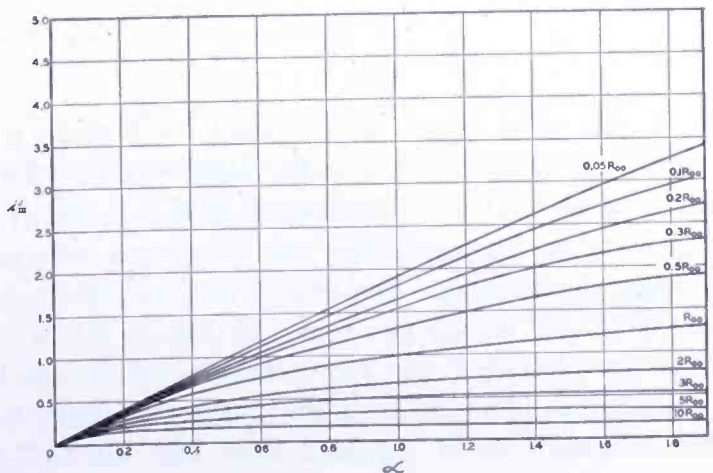
the power-transfer efficiency will increase from zero to maximum and will then decrease as I_0 is increased beyond this point. For the optimum load resistance, R_{00}, the maximum power-transfer efficiency will, of course, take place when $I_0 = I_{00}$. Although a transfer efficiency of 100 per cent is seen in Figure 11 to be theoretically realizable for *any* pure resistive load, the actual power transferred will depend upon αI_{00}. For large γ the power absorbed by the beam in Region I will be small even though the power-transfer efficiency is maximum. When γ is small, the current necessary to achieve maximum power-transfer efficiency may be unobtainable due to space-charge limitations thereby limiting the overall efficiency of the device during modulation.

B. Power-Transfer Modulation Using Transit Time Variation

The expressions for η and i_{III} in Equations (54) and (56) are dependent on the ratio of the transit times through Region I and Region III. Assume a transit-time factor, β, where

$$\beta = \frac{V_{b3}}{V_{b1}} \tag{63)p}$$

such that

$$\eta = 100 \left[1 - \left(1 - \frac{K}{\sqrt{\beta}} \right) \right]. \tag{54-a)p}$$

Also let

$$i_{III}'' = \left[-\frac{K}{\beta} + \frac{2}{\sqrt{\beta}} \right] \tag{56-a)p}$$

where

$$i_{III}'' = i_{III} \frac{16 \, d_3 \, V_{b1}}{E_I \, l_I \, l_{III} \, I_{00}} e^{-j\omega_c t}. \tag{64)p}$$

A plot of η versus K for values of β from $\beta = 0.33$ to $\beta = 10$ is shown in Figure 13. The curve for $\beta = 1.0$ is the same curve as that pictured in Figure 9. The result of increasing β is a lengthening of the distance between base line intercepts whereas decreasing β decreases the distance. For any β, however, the maximum power transfer efficiency is 100 per cent. In Figure 14, a set of i_{III}'' versus K lines are plotted, — one for each value of β used in Figure 13. A set of load lines identical to those in Figure 10 are included. By plotting the intersections of the load lines and the i_{III}'' versus K lines, the
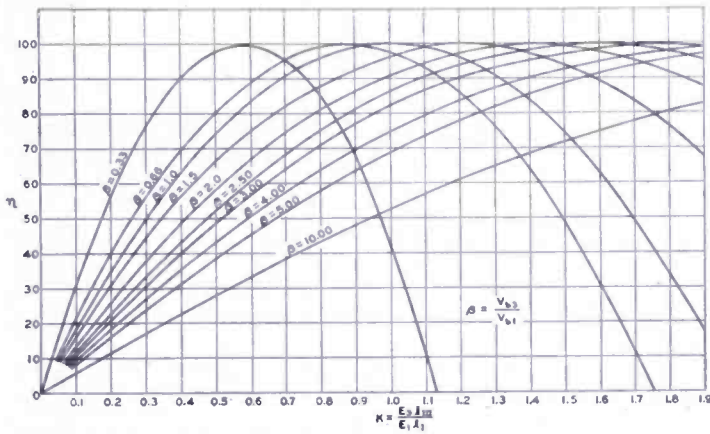
Fig. 13—Curves of η versus K for values of β from 0.33 to 10. β is the ratio of the beam voltage in Region III to the beam voltage in Region I;

i.e. $\beta = \dfrac{V_{b3}}{V_{b1}}$.

curves shown in Figures 15 and 16, which correspond to various values of resistive loads for η versus β and i_{III}'' versus β respectively, are obtained.
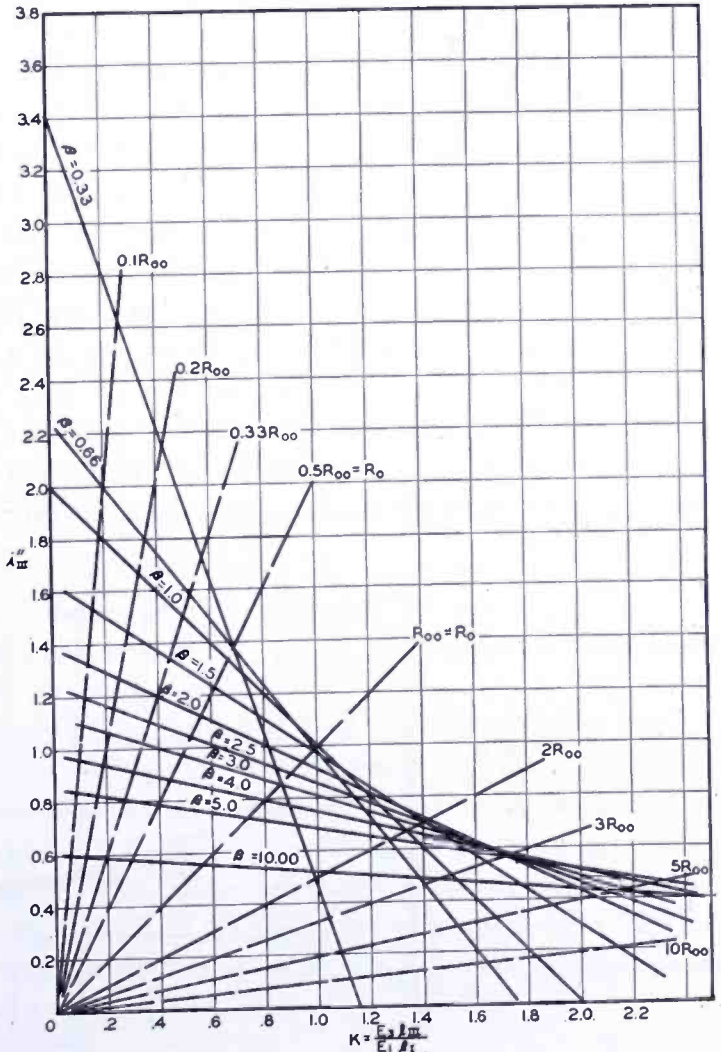

Fig. 14—Characteristic lines and load lines for the output-cavity system which yield i_{III}'' versus K as a function of α and γ.
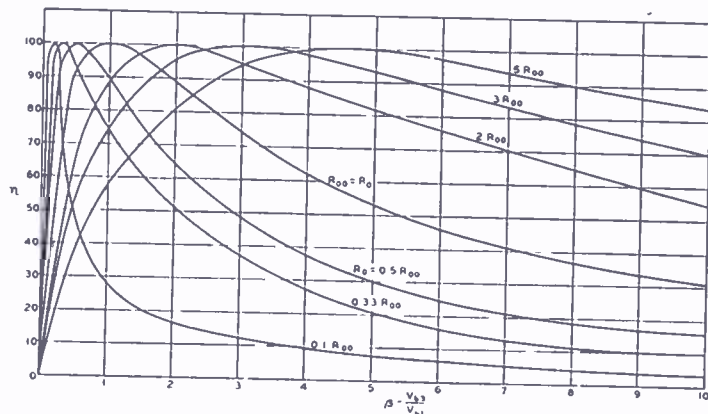
Fig. 15 — Curves of η versus β as a function of γ.

As V_{b3} increases with respect to V_{b1}, η, in Figure 15, rises to a maximum which is equal to 100 per cent for all values of R_0, and then falls off. The rate of rise and fall increases and the maximum moves toward smaller values of β as R_0 decreases in magnitude.

In Figure 16, the output-current behavior for various values of R_0 as β is varied is shown. The current rises to a maximum determined by γR_{00} and then falls off. If V_{b1} is assumed to be constant as V_{b3} is varied, the increase in peak current as γ is decreased is readily seen to be due to the fact that since the power is the same at the maximum points, the current through the output load must increase by a proper amount as the load resistance is decreased in order to maintain this value of maximum power. If the optimum beam current, I_{00}, is sustained by a beam voltage V_{b1}, in Region I and if no grazing takes place as it passes into Region III, there will be a minimum value to which V_{b3} can be adjusted before Region III fails to sustain the current causing an instability which will return current to Regions II and I. Because of this, the regions of Figures 15 and 16 in which β approaches zero apply only to small-beam-current Electron Couplers.
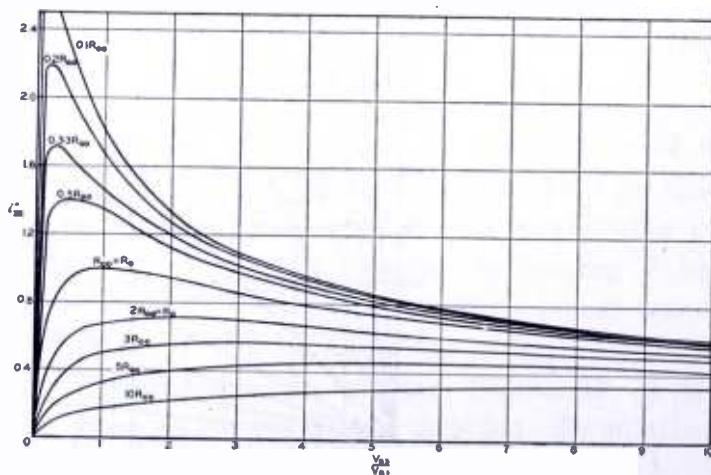
Fig. 16 — Curves of $i_{III}{}''$ versus β as a function of γ.

Transit time modulation of Electron Couplers is, in general, practical only for variations of β in the ranges where V_{b_3} is equal to or greater than V_{b_1}.

LIMITATION IN THE POSITION OF THE CROSSOVER POINT IN REGION III

When $l_{III} = 2 \, l_{3_c}$, i_{III} as described by Equation (56) will be equal to zero. This is the case for which the i_{III}' and i_{III}'' versus K lines intersect the axes of the abscissas in Figures 10 and 14 respectively. However, intersections with load lines for *all* values of pure resistance can only take place in the first quadrant. These intersections represent the operating points of the resistance loaded Electron Coupler and it is evident that as an extreme case as either $\gamma \rightarrow \infty$ or $V_{b_3} \rightarrow 0$, the crossover will take place at $\dfrac{l_{III}}{2} = l_{3_c}$. This is to be expected since if $\dfrac{l_{III}}{2} > l_{3_c}$, the electron beam would emerge from Region III with more rotational energy than it had when it entered. This is, of course, impossible when the transverse electric field is produced by an induced current flowing through the load resistance since a resistance can only absorb power. As a result, no grazing theoretically can take place on the transverse electric field boundaries in Region III.

ACKNOWLEDGMENT

APPENDIX

EQUIVALENT-CIRCUIT SOLUTION OF THE ELECTRON COUPLER

Since the Electron Coupler is, essentially speaking, a Class A device, an equivalent-circuit representation of Region III, due to D. O. North,* permits a circuit solution which will effectively complement and extend the solution already presented.

It is evident from Equation (42), that it is possible to think of the beam configuration in Region III in terms of two separate electron beams. One beam will enter Region III with rotational radius r_0, and will continue through this region with each electron pursuing a helical path of constant radius. The other beam will enter Region III at $x = y = 0$ with no radial motion, and each electron will spiral with its spiral radius increasing linearly with time as it proceeds through the region.

---

* of these laboratories.

This is identical to the electron behavior in Region I. If the beams are of vanishingly small cross section, then the first beam will form the line directrix of a cylinder and the second beam will form the line directrix of a cone whose apex is at the entrance to the region. These beams will be 180 degrees out of phase with respect to each other as they rotate.

Substituting Equation (37) into Equation (47) yields the complete solution for the induced current in the incremental distance, $d\tau_3$. The sum of all of the induced currents, i_{III}, is written as follows:

$$i_{III} = \left\{ -\frac{I_0}{d_3} \int_0^{\tau_{III}} \left[\omega_c\, r_o - \frac{1}{2} \cdot \frac{|e|}{m} \cdot E_3\, \tau_3 \right.\right.$$

$$\left.\left. + \frac{1}{2} \frac{|e|}{m} \frac{E_3}{\omega_c} \sin \omega_c\,(t - t_3) \right] d\tau_3 \right\} e^{j\omega_c t}. \tag{A-1}$$

Equation (A-1) is readily solved; its solution is written in practical units as follows:

$$i_{III} = -\frac{I_0\, d_1\, E_1}{4\, \sqrt{V_{b_1}\, V_{b_3}}} \cdot \frac{l_I}{d_1} \cdot \frac{l_{III}}{d_3} \cdot e^{j\omega_c t}$$

$$+ \frac{d_3\, E_3\, I_0}{8\, V_{b_3}} \left[\frac{l_{III}}{d_3} \right]^2 \left\{ 1 + \frac{2\cos\theta_{III}}{\theta^2_{III}} \right\} e^{j\omega_c t} \tag{A-2}*$$

$$= i_a + i_b \tag{A-3}$$

where $\theta_{III} = \omega_c\, \tau_{III}$ and is the transit angle through the output cavity.

The first current term, i_a, is due to the constant-radius electrons which form the helix and is seen to be independent of E_3 or of the load of Region III. It may then be considered to be the output of a constant-current generator. The second term, i_b, when divided by the voltage $d_3\, E_3\, e^{j\omega_c t}$, yields a conductance $\dfrac{1}{R_s}$, which internally shunts the constant-current generator. Note that when $\dfrac{2\cos\theta_{III}}{\theta^2_{III}}$ goes to zero, R_s becomes R_{00}.

---

* Equations (A-2) — (A-18) are in practical units.

The equivalent circuit involving i_a, R_s, and the output load is pictured in Figure 17. The voltage, V_3, across the output load may be written as follows:

$$V_3 = d_3\, E_3\, e^{j\omega_c t} = i_a\, \frac{R_o}{1 + \dfrac{R_o}{R_s}} \tag{A-4}$$

$$= i_a\, \frac{R_o}{1 + \gamma\left[1 + \dfrac{2\cos\theta_{III}}{\theta^2_{III}}\right]} \tag{A-5}$$

(A-5) may be expanded into the form

$$V_3 = i_a\, \frac{R_o}{1+\gamma}\left[1 - \frac{2\gamma}{1+\gamma}\cdot\frac{\cos\theta_{III}}{\theta^2_{III}} + \cdots\right] \tag{A-6}$$

It is evident from (A-6) that as θ_{III} increases, the term $\dfrac{2\gamma}{1+\gamma}\cdot\dfrac{\cos\omega_c\tau_{III}}{\theta^2_{III}}$ may be neglected and the voltage will be dependent upon i_a, R_0 and R_{00} only.

Since i_a contains $d_1 E_1$, the ratio of the output voltage, V_3, to the input voltage, V_1, is easily obtained. When θ_{III} is large, it follows from (A-6) that
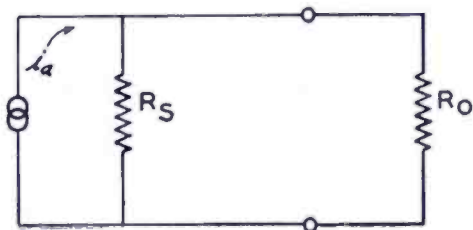
Fig. 17—Equivalent circuit representation of the output cavity system of the Electron Coupler.

$$\left|\frac{V_3}{V_1}\right| = \frac{I_0}{4\sqrt{V_{b_1} V_{b_3}}}\cdot\frac{l_I}{d_1}\frac{l_{III}}{d_3}\cdot\frac{R_0}{1 + \dfrac{R_0}{R_{00}}}\cdot \tag{A-7}$$

Substituting the expression for R_{00} as given by Equation (53) into (A-7) yields

$$\left| \frac{V_3}{V_1} \right| = 2 \sqrt{ \frac{V_{b_3}}{V_{b_1}} \cdot \frac{l_I}{d_1} \cdot \frac{l_{III}}{d_3} \cdot \frac{R_0 I_0}{\left[8 V_{b_3} + R_0 I_0 \left(\dfrac{l_{III}^2}{d_3^2} \right) \right]} }. \qquad (A\text{-}8)$$

If αI_{00} and γR_{00} are substituted for I_0 and R_0 respectively in (A-8), the resulting expression will include a factor $\dfrac{2\alpha}{1 + \alpha\gamma}$. This factor will yield the curves for $i_{III}{}'$ in Figure 12; $i_{III}{}'$ being proportional to V_3.

As a further illustration of the use of the equivalent circuit formulation, consider the solution for the power-transfer efficiency, η, for the case when $\alpha = \beta = 1$. For this solution let the output load, R_0, be expressed in terms of the input beam resistance, R_1, as follows:

$$R_0 = \gamma R_{00} \qquad (A\text{-}9)$$

$$= \gamma \left[\frac{d_3}{l_{III}} \cdot \frac{l_I}{d_1} \right]^2 R_1. \qquad (A\text{-}10)$$

For the sake of simplifying the derivation, let $l_I = l_{III}$ and $d_1 = d_3$. The load current i_{III} may then be written

$$i_{III} = i_a \frac{R_{00}}{R_{00} + \gamma R_1}. \qquad (A\text{-}11)$$

Substituting (18) and (53) into (A-11) yields

$$i_{III} = i_a \frac{1}{1 + \gamma}. \qquad (A\text{-}12)$$

The output voltage is therefore (see (A-6))

$$V_3 = i_a \frac{R_0}{1 + \gamma}. \qquad (A\text{-}13)$$

The transfer efficiency, η, may be found as follows:

$$\eta = \frac{P_0}{P_{in}} \cdot 100 \qquad (A\text{-}14)$$

$$= \frac{R_1 V_3 i_{III}}{d_1^2 E_1^2} \cdot 100 \tag{A-15}$$

$$= \frac{R_1^2}{d_1^2 E_1^2} \cdot \frac{\gamma}{[1 + \gamma]^2} \cdot i_a^2 \cdot 100. \tag{A-16}$$

Substituting the value for i_a from (A-2) into (A-16) yields

$$\eta = \frac{4 \gamma}{(1 + \gamma)^2} \cdot 100. \tag{A-17}$$

This equation will give the various values of η corresponding to γ along the line $\alpha = 1$ in Figure 11.

In like manner it can be shown that for general values of β

$$\eta = \frac{4}{\beta} \frac{\gamma}{\left[1 + \dfrac{\gamma}{\beta} \right]^2} \cdot 100 \tag{A-18}$$

which yields the curves of Figure 15.

This solution may be extended to include the case when the output load is not a pure resistance.

VIDEO ANNOUNCER*

By

Edward P. Bertero

Engineering Development Group, National Broadcasting Company, Inc.,
New York, N. Y.

Summary—The Video Announcer is a mechanical device which can be installed on a television field camera to permit the televising of specially edited 35-millimeter film strips. The film strip contains single frame exposures of static type commercials or announcements along with frames of RMA or television station test patterns.

The Video Announcer makes possible the origination of static type commerical announcements at a television field pickup point, and, if desired, their superposition over the background of the local program without the need for interlocking synchronizing generators. In addition it simplifies camera alignment procedure.

Introduction

THERE has long been a need in television field operation for a simple compact device to facilitate camera alignment particularly when adverse weather conditions prevail. Such a device could also provide a means of presenting static type commercial announcements.

An experimental model of such a device which used 35-millimeter film proved to be of great interest to those concerned. It was therefore decided to develop a practical working model later to be called the Video Announcer.

A developmental model of the Video Announcer has been built and used successfully on the air. As in the earlier version, the developmental model uses single frame exposures of 35-millimeter film strip. Adjustments are provided for proper alignment, framing and illumination of the film. The device can be quickly and easily installed on most television field cameras and uses the 50-millimeter lens normally supplied with the camera. See Figures 1 and 2 .

Theoretical Considerations

Normally in a television camera optical system, as in a photographic camera, the image is much smaller than the object. In this method of televising a 35-millimeter frame the opposite situation exists; i.e., magnification is required. Therefore, the lens placement must be changed relative to the image orthicon tube.
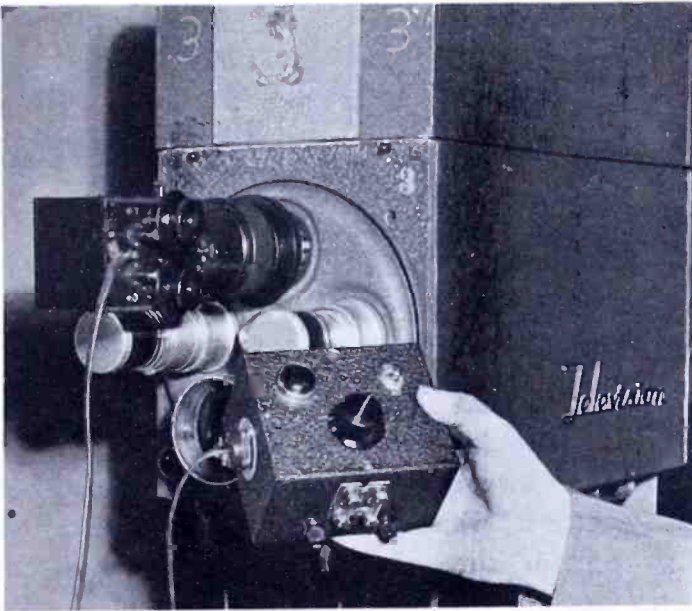
---

* Decimal Classification: R583.

Fig. 1 — Video Announcer installed in lens turret, and control box.

Using the lens with a focal length of 50-millimeters, the object and image distances were computed to be approximately three inches and five inches respectively.

MECHANICAL CONSIDERATIONS

Means are provided for image and object distance adjustments. See Figure 3. The object distance adjustment is primarily used to obtain proper image size. The lens extension or image distance adjustment permits proper focusing at a point midway of the travel of the image orthicon tube.

The film aperture (ASA 0.6 inch × 0.825 inch) is fixed and is centered on the optical center of the system. Because of the differences in scanning centering in image orthicon tubes, adjustments are provided to move the film strip relative to the aperture in both the horizontal and vertical planes, thereby assuring proper framing.

The film strip wraps around and is guided by two standard 35-millimeter sprockets. A detent is added to the sprocket shafts. The relation of sprocket teeth to detents, which is adjustable, is such that the

Fig. 2 — Video Announcer and control box.
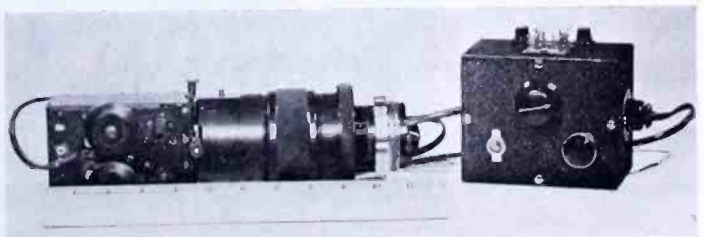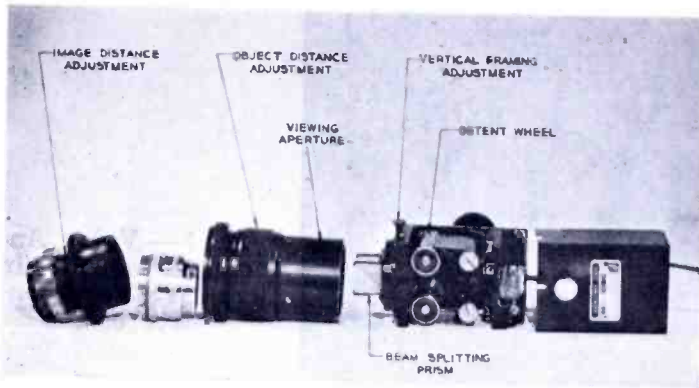
Fig. 3—Exploded view of the Video Announcer.

spacing between detents is exactly one frame of movement of the film strip relative to the aperture. See Figure 4.

Two small spindles act as storage reels for the film strip. This arrangement permits movement of the film strip in either direction since movement is provided for through the storage spindles. A ratchet arrangement activates the spindles. When movement of the film strip is desired the appropriate knob is pushed toward the body of the unit causing the ratchet to engage the spindle shaft and, as the knob is turned, to move the film. If the rotation of the knob is in the wrong direction, the ratchet will not engage the spindle shaft and the film will not move. Both spindles and sprocket shafts are spring loaded to keep the film strip taut at all times.

The film threading and storage portion of the Video Announcer is entirely enclosed by metal except for opal glass which permits illumination of the film strip, and a prism covering the film aperture.

ELECTRICAL CONSIDERATIONS

A simple electrical circuit is used to control the illumination of the film strip. In the Video Announcer proper, two microswitches, which are actuated by the knobs, are so wired that when movement of
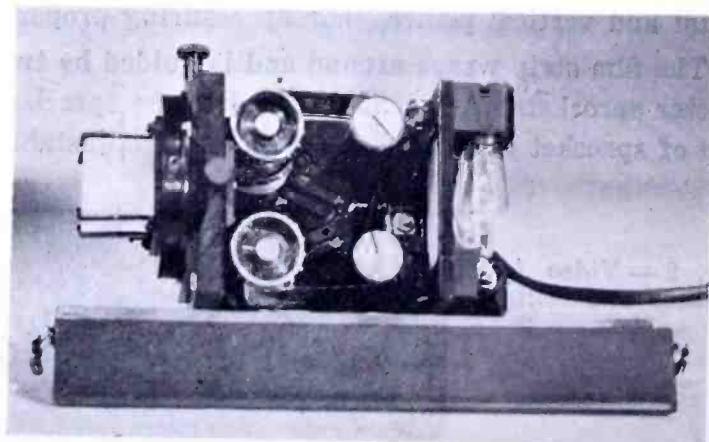
Fig. 4 — Film positioning mechanism.

the film is desired the source of illumination is cut off before the film is moved. If illumination is desired while moving the film, a slide type switch is provided which shorts the microswitch circuits.

The illumination source for the film strip consists of two 6-watt 110-volt candelabra base bulbs. A control box located at the camera operator's position is used to adjust the illumination to the desired intensity. The control box consists of a rheostat, an on-off switch, a pilot light, and fuses. The rheostat adjusts the voltage to the two bulbs. The power cord from the control box to the Video Announcer proper is fused. A lead from the 110-volt 60-cycle duplex outlet located on the bottom of the camera to the control box provides the power for illumination of the film strip.

OPTICAL CONSIDERATIONS

Sufficient dispersion of light from the source of illumination is obtained by using opal glass.

By looking into the viewing aperture at the end of the lens barrel a mirror image of the frame being televised can be seen. The reflected image is obtained by means of a beam splitting prism located at the film aperture.

The lens used in the Video Announcer is the 50-millimeter lens supplied with the camera. It is adjusted to focus at 1.5 feet with an F opening of 4.5.

FILM EDITING AND PROCESSING

Film strips may have program material for one or more programs. RMA and local station test patterns are generally included at the ends of each strip along with a few transparent frames and about six inches of leader for threading purposes. The Video Announcer can conveniently accommodate a film with a maximum of approximately 70 frames.

The art copy and test patterns are photographed with a 35-millimeter motion picture film camera capable of taking single frame exposures (ASA mask size 0.631 inch × 0.868 inch). Since no sound is recorded, the frame can be centered on the film strip. All material should be photographed at the proper light intensity to assure a uniform density of prints. In obtaining prints, it has been found advisable to specify three safety film positive prints, standard, medium and light copies. The light positive copy has usually been found to be the most satisfactory of the three. The other two can be used for emergency and protection purposes.

Installation and Operation of the Video Announcer

The Video Announcer can be installed easily and quickly on most television field cameras. The 50-millimeter lens is first removed from the camera turret and the lens extension portion of the Video Announcer is inserted in its place. After adjusting the 50-millimeter lens for a focal length of 1.5 feet and an F opening of 4.5 it is inserted into the lens extension. The remaining portion of the unit slides over and cinches on the lens extension assembly. After plugging in the Video Announcer power cord and reducing the illumination so that the frame is barely visible at the viewing aperture, the unit is ready to be adjusted. Adjustment is achieved by first rotating the lens turret to position the Video Announcer in line with the camera pickup tube. Then under the direction of the camera man, who is viewing the electronic monitor and has increased the illumination of the frame sufficiently to properly focus an image, the film assembly portion of the Video Announcer is rotated to assure that the sides of the image are vertical. Next the horizontal and vertical adjustments are made to center the film strip relative to the aperture. Proper framing is achieved only when a frame of the film strip is located directly over the aperture and the sprocket holes of the film strip match the sprocket teeth. Final adjustment is for proper image size. Camera alignment is done with the RMA test pattern on the film strip. The transparent frames on the film strip can be used to "wipe off" any images "burned on" the image orthicon tube if this should happen while using the unit. The Video Announcer can be left on the turret if it is so desired.

If frames are to be changed on the air there will be no picture or black picture transmitted while the operator turns the knob to change frames. The operation to change a frame is simply to push the appropriate knob toward the body of the unit, turn it about 90 degrees, then release it when the pressure of the detent is felt.

Certain precautions must be observed in handling the unit. Care must be taken not to burn an image on the photo cathode of the image orthicon tube because of too much illumination of the film strip or leaving an image on the tube too long.

Conclusion

The Video Announcer is now being used successfully on several NBC television programs. It has provided television program personnel with a means of presenting commercial material in a more interesting and subtle fashion. The use of the Video Announcer has also simplified camera alignment at television field pickup points and minimized the

need for switching from pickup point to film studio for slide or static type commercials.

ACKNOWLEDGMENT

The development and design of the Video Announcer was done under the supervision of E. D. Goodale and the actual fabrication of the developmental model was carried out by Clarkson U. Bundick of the Model Shop of the National Broadcasting Company. The many suggestions and valuable criticisms of several members of the television operating groups are gratefully acknowledged.

RCA TECHNICAL PAPERS†

First Quarter, 1949

Any request for copies of papers listed herein should be addressed to the publication to which credited.

† Report all corrections or additions to RCA Review, Radio Corporation of America, RCA Laboratories Division, Princeton, N. J.

"How to Make FM Proof-of-Performance Measurements", F. E. Talmage, *Broadcast News* (February) 1949

"How to Shock Mount 70 Series Turntables", W. E. Stewart, *Broadcast News* (February) 1949

"Improved Lacquer Disk Recording Head," H. E. Roys, *Broadcast News* (February) 1949
Audio Eng. (February) 1949

"Internal Structure and Nuclei in Cells of Escherichia Coli as Shown by Improved Electron Microscopic Techniques", J. Hillier (Co-author), *Jour. Bacteriology* (March)........ 1949

"Luminescent Solids (Phosphors)", H. W. Leverenz, *Science* (February 25) 1949

"Mixer-Oscillator Circuit for FM and AM Using RCA-6J6 or RCA-19J6", *RCA Application Note AN-138*, RCA Tube Department, Harrison, N. J. (March 15)................. 1949

"Omnidirectional Ranger" (letter), D. G. C. Luck, *Flying* (March) 1949

"Overall Fidelity of Standard Broadcast and FM Receivers Manufactured in 1948", J. Weinberger, *RCA Licensee Bulletin LB-765* (February 10) 1949

"Phase and Amplitude Equalizer for Television Use", E. D. Goodale and R. C. Kennedy, *RCA Review* (March)........ 1949

"Philosophy of Our Television System", J. H. Roe, *Broadcast News* (February) 1949

"Preliminary Observations on the Germination of the Endospore in Bacillus Megatherium and the Structure of the Spore Coat", J. Hillier (Co-author), *Journal of Bacteriology* (January) 1949

"The Preparation of Luminescent Screens", Meier Sadowsky, *Electrochemical Society Journal* (March) 1949

"Properties of Some Wide-Band Phase-Splitting Networks", D. G. C. Luck, *Proc. I.R.E.* (February) 1949

RCA TECHNICAL PAPERS (1948)—INDEX, Volume II(c), *RCA Review*, RCA Laboratories Division, Princeton, N. J. (February) 1949

"Reading Aid for the Blind Pronounces Printed Letters", L. E. Flory and W. S. Pike, *Electronics* (January) 1949

"A Reversible Beam Antenna for Twelve Channel Television Reception", O. M. Woodward, Jr., *RCA Licensee Bulletin LB-768* (March 7) 1949

"A Simple Keyed AGC System for Television Receivers", G. F. Rogers and E. I. Anderson, *RCA Licensee Bulletin LB-769* (March 15) 1949

"Single-Element Unidirectional Microphone", H. F. Olson and J. Preston, *Jour. Soc. Mot. Pic. Eng.* (March) 1949

"Some Characteristics of Diodes with Oxide-Coated Cathodes", W. R. Ferris, *RCA Review* (March) 1949

"Some Novel Circuits for the Three-Terminal Semiconductor Amplifier", W. M. Webster, E. Eberhard and L. E. Barton, *RCA Review* (March) 1949

NOTE—Omissions or errors in these listings will be corrected in the yearly index.

Corrections:

The following corrections refer to the paper entitled "Small-Signal Analysis of Traveling-Wave Tube", published in the December, 1947 issue, Vol. VIII, No. 4, pp. 585-611.

A list of errata for this paper was published in the June, 1948 issue. Subsequent to publication of this list, an error in Equation (20) of the paper was discovered, which necessitates changes in most of the published errata, and alters Figures 8 and 9 of the paper. It seems best, therefore, to withdraw the first errata sheet and publish a completely new one. Furthermore, these changes allow simplification of the expressions for noise factor. For completeness, the simplifications are mentioned here. The changes follow:

p. 590, Equation (9)—the term in the 6th row, 4th column, should read H_m' instead of H_m.

p. 592, Equations (14)—delete the prime in the element of the 3rd row 1st column.

p. 595, Equation (17)—multiply the left side of the equation by $J_0(\eta_0 a)$.

p. 596, Equation (20) should read—

$$-x \frac{H_m(ix)}{J_m(ix)} \frac{1}{h_m(ix)} = \frac{4}{1 + \frac{m\nu}{x}\sqrt{1 + \frac{\mu^2}{x^2\nu^2}}} + \frac{1}{1 + \frac{\mu^2}{x^2\nu^2}}\left(2 - \frac{2}{1 + \frac{m\nu}{x}\sqrt{1 + \frac{\mu^2}{\nu^2 x^2}}}\right)$$

$$+ x\left[\frac{iJ_m'(ix)}{J_m(ix)} + \frac{iH_m'(ix)}{H_m(ix)}\right]\left[1 + \left(1 + \frac{m^2}{x^2}\right)\left(\frac{\mu}{x + m\nu\sqrt{1 + \frac{\mu^2}{\nu^2 x^2}}}\right)^2\right]$$

p. 599, Equation (28) should read—

$$V_0 = \frac{1}{2}\frac{m}{e}v_p{}^2 = \frac{1}{2}\frac{c^2}{\frac{e}{m}\left(1 + \frac{x^2\nu^2}{\mu^2}\right)}$$

p. 601, Figure 8—the curves shown here are in error, for $y_0(ix)$ depends on $h_0(ix)$. New curves are shown below.

p. 602—multiply the right-hand side of Equations (30) and (31) by $(2\mu)^{1/3}$.

p. 602, Equation (28a) and p. 610—invert the quantity $\dfrac{\lambda}{2\pi b}$.

p. 603, Equation (35)—change the factor 8 to 16.

p. 605, Equation (40)—change the exponent of b from 2 to 4. Furthermore, there now exists a simple relation between $p_m(ix)$ and $h_m(ix)$. This relation did not exist before because of the error in Equation (20). We now find:

$$(-1)^m p_m(ix) = \frac{-2b^4\Gamma_0}{x^3\lambda} \cdot \frac{1}{ih_m(ix)}.$$

p. 606, Equation (44)—delete the factor 2 in the denominator, and change the exponent of $\dfrac{e}{m}$ from 4/3 to 2/3.

p. 606, Equation (45) should read—

$$(F)_{m=0} = 1 + \frac{a^2 \, ec}{kT} \, \frac{b}{\lambda} \, \frac{\pi^{7/3} \, I_0^{1/3}}{(e/m)^{2/3}} \, \frac{Q_0}{\mu} \left(ix, \frac{a}{b} \right)$$

where the original definition of $Q_0 \left(ix, \dfrac{a}{b} \right)$ is preserved.

Applying the new simple relation written above, $Q_0 \left(ix, \dfrac{a}{b} \right)$ is given by

$$\frac{Q_0}{\mu} \left(ix, \frac{a}{b} \right) = \frac{2}{\pi} \frac{y_0 \left(ix, \dfrac{a}{b} \right)}{\left(x^2 + \dfrac{\mu^2}{\nu^2} \right)^{3/2}}$$

p. 607, Equation (46) should read—

$$(F)_{m=0} = 1 + 2 \frac{a^2 \, ec}{kT} \, \frac{b}{\lambda} \, \frac{\pi^{4/3} \, I_0^{1/3}}{\left(\dfrac{e}{m} \right)^{2/3}} \, \frac{e^{-2/3 \, \mu}}{\mu} \, J_0^{2/3} \left(i\mu \frac{a}{b} \right)$$

p. 607, Figure 9—these curves are in error because $Q_0(ix)$ depends on $h_0(ix)$. Correct values may be taken from the curves of $y_0 \left(ix, \dfrac{a}{b} \right)$ via the relation shown above. For completeness, curves of $\dfrac{Q_0}{\mu} \left(ix, \dfrac{a}{b} \right)$ versus μ are shown below.

p. 609, Equation (49) should read—

$$(F)_{m=0} = 1 + \frac{a^2 \, ec}{kT} \, \frac{b}{\lambda} \, \frac{\pi^{7/3} \, I_0^{1/3}}{\left(\dfrac{e}{m} \right)^{2/3}} \, \frac{Q_0}{\mu} \left(ix, \frac{a}{b} \geqslant 1 \right)$$

p. 609, Equation (51) should read—

$$(F)_{m=0} = 1 + \frac{a^2 \, ec}{kT} \, \frac{b}{\lambda} \, \frac{\pi \, I_0^{1/3} \, 2^{2/3} \, e^{-2/3 \left(\frac{a}{b} - 1 \right) \mu}}{\left(\dfrac{e}{m} \right)^{2/3} \left(\dfrac{a}{b} \right)^{1/3} \mu^{4/3}}$$

The general conclusions of the paper are not changed, but the conditions for maximum gain are moved toward values of higher μ.
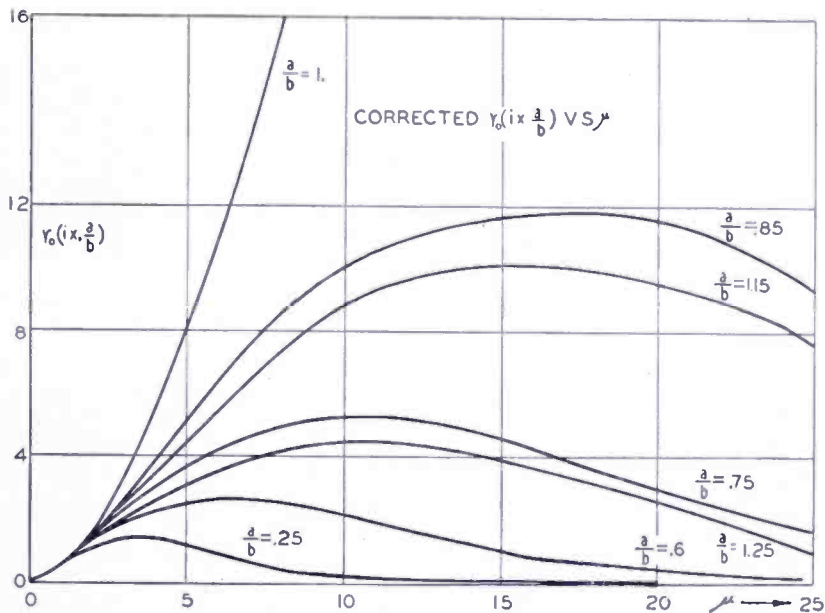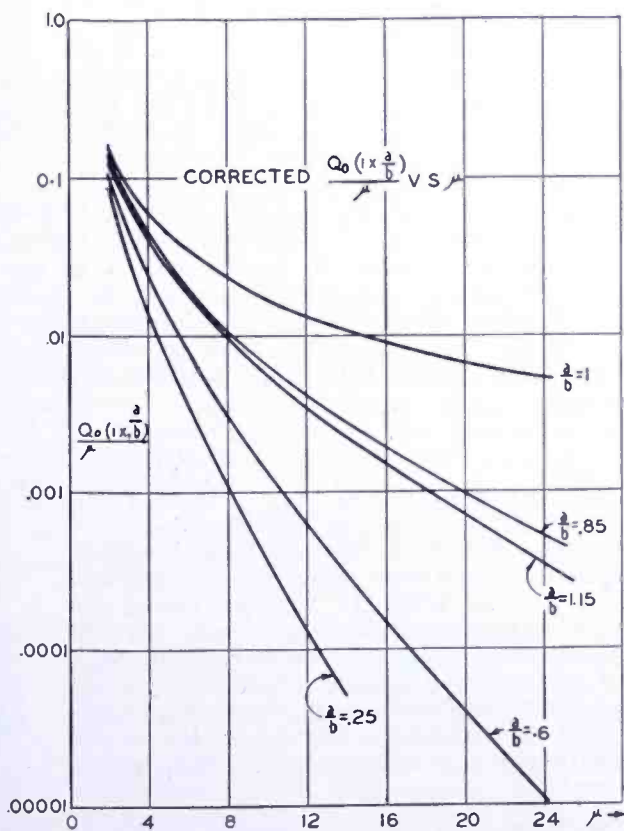
Fig. 8 (Corrected)

Fig. 9 (Corrected)

AUTHORS

WILLIAM L. BEHREND received the B.S. degree in electrical engineering from the University of Wisconsin in 1946 and the M.S. in 1947. From 1944 to 1946 he served as an electronic technician in the Navy. In 1947 he joined the RCA Laboratories Division, Princeton, N.J., where he is now engaged in work on antennas and transmitters. Mr. Behrend is a member of the Institute of Radio Engineers.

EDWARD P. BERTERO received the B.S. degree in electrical engineering in 1942 from New York University. He has been associated with the National Broadcasting Company since 1932. In 1937 he became an apprentice engineer of the Operations Group of the Engineering Department. From 1939 to 1942 he was assigned to both the Field and Studio Groups. While on leave of absence from 1942 to 1945 he served as an officer in the U. S. Naval Reserve as an Electronic Specialist. Upon his return to NBC, he joined the Development Laboratory group to assist in the modernization program of improving field equipment. Currently he is engaged in the design of television apparatus for both field and studio use. Mr. Bertero is a Member of Eta Kappa Nu and an Associate Member of the Institute of Radio Engineers.

GEORGE H. BROWN received the B.S. degree at the University of Wisconsin in 1930; the degree of M.S. in 1931; the Ph.D. degree in 1933; and his professional degree of E.E. in 1942. From 1930 until 1933 he was a Research Fellow in the Electrical Engineering Department at the University of Wisconsin, and from 1933 to 1942 he was in the Research Division of the RCA Manufacturing Company at Camden, N. J. Since 1942, he has been at RCA Laboratories Division, Princeton, N. J. Dr. Brown is a Member of Sigma Xi, the American Institute of Electrical Engineers, New York Academy of Sciences, and a Fellow of the Institute of Radio Engineers, and the American Institute of Electrical Engineers.

ALEXANDER D. BURT attended Drexel Institute of Technology where he studied electrical engineering from 1924 to 1928 and the Moore School of Electrical Engineering, University of Pennsylvania where he studied physics and mathematics from 1930 to 1933. In 1925 he joined the General Electric Company in Philadelphia and in 1928 transferred to Schenectady. In 1930 he joined the RCA Manufacturing Company in Camden where he was engaged in the development of radio and phonograph components. Mr. Burt is presently Section Manager of Record Changers in the Home Instrument Department.

C. LOUIS CUCCIA—(See RCA Review, Volume X, No. 1, March 1949, page 153).

www.americanradiohistory.com

BENJAMIN R. CARSON attended Drexel Institute in Philadelphia. He was employed by the Standard Roller Bearing Company from 1912 until 1916 when he went to the Eddystone Rifle Plant of Midvale Steel. In 1918 he joined the Wright Roller Bearing Company; in 1920, the Electric Service Supplies Company; in 1923, the Miller Lock Company; in 1924 the Victor Talking Machine Company; in 1928, the Philco Radio Company; and in 1929, the M. Tucker Company. In 1930 he joined the Engineering Department of the RCA Manufacturing Company. Since 1945 Mr. Carson has been retained as a consultant by the RCA Victor Division.

MURLAN S. CORRINGTON received the B.S. degree in electrical engineering in 1934, from the South Dakota School of Mines and Technology, and the M. Sc. degree in 1936, from Ohio State University. From 1935 to 1937 he was a graduate assistant in the Physics Department of Ohio State University. In 1937 he joined the Rochester Institute of Technology, and taught mathematics, mechanics, and related subjects. Since 1942 he has been engaged in mathematical engineering in the Advanced Development Section of the RCA Victor Division, Radio Corporation of America, at Camden, N. J.

ROBERT B. JANES received the B.S. degree in physics from Kenyon College in 1928. He did graduate work in physics at Harvard and the University of Wisconsin where he received a Ph.D. in 1935. From 1929 to 1931 he served as instructor in physics at Colgate University and from 1931 to 1935 as research assistant at the University of Wisconsin. In 1935, he joined the Tube Department of the RCA Manufacturing Company at Harrison, N.J. where he worked on television camera tubes and phototubes. Since 1943 he has been in the Tube Department at Lancaster, Pa. in charge of the development and design of television camera tubes. Dr. Janes is a member of Phi Beta Kappa, Sigma Xi, Gamma Alpha and the Institute of Radio Engineers.

RALPH E. JOHNSON received the B.S. degree in electrical engineering from the University of Pittsburgh in 1942. Soon after graduation he was employed as a design engineer in the Cathode-Ray Tube Development Group of the Tube Department of the RCA Victor Division at Harrison, N.J.; he is now with the same group at Lancaster, Pa. He was engaged in the development of radar indicators until 1946 at which time he assumed similar responsibilities in the design and development of camera tubes. Mr. Johnson is a member of Sigma Tau, Eta Kappa Nu, and Sigma Pi Sigma.

ROBERT S. MOORE received the B.S. degree in electrical engineering with a major in communications from Michigan State College in 1943. He joined the Tube Department of the RCA Victor Division at Lancaster, Pa. in the same year as an engineer on television camera tubes. He has worked on the design of various camera and storage tubes with special attention to the development of the target and mesh structure of the image orthicon. Mr. Moore is a member of the American Institute of Electrical Engineers.

WENDELL C. MORRISON received the A.B. degree in 1937 from Morningside College, and the B.S. degree in 1939 and the M.S. degree in 1940, from the University of Iowa. He joined the RCA Manufacturing Company in Camden, N.J. in 1940. In 1942 he transferred to the RCA Laboratories at Princeton, New Jersey, where he is employed at present in the Transmitter Research Section. Mr. Morrison is a member of Sigma Xi, Tau Beta Pi, and Eta Kappa Nu.

JOE REDDECK was discharged from the Army Signal Corps in 1946. He received the B.S. degree in electrical engineering from North Carolina State College in 1947. In the same year he joined the Training Program at RCA Laboratories Division, Princeton, N.J., and is now assigned to the Transmitter Research Section. Mr. Reddeck is an Associate Member of the Institute of Radio Engineers.

HILLEL I. REISKIND received the E.E. degree from Rensselaer Polytechnic Institute in 1928. He was a motion picture recording engineer with Paramount Pictures from 1929 to 1932 and with Eastern Service Studios from 1932 to 1936. In 1936, he joined the Photophone Engineering Department of the RCA Manufacturing Company and was associated with various phases of film recording activities in Camden, New York, Hollywood, and Indianapolis until 1941. In that year, he organized in Indianapolis the Phonograph Record Development Group. He is now Chief Engineer of the Record Department. Mr. Reiskind is a member of the Society of Motion Picture Engineers, the Audio Engineering Society, the American Association for the Advancement of Science, and an Associate Member of Sigma Xi.

H. E. ROYS received the B.S. degree in electrical engineering from the University of Colorado in 1925. From 1925 to 1930 he was with the General Electric Company in Schenectady on radio transmitter test and later on receiver engineering. He was transferred to the RCA Manufacturing Company at Camden, N.J. in 1930 and in 1931 became associated with the Phonograph Section. In 1937 he became a member of the Advanced Development Group of the Photophone Section, which later became part of the Engineering Products Department. From 1941 to 1946 he was located with this group in Indianapolis, working mainly on disk recording and reproducing problems. At present he is located in Camden and is still associated with the same group. Mr. Roys is a member of Tau Beta Pi and Eta Kappa Nu, and is a Senior Member of the Institute of Radio Engineers.

OAKLEY M. WOODWARD, JR. received the degree of Bachelor of Science in electrical engineering from the University of Oklahoma in 1938. He joined the Seismograph Service Corporation of Tulsa, Oklahoma, after graduation. During 1941, he was a research engineer at the RCA Manufacturing Company, Camden, N. J. Since January 1942, he has been with RCA Laboratories Division, Princeton, N. J. Mr. Woodward is a Member of Sigma Xi, and an Associate Member of the Institute of Radio Engineers.